Coffin, M.F., Frey, F.A., Wallace, P.J., et al., 2000
Proceedings of the Ocean Drilling Program, Initial Reports Volume 183

1. Leg 183 Summary: Kerguelen Plateau–Broken Ridge—A Large Igneous Province[1]

Shipboard Scientific Party[2]

ABSTRACT

Most of the Kerguelen Plateau and Broken Ridge formed as a single giant oceanic plateau in Cretaceous time. During Ocean Drilling Program Leg 183, igneous basement rock and sediment cores were obtained from five sites on the Kerguelen Plateau and two on Broken Ridge. Based on the recovery of basalt, other igneous rocks, and interbedded and overlying sediment, we found that

1. From south to north, the age of the uppermost crust forming this very large igneous province (LIP) decreases, possibly in steps (i.e., ~110 Ma in the southern Kerguelen Plateau, ~85 to 95 Ma in the central Kerguelen Plateau, Broken Ridge, and Elan Bank, and ≤35 Ma in the northern Kerguelen Plateau); the submarine igneous basement of Elan Bank and the northern Kerguelen Plateau had not been previously sampled.
2. The growth rate of the LIP at five of seven basement sites was sufficient to form a subaerial landmass. This was most spectacularly revealed at central Kerguelen Plateau Site 1138 by wood fragments in a dark brown sediment overlying the subaerially erupted lava flows, a result consistent with the charcoal and wood fragments in sediments overlying igneous rocks at Site 750 in the southern Kerguelen Plateau.
3. The terminal stage of volcanism forming the LIP included explosive eruptions of volatile-rich felsic magmas formed from cooling basaltic magmas that were trapped within the crust when the flux of basaltic magma from the mantle decreased.

[1]Examples of how to reference the whole or part of this volume.
[2]Shipboard Scientific Party addresses.

Ms 183IR-101

4. Previous geochemical studies of basalt from the southern Kerguelen Plateau and eastern Broken Ridge had identified a component derived from continental crust (e.g., Mahoney et al., 1995), but the mechanism for incorporation of a continental component into the oceanic plateau was unconstrained. Possible processes range from recycling of continental material into a deep mantle plume to contamination of mantle-derived basaltic magma by fragments of continental crust isolated in the embryonic Indian Ocean crust during rifting of Gondwana. At Site 1137 on Elan Bank, a 26-m sequence of fluvial conglomerate was intercalated between basaltic flows; the clasts in this conglomerate show that a wide range of rock types were subaerially exposed on Elan Bank. Most notable are clasts of garnet-biotite gneiss, a rock type that is commonly found only in continental crust, thereby indicating that a continental fragment is present in this oceanic environment.

INTRODUCTION

Large igneous provinces (LIPs) are a significant type of planetary volcanism found on Earth, the moon, Venus, and Mars (Coffin and Eldholm, 1994; Head and Coffin, 1997). They represent large volumes of magma emplaced over relatively short time periods, such as expected from decompression of upwelling, relatively hot or wet mantle. This process explains hot spot magmatism at the Earth's surface and is conceptually described by various plume head and tail models applicable to the Earth's sublithospheric mantle. In such models, the plume head leads to oceanic plateaus and continental flood basalts, and the tail leads to volcanic chains known as hot spot tracks. Terrestrial LIPs are dominantly mafic rocks formed during several distinct episodes in Earth's history, perhaps in response to fundamental changes in the processes that control energy and mass transfer from the Earth's interior to its surface. The ocean basins contain several Cretaceous LIPs; the two largest are the Kerguelen Plateau–Broken Ridge in the Indian Ocean (Fig. **F1**) and the Ontong Java Plateau in the Pacific Ocean. Both are elevated regions of the ocean floor encompassing areas of ~2 × 10^6 km^2 (Coffin and Eldholm, 1994). These giant LIPs are important for several reasons. They provide information about mantle compositions and dynamics that are not revealed by volcanism at spreading ridges. For example, today's plume-associated volcanism (principally, oceanic islands) accounts for only 5% to 10% of the mass and energy expelled from Earth's mantle, but the giant LIPs may have contributed as much as 50% in Early Cretaceous time (Coffin and Eldholm, 1994), thereby indicating a substantial change in mantle dynamics from Cretaceous to present time (e.g., Stein and Hofmann, 1994). Because magma fluxes represented by oceanic plateaus are not evenly distributed in space and time, their episodicity punctuates the relatively steady-state production of crust at seafloor spreading centers. These intense episodes of igneous activity temporarily increase the flux of magma and heat from the mantle to the crust, hydrosphere, and atmosphere, possibly resulting in global environmental changes, such as excursions in the composition and isotope characteristics of seawater (e.g., Larson, 1991; Ingram et al., 1994; Jones et al., 1994; Bralower et al., 1997). Finally, because oceanic LIPs apparently resist subduction, they contribute to the growth of continents.

F1. Map of the eastern Indian Ocean showing major physiographic features and pre-Leg 183 sites where igneous basement was recovered, **p. 49.**

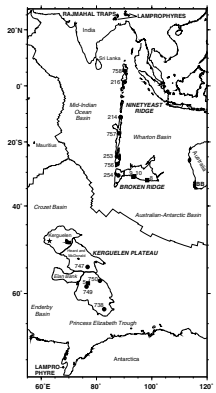

The Kerguelen Plateau–Broken Ridge LIP is interpreted to represent voluminous Cretaceous volcanism associated with the arrival of the Kerguelen plume head below young Indian Ocean lithosphere (Fig. F2) (e.g., Morgan, 1971; Duncan and Storey, 1992; Pringle et al., 1994; Storey et al., 1996). Subsequently, rapid northward movement of the Indian plate over the plume formed a 5000-km-long, ~82- to 38-Ma, hot spot track, the Ninetyeast Ridge (Duncan, 1991). At ~40 Ma the westward-propagating Southeast Indian Ridge (SEIR) intersected the plume's position. As the SEIR migrated northeast relative to the plume, hot spot magmatism became confined to the Antarctic plate. From ~40 Ma to the present, the Kerguelen Archipelago, Heard and McDonald Islands, and a northwest-southeast–trending chain of submarine volcanoes between these islands were constructed on the northern and central sectors of the Kerguelen Plateau (Figs. F1, F2, F3, F4). Thus, an ~115-m.y. record of volcanism is attributed to the Kerguelen plume (e.g., Mahoney et al., 1983; Weis et al., 1992; Pringle et al., 1994; Storey et al., 1996).

Despite their huge size and distinctive morphology, oceanic plateaus remain among the least understood features in the ocean basins. This drilling leg focused on sampling the Kerguelen Plateau–Broken Ridge LIP to determine (1) the age and composition of the basement volcanic rocks in all major parts of the LIP, (2) the mantle and crustal components that contributed to the magmatism, (3) the mass transfer and chemical fluxes between the volcanic crust and atmosphere-hydrosphere-biosphere system, and (4) the tectonic history of the LIP beginning with the mechanisms of growth and emplacement and continuing with the multiple episodes of postconstructional deformation that created the present complex bathymetry (Figs. F3, F4).

STUDY AREA

Physical Description

The Kerguelen Plateau is a broad bathymetric high in the southern Indian Ocean surrounded by deep ocean basins—to the northeast by the Australian-Antarctic Basin, to the south by the 3500-m-deep Princess Elizabeth Trough, to the southwest by the Enderby Basin, and to the northwest by the Crozet Basin (Figs. F1, F3). The plateau stretches ~2300 km between 46°S and 64°S in a southeast-trending direction toward the Antarctic continental margin. It is between 200 and 600 km wide and stands 2–4 km above the adjacent ocean basins. Variable age oceanic crust abuts the Kerguelen Plateau. As summarized by Schlich and Wise (1992), the oldest magnetic anomalies range from Chron C11n.2n (o) (30.1 Ma), in the northeast, to Chron C18n.2n (o) (40.1 Ma) off the central part of the eastern plateau (we use the geomagnetic polarity time scale of Cande and Kent, 1995). Farther south, the eastern flank of the Southern Kerguelen Plateau is bounded by the Labuan Basin. Basement of the Labuan Basin has not been sampled by drilling, but its structure resembles that of the main Kerguelen Plateau (Rotstein et al., 1991; Munschy et al., 1992). To the northwest, magnetic anomaly sequences from Chrons C23 to C34 have been identified in the Crozet Basin, but to the southwest no convincing anomalies have been identified in the Enderby Basin, although Mesozoic anomalies have been suggested (Li, 1988; Nogi et al., 1996). An Early Cretaceous age for the

F2. Plate reconstructions of the southern Indian Ocean, p. 50.

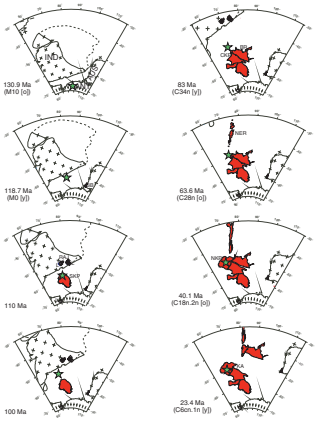

F3. Bathymetry of the Kerguelen Plateau, p. 52.

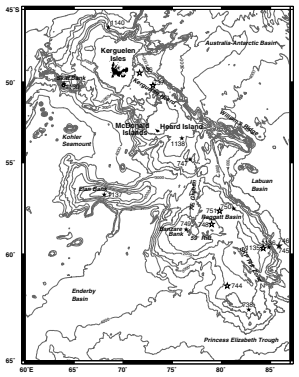

F4. Satellite-derived free-air gravity map of the Kerguelen Plateau, p. 53.

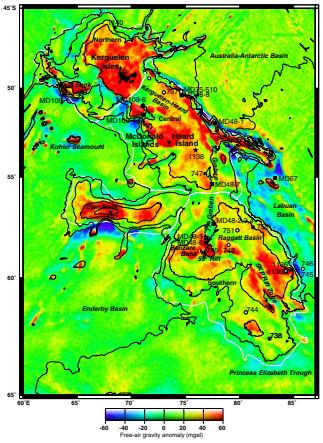

Enderby Basin is assumed in most plate reconstructions (e.g., Royer and Coffin, 1992).

Beginning with early studies (Schlich, 1975; Houtz et al., 1977), the Kerguelen Plateau province has been divided into distinct domains. Coffin et al. (1986) and Könnecke et al. (1998) recognize five domains: northern, central, and southern Kerguelen Plateau; Elan Bank; and the Labuan Basin (Figs. **F3, F4**). The northern Kerguelen Plateau (NKP), ~46°S to 50°S, has shallow water depths (<1000 m) and basement elevations 3000–4000 m above adjacent seafloor, with maximum elevations forming the Kerguelen Archipelago. A lack of rocks older than ~40 Ma from the Kerguelen Archipelago (Nicolaysen et al., 1996, in press), as well as plate reconstructions (Royer and Sandwell, 1989; Royer and Coffin, 1992), suggests that the age of the NKP is ≤40 Ma, whereas the central and southern domains of the submarine Kerguelen Plateau appear to be of Cretaceous age (Pringle et al. 1994; Storey et al., 1996). However, the basement of the submarine NKP had not been sampled before Leg 183. The central Kerguelen Plateau (CKP), ~50°S to 55°S, is also relatively shallow, contains a major sedimentary basin (Kerguelen-Heard Basin), and includes the volcanically active Heard and McDonald Islands. Broken Ridge and the CKP are conjugate Late Cretaceous provinces (Fig. **F1**) that were separated by seafloor spreading along the SEIR during Eocene time (Mutter and Cande, 1983).

The southern Kerguelen Plateau (SKP) apparently formed in Early Cretaceous time (Pringle et al., 1994; Storey et al., 1996). Relative to the NKP, water depths are greater (1500 to 2500 m), and it is tectonically more complex (Figs. **F3, F4**). There are several large basement uplifts and evidence for multiple stages of normal faulting, graben formation, and strike-slip faulting (e.g., Coffin et al., 1986; Fritsch et al., 1992; Rotstein et al., 1992; Royer and Coffin, 1992; Angoulvant-Coulon and Schlich, 1994; Könnecke and Coffin, 1994; Gladczenko et al., 1997). Elan Bank, a salient extending westward from the boundary between the CKP and SKP, has water depths from <1000 to 2000 m. Before Leg 183, basement had not been sampled from Elan Bank and its age was, therefore, unknown. The Labuan Basin, which adjoins the CKP and SKP to the east, is a deep (>3500 m), extensively faulted, thickly sedimented (>2 s two-way traveltime in places, or >2000 m, assuming a sediment velocity of 2000 m/s) basin. Dredging of an exposed faulted basement block in the Labuan Basin recovered metamorphic and granitic rock; these rocks have been interpreted as ice-rafted debris (Montigny et al., 1993). Thus, the basin's age and the nature of its crust (i.e., oceanic or continental) remain uncertain.

The CKP was contiguous with Broken Ridge when these domains formed during Cretaceous time (Duncan, 1991; Houtz et al., 1977; Pringle et al., 1994; Storey et al., 1996). Subsequently, at ~40 Ma, Broken Ridge and the CKP began to separate along the westward-propagating SEIR. Broken Ridge, now ~1800 km north of the Kerguelen Plateau, is a narrow and elongated oceanic plateau (100–200 km by ~1000 km at ~2000 m water depth) that trends west-northwest (Figs. **F5, F6**). It is markedly asymmetric in cross section, dipping gently (<2°) toward the north but with a steeply dipping (>10°) southern face (Fig. **F5**). This southern flank was uplifted, perhaps more than 2000 m, during the early Tertiary breakup between Broken Ridge and the Kerguelen Plateau (Peirce, Weissel, et al., 1989; Weissel and Karner, 1989).

F5. Bathymetry of Broken Ridge, **p. 55.**

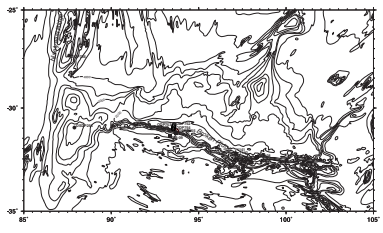

F6. Satellite-derived gravity field for Broken Ridge, **p. 56.**

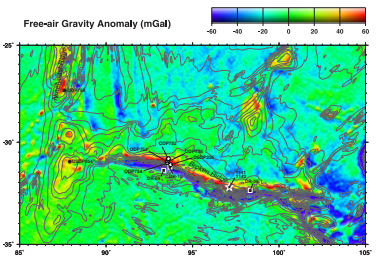

Crustal Structure

Ocean Drilling Program (ODP) Legs 119 and 120 drilling results (Barron, Larsen, et al., 1989; Schlich, Wise, et al., 1989), dredging data (Leclaire et al., 1987; Davies et al., 1989; Duncan, 1991; Weis et al., 1998a), and multichannel seismic reflection data (Coffin et al., 1990; Schaming and Rotstein, 1990; Schlich et al., 1993) have shown that igneous basement of the Kerguelen Plateau and conjugate Broken Ridge is basaltic. Numerous dipping intrabasement reflections interpreted as flood basalts have been identified in the crust of the CKP and SKP and on Elan Bank (Könnecke et al., 1997). Wide-angle seismic data from the Kerguelen Archipelago on the NKP show an upper igneous crust 8–9.5 km thick and a lower crust 6–9.5 km thick (Charvis et al., 1995; Recq and Charvis, 1986; Recq et al., 1990, 1994). Wide-angle reflection and refraction experiments employing ocean-bottom seismometers have been undertaken recently on both the CKP and SKP (Charvis et al., 1993, 1995; Operto and Charvis, 1995, 1996; Könnecke et al., 1998; Charvis and Operto, 1998, 1999). The crustal structure beneath the Kerguelen Archipelago differs significantly from that of the CKP. Igneous crust of the CKP is 19 to 21 km thick and is composed of three layers. The upper layer is 1.2 to 2.3 km thick, and velocities range from 3.8 to 4.9 km/s. It could be composed of either lava flows or interlayered volcanic and sedimentary beds. The second layer is 2.3 to 3.3 km thick, and velocities increase downward from 4.7 to 6.7 km/s. In the ~17-km-thick lower crust, velocities increase from 6.6 km/s at ~8.0 km depth (near the top of the layer) to 7.4 km/s at the base of the crust, with no internal discontinuity. On the southern plateau, the ~22-km-thick igneous crust can be divided into three layers: (1) an upper crustal layer ~5.3 km thick with velocities ranging from 3.8 to 6.5 km/s; (2) a lower crustal layer ~11 km thick with velocities of 6.6 to 6.9 km/s; and (3) a 4- to 6-km-thick transition zone at the base of the crust characterized by velocities of 6.7 to 6.9 km/s (Operto and Charvis, 1995, 1996). This low-velocity, seismically reflective transition zone at the crust/mantle interface has not been imaged on the NKP or CKP; it is the basis for the hypothesis that parts of the SKP contain fragments of continental crust (Operto and Charvis, 1995; 1996).

Previous Sampling of Igneous Basement: Ages and Geochemical Characteristics

In this section we summarize results of previous sampling (Legs 119 and 120 and dredging) of the Kerguelen Plateau–Broken Ridge LIP. Based in large part on ODP-related studies, there is a consensus that the Kerguelen plume was the major source of magma for constructing the Kerguelen Plateau–Broken Ridge LIP. Although samples and dates from the entire LIP are meager, sampling of the SKP at four spatially diverse locations (Sites 738, 749, and 750, and dredge Site MD48-05; see Figs. **F3, F4**) shows that the uppermost igneous crust of SKP formed over a relatively short interval at ~110 Ma (K/Ar data from Leclaire et al., 1987; Whitechurch et al., 1992; and $^{40}Ar/^{39}Ar$ data from Pringle et al., 1994; Storey et al., 1996). In contrast, basement basalts from Site 747 on the CKP may be much younger, ~85 Ma (Pringle et al., 1994; Storey et al., 1996). This age is similar to the 83- to 88-Ma age for lavas from Broken Ridge dredge sites 8 and 10 ($^{40}Ar/^{39}Ar$ data from Duncan, 1991), which coincide spatially with the prebreakup position of Site 747 (Figs. **F1, F2**). Also, piston coring of sediments on the northeast flank of the CKP

between the Kerguelen Archipelago and Heard Island (MD35-510 in Fig. F4) recovered cherts and calcareous oozes of probable Santonian age (Fröhlich and Wicquart, 1989). In summary, we have very few high-quality age data for the 2.3 × 10^6 km^2 (equivalent to approximately eight Icelandic plateaus) of the Kerguelen Plateau–Broken Ridge LIP. These sparse data support the hypothesis that large magma volumes erupted over short time intervals, possibly as two pulses during Cretaceous time—the SKP at ~110 Ma; the CKP, Broken Ridge, and perhaps Elan Bank at ~85 Ma (Fig. F7). In contrast, Cenozoic volcanism (~38 Ma to present) has formed the Kerguelen Archipelago (e.g., Nicolaysen et al., 1996, in press), Heard and McDonald Islands (Clarke et al., 1983; Quilty et al., 1983), and the bathymetric/gravity highs between the Kerguelen Archipelago and Heard Island (Weis et al., 1998a). A major goal of Leg 183 was to drill at other sites throughout the plateau to determine whether formation of this LIP was truly episodic or continuous with a south to north decrease in age of volcanism.

Although the southern and central domains of the Kerguelen Plateau formed in a young oceanic basin (Royer and Coffin, 1992; Munschy et al., 1994), evidence is equivocal as to whether it formed at a spreading center, like Iceland, or off-ridge, like Hawaii (Coffin and Gahagan, 1995). Before Leg 183, several observations had indicated that much of the uppermost basement of the southern and central Kerguelen Plateau erupted in a subaerial environment—specifically, (1) oxidized flow tops and vesicularity of lava flows at Sites 738 and 747; (2) nonmarine, organic-rich sediments containing up to 5-cm pieces of charcoal overlying the basement at Site 750; and (3) claystone overlain by a basalt cobble conglomerate and glauconitic sediment with wood fragments in the lowermost core at Site 748 (Schlich, Wise, et al., 1989). Coffin (1992) concluded that the drill sites in the SKP had long (>10 to ≤50 m.y.) histories of subaerial volcanism and erosion, followed by subsidence caused by cooling. Zeolite mineralogy of the basaltic basement indicates temperatures of ≤120°C at Sites 747 and 750, but higher temperatures (≤225°C) at Site 749, perhaps indicating deeper levels of erosion (Sevigny et al., 1992).

The islands on the Kerguelen Plateau are dominantly formed of <40-Ma transitional and alkaline lavas (Fig. F8) (Weis et al., 1993, 1998b; Barling et al., 1994; Yang et al., 1998; Nicolaysen et al., 1996, in press). Before Leg 183, the only alkaline basalt recovered from the Kerguelen Plateau, Broken Ridge, and Ninetyeast Ridge was a flow ~200 m above basement at Site 748. Tholeiitic basalt of Cretaceous age has been recovered from four dredge and four drill sites on the central and southern Kerguelen Plateau and three dredge sites on Broken Ridge (Figs. F3, F4, F5, F6, F8); seven drill sites on Ninetyeast Ridge have yielded solely tholeiitic basalt ranging from 38 to 82 Ma (Fig. F1). Tholeiitic basalts from each of these sites are geochemically distinct, but as a group, their incompatible element abundances resemble those of ocean-island tholeiitic basalts, rather than typical mid-ocean-ridge basalts (MORBs) (data sources: Kerguelen Plateau and Broken Ridge: Davies et al., 1989; Weis et al., 1989; Storey et al., 1992; Mahoney et al., 1995; Ninetyeast Ridge: Frey et al., 1991; Saunders et al., 1991; Frey and Weis, 1995). We infer that tholeiitic basalt was the dominant magma type produced by the Kerguelen plume from ~110 to 38 Ma during formation of the Kerguelen Plateau, Broken Ridge, and Ninetyeast Ridge. The significance is that tholeiitic basalts are derived from relatively high (>5%) extents of partial melting (Kent and McKenzie, 1994), and the inference is that the Kerguelen plume was a high-flux magma source for a long time (Figs.

F7. Kerguelen hot spot magma output since ~130 Ma, p. 57.

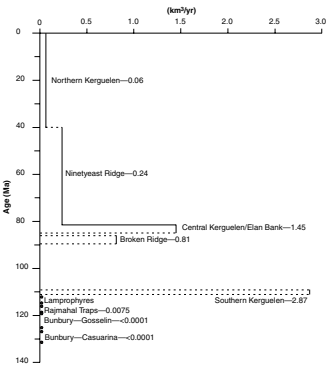

F8. Total alkalis vs. SiO_2 plot for classifying tholeiitic and alkalic basalts, p. 58.

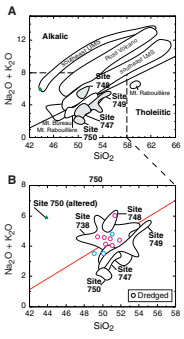

F2, F7). However, the MgO-rich melts expected from large extents of melting of high-temperature plumes (e.g., Storey et al., 1991) have not been recovered from Cretaceous parts of the Kerguelen Plateau. Picritic (i.e., olivine rich) alkaline lavas of Quaternary age are found on Heard Island (Barling et al., 1994), and transitional picritic lavas (14 to 19 Ma) were recently dredged from one of the bathymetric/gravity highs between the Kerguelen Archipelago and Heard Island (Weis et al., 1998a) (see Figs. F3, F4). All of these picrites are olivine-rich cumulates rather than crystallized MgO-rich melts.

Most lavas from the Kerguelen Plateau and Broken Ridge have Sr and Nd isotope ratios that range from the high $^{87}Sr/^{86}Sr$-low $^{143}Nd/^{144}Nd$ end of the field for SEIR MORB to the field proposed for the Kerguelen plume (Fig. F9). In Pb-Pb isotope plots, Kerguelen Plateau lavas from Sites 747, 749, and 750 define an elongate field subparallel to that for SEIR MORB (Fig. F10); however, like lavas forming the Kerguelen Archipelago, the Kerguelen Plateau lavas are offset from the MORB field to higher $^{208}Pb/^{204}Pb$ and $^{207}Pb/^{204}Pb$ at a given $^{206}Pb/^{204}Pb$ ratio. In addition, submarine Kerguelen Plateau lavas extend to lower $^{206}Pb/^{204}Pb$ than Kerguelen Archipelago lavas (Fig. F10). These Sr, Nd, and Pb isotope data have been interpreted as a result of mixing between the Kerguelen plume and entrained depleted (MORB related) asthenosphere (e.g., Weis et al., 1992).

In contrast, basalts from Site 738 on the southernmost SKP and dredge 8 from eastern Broken Ridge (Figs. F1, F2, F3, F4, F5, F6) have atypical geochemical characteristics for oceanic lavas. These lavas have very high $^{87}Sr/^{86}Sr$, low $^{143}Nd/^{144}Nd$, and very high $^{208}Pb/^{204}Pb$ and $^{207}Pb/^{204}Pb$ ratios that accompany relatively low $^{206}Pb/^{204}Pb$ (Figs. F9, F10). They also have relative depletions in abundances of Nb and Ta (Fig. F11A); moreover, La/Nb correlates positively with $^{87}Sr/^{86}Sr$ (Fig. F12). Mahoney et al. (1995) concluded that these isotope characteristics, coupled with depletions of Nb and Ta, arose from a continental lithosphere component that contributed to these basalts, a hypothesis also proposed by Storey et al. (1989) to account for Ta depletion in basalts dredged from the Kerguelen Plateau. Significant relative depletion in Nb is also evident in basalts dredged from the 77° graben on the SKP and from Site 747 on the CKP (Fig. F11A). Trends to anomalously high Th/Nb and La/Nb and a positive correlation between $^{87}Sr/^{86}Sr$ and La/Nb are also defined by the Bunbury Basalt, southwest Australia, and the Rajmahal Basalt, northeast India (Figs. F11B, F12). These continental basalts, erupted at ~123–130 Ma and 116 Ma, respectively, are contaminated to varying degrees by continental crust (Frey et al., 1996; Kent et al., 1997). The combination of geochemical features in basalts from Site 738 and eastern Broken Ridge (i.e., very high $^{87}Sr/^{86}Sr$ and low $^{143}Nd/^{144}Nd$; high $^{208}Pb/^{204}Pb$ and $^{207}Pb/^{204}Pb$ that accompany relatively low $^{206}Pb/^{204}Pb$; anomalously high Th/Nb and La/Nb; see Figs. F9, F10, F11, F12) is consistent with continental crust as the continental component. In particular, the low $^{206}Pb/^{204}Pb$ requires aged crust with low U/Pb, such as some types of Archean crust.

In detail, the trend for Site 747 lavas (Fig. F11A) differs from that of other Kerguelen Plateau basalts because Site 747 lavas trend to high La/Nb without elevated Th/Nb. This trend is similar to that for North Atlantic MORB from the lower flow units at Hole 917A (Fig. F11B), which are contaminated by the Archean crust of eastern Greenland, specifically, lower crustal granulite-facies gneiss (Fitton et al., 1998a, 1998b). The effects of continental contamination are very evident in these Hole

F9. $^{143}Nd/^{144}Nd$ vs. $^{87}Sr/^{86}Sr$ showing data points for basalts recovered from the Kerguelen Plateau and Broken Ridge, p. 59.

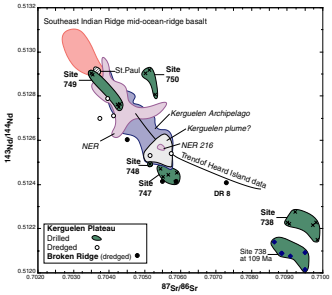

F10. $^{208}Pb/^{204}Pb$ vs. $^{206}Pb/^{204}Pb$ showing measured data points for basalts recovered from the Kerguelen Plateau and Broken Ridge, p. 60.

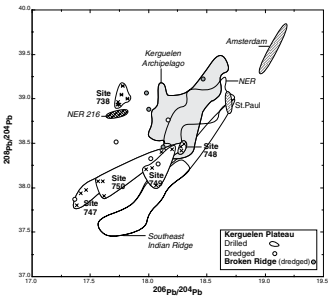

F11. Abundance ratios of $(Th/Nb)_N$ vs. $(La/Nb)_N$, p. 61.

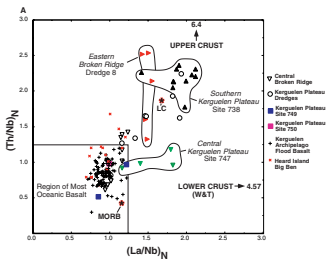

917A basalts because their parental magmas were MORB-like with much lower incompatible element abundances than are found in most plume-related lavas. Note that the combination of elevated La/Nb with low Th/Nb is unlike recent estimates of average lower crust composition (e.g., Fig. **F11;** Rudnick and Fountain, 1995) but is typical of Lewisian granulites (Fig. **F11;** lower crust estimates are from Weaver and Tarney, 1984). Although not as extreme as some basalts from the lower units of Hole 917A, several geochemical characteristics of Site 747 basalts are consistent with crustal contamination—namely, (1) the trend to high La/Nb without high Th/Nb; (2) the offset to low $^{143}Nd/^{144}Nd$ from the $^{87}Sr/^{86}Sr$-$^{143}Nd/^{144}Nd$ trend defined by Kerguelen Archipelago lavas; and (3) the low $^{206}Pb/^{204}Pb$ ratios, which are lower than those of all other lavas from the Kerguelen Plateau, Ninetyeast Ridge, Kerguelen Archipelago, and Heard Island (Figs. **F9, F10, F11, F12**). These characteristics are consistent with ancient continental crust as the contaminant; the high La/Nb–low Th/Nb (Fig. **F11A**) trend suggests a component similar to Lewisian granulites. Archean granulites on the conjugate Antarctic and Indian margins (e.g., Black et al., 1992) raise the possibility that fragments of such crust were incorporated into the embryonic Indian Ocean and subsequently sampled during formation of the Kerguelen Plateau. In addition, the Os and Pb isotope ratios of peridotite xenoliths in basalts from the Kerguelen Archipelago are interpreted as reflecting Gondwanan lithospheric mantle that was incorporated into the Indian Ocean mantle during rifting (Hassler and Shimizu, 1998; Mattielli et al., 1999).

The geochemical evidence for a continental component in basalts forming the Kerguelen Plateau and Broken Ridge is consistent with a crustal velocity structure suggesting that the SKP contains a stretched continental fragment (Operto and Charvis, 1995; 1996); this geophysical evidence is at ~58°S in the vicinity of the basalts dredged from the 77° graben and cored at Site 750, whereas Site 738 is much farther south at ~63°S and Site 747 is to the north at ~55°S (Fig. **F3, F4**). These results suggest that continental lithosphere may be widespread in the Kerguelen Plateau.

F12. Initial $^{87}Sr/^{86}Sr$ vs. $(La/Nb)_N$ showing the positive correlation that arises from an increasing proportion of a continental crust component in the Bunbury Basalt of southwest Australia, **p. 63.**

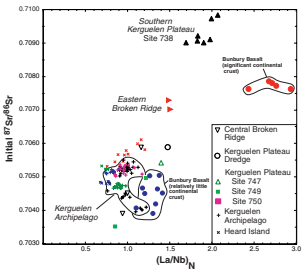

SCIENTIFIC OBJECTIVES

Leg 183 objectives focused on four major problems related to the formation and evolution of a giant LIP:

1. Chronology of Kerguelen Plateau–Broken Ridge magmatism: The goal was to quantify magma flux as a function of time.
2. Petrogenesis of basement igneous rocks: The goal was to constrain the mineralogy and composition of the mantle sources that contributed to the magmatism, the melting processes that created the magmas, and the postmelting magmatic evolution; in particular, we sought to evaluate the role of continental lithosphere in the magmatism that formed the different domains of this LIP.
3. Environmental impact: The goal was to understand the postmagmatic processes that affected the igneous crust and evaluate the effects of LIP magmatism on the environment.
4. Tectonic history: The goal was to identify and interpret relationships between LIP development and tectonism.

Chronology of Kerguelen Plateau–Broken Ridge Magmatism

The most significant question to answer is "how much magma was erupted over what time interval"?—more specifically (1) "what is the age of the uppermost volcanic basement"? (2) "do eruption ages vary systematically with location on the plateau"? (3) "was the growth episodic or continuous"? and (4) "did the plateau grow by lateral accretion (i.e., similar to Iceland) or by vertical accretion and underplating"? Answers to these questions are provisionally provided by dating the oldest sediment above basaltic basement; more definitive results will come from postcruise $^{40}Ar/^{39}Ar$ dating of the lavas.

Other important questions related to magma flux are (1) "did volcanism end abruptly or gradually"? (2) "did volcanism change from tholeiitic/transitional basalt to alkaline basalt as in the Kerguelen Archipelago, or did it remain exclusively tholeiitic like the Ninetyeast Ridge"? and (3) "were evolved (nonbasaltic) magmas erupted"? These questions were answered by drilling several holes with >100-m basement penetration.

Answers to all of these questions related to magma flux are required to understand the physical and chemical processes that formed the Kerguelen Plateau–Broken Ridge LIP.

Petrogenesis of Basement Igneous Rocks

Several lines of evidence support the interpretation that the Kerguelen plume has been a long-term source of magma for major bathymetric features in the eastern Indian Ocean. For example, the systematic south to north age progression on Ninetyeast Ridge is consistent with a hot spot track formed as the Indian plate migrated northward over the Kerguelen plume (Mahoney et al., 1983; Duncan, 1991). Also, isotope similarities among lavas from the Ninetyeast Ridge, the younger lavas forming the Kerguelen Archipelago and Heard Island, and the older lavas forming the Kerguelen Plateau and Broken Ridge (Figs. **F9, F10**) are consistent with the Kerguelen plume as an important source component (Weis et al., 1992; Frey and Weis, 1995, 1996). The preservation of a LIP resulting from partial melting of a decompressing plume head and its associated hot spot track derived from the plume stem presents an excellent opportunity to understand the evolution of a long-lived plume.

Many studies of oceanic island volcanoes have demonstrated that geochemically distinct sources (e.g., plume, entrained mantle, and overlying lithosphere) contribute to plume-related volcanism. Because isotope characteristics of plume, asthenosphere, and lithosphere sources are usually quite different, temporal geochemical variations in stratigraphic sequences of lavas can be used to determine the relative roles of different sources in plume-related volcanism. Establishing how the proportions of these sources change with time and location aids our understanding of how plumes "work" (Chen and Frey, 1985; Gautier et al., 1990; White et al., 1993; Peng and Mahoney, 1995).

What was the role of depleted asthenosphere in creating the Kerguelen Plateau–Broken Ridge LIP? We use "depleted" to indicate relative depletion in abundances of highly incompatible elements (e.g., depleted asthenosphere is the source of most MORB [see Hofmann, 1997, for additional discussion]). Such asthenosphere can be entrained into an ascending plume head, or, when a plume is located at a spreading

ridge axis, plume-derived and MORB magmas can mix. For example, much of the Ninetyeast Ridge formed when the Kerguelen plume was close to a ridge axis (Royer et al., 1991). Weis and Frey (1991) inferred that the relatively low $^{87}Sr/^{86}Sr$ and high $^{143}Nd/^{144}Nd$ ratios of lavas from Deep Sea Drilling Project (DSDP) Site 756 on the Ninetyeast Ridge are a consequence of the plume being close to a spreading ridge axis during formation of the Ninetyeast Ridge. Also, depleted material may be intrinsic to a plume (e.g., Saunders et al., 1998). Fitton et al. (1998) suggested that a plot of Zr/Y vs. Nb/Y is a geochemical discriminant for distinguishing depleted material intrinsic to the Icelandic plume from North Atlantic MORB. In the case of the Kerguelen plume, however, this discriminant is compromised by the presence of a continental lithosphere component in some of the lavas.

A continental lithospheric component has been recognized geochemically in lavas from the southern SKP (Site 738 at ~63°S) and in dredge 8 lavas from eastern Broken Ridge (Mahoney et al., 1995). A less obvious but significant continental lithospheric component is also present in basalts from Site 747 on the CKP and in basalts dredged from the 77° graben in the SKP (Figs. **F9, F10, F11, F12**). In addition, wide-angle seismic data from the Raggatt Basin (58°S) of the SKP show a reflective zone at the base of the crust that has been interpreted to be stretched continental lithosphere (Operto and Charvis, 1995, 1996). In contrast, no compelling geochemical evidence supports a continental lithosphere component in lavas from the Ninetyeast Ridge and the Kerguelen Archipelago (Frey et al., 1991; Weis et al., 1993, 1998; Frey and Weis, 1995, 1996; Yang et al., 1998), but such a component is present in the Big Ben basaltic series on Heard Island (Barling et al., 1994) (Figs. **F9, F11A, F12**) and in mantle xenoliths found in Kerguelen Archipelago lavas (Hassler and Shimizu, 1998; Mattelli et al., 1999). Determination of the spatial and temporal role of continental lithosphere components in the Kerguelen Plateau–Broken Ridge LIP is required to evaluate whether these continental components are a piece of Gondwana lithosphere that was incorporated into the plume.

Relatively shallow basement holes (>100 m) in the Kerguelen Plateau and Broken Ridge can be used to define spatial and short-term variability in the geochemical characteristics of the lavas erupted during the waning phase of plateau volcanism. A surprising result of previous drilling (Legs 119 and 120) on the Kerguelen Plateau is that sampling of the uppermost 35 to 50 m of igneous basement at several plateau sites shows that lavas at each site have distinctive geochemical characteristics (e.g., basalts from each site have a distinct combination of Sr and Nd isotope ratios [Fig. **F9**] and incompatible element abundance ratios, such as Ti/Zr [Fig. **F13**]). The latter ratio is useful because it can be precisely determined by the shipboard X-ray fluorescence (XRF) spectrometer. In many continental flood basalts, relatively low Ti/Zr is diagnostic of significant contamination by continental crust (e.g., the Bunbury and Rajmahal Basalts; Frey et al., 1996; Kent et al., 1997). In summary, we sought to determine whether the geochemical heterogeneity of basalts from different domains of the Kerguelen Plateau and Broken Ridge reflect spatial and temporal heterogeneities in a plume or localized differences in mixing proportions of components derived from asthenosphere, plume, and slivers of continental lithosphere. Answering this question requires knowledge of temporal variations in geochemical characteristics at several locations within this LIP. Preliminary data relevant to these questions are provided by shipboard geochemical results.

F13. Ti/Zr vs. MgO for basalts from Broken Ridge and the Kerguelen Plateau, **p. 64.**

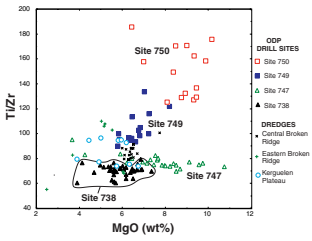

These topics are also the main focus of postcruise geochemical and isotope studies.

Environmental Impact

A major goal of Leg 183 was to address the environmental impact of the formation of the Kerguelen Plateau and Broken Ridge. Important goals for this assessment are to (1) define postmagmatic compositional changes resulting from interaction of magmas with the surficial environment, (2) determine the relative roles of submarine and subaerial volcanism in constructing the upper part of the plateau, (3) estimate volatile contents of magmas from compositional studies of phenocrysts and their inclusions, and (4) evaluate the extent of degassing by determining the abundance and distribution of vesicles. The study of altered and metamorphosed basement rocks will be a major source for this information, but overlying sediments will also provide important data (e.g., the presence of terrestrial and terrigenous sedimentary components, as at Site 750, establishes an important role for subaerial volcanism). For subaerial eruptions, the input of volcanic gases into the atmosphere is controlled by the volatile content of the magmas and eruption rate. For submarine eruptions, it is essential to determine if hydrothermal systems developed that were significant in controlling local, regional, and global elemental and isotope fluxes. Our overall goal was to assess the environmental impact of the Kerguelen/Broken Ridge LIP by estimating fluxes of elements, volatiles, particulates, and heat into the atmosphere-hydrosphere-biosphere system.

Tectonic History

To understand relationships between tectonism and LIP magmatism, we will study the seismic volcanostratigraphy of the Kerguelen Plateau and Broken Ridge by linking seismic facies analysis with petrophysics, borehole data, and synthetic seismic modeling. We will determine stratigraphic and structural relationships both within the various Kerguelen Plateau domains and Broken Ridge and between these features and adjacent oceanic crust. Seismic volcanostratigraphic studies can reveal temporal and spatial patterns of LIP extrusion in a regional tectonic framework, as well as test for synchronous or asynchronous postemplacement tectonism of the Kerguelen Plateau, Broken Ridge, and adjacent ocean basins. Knowledge of the uplift and subsidence histories of the Kerguelen Plateau and Broken Ridge will provide much-needed boundary conditions for models of mantle upwelling, crustal thinning, crustal growth, and postconstructional subsidence and faulting.

Observations of physical volcanology, such as (1) flow thicknesses and directions, (2) flow morphologies, (3) relative thickness of marginal breccia zones and massive interiors of flows, (4) vesicle distribution within flows, (5) the presence and nature of interbeds, and (6) evidence for subaerial vs. submarine extrusion, will provide important information on eruption parameters and the distribution of melt conduits. In addition, physical volcanological observations coupled with shipboard measurements of physical properties and downhole logging data will provide ground truth for seismic volcanostratigraphy. We seek to determine the types of eruptive activity that formed the volcanic rocks and sediments of the Kerguelen Plateau and Broken Ridge. This includes distinguishing between subaerial and subaqueous eruptions, for example,

by recognizing oxidized crusts on lava flow surfaces and analysis of intercalated soils developed on flow tops. In conjunction with seismic volcanostratigraphic studies, we will attempt to identify surficial and shallow subsurficial sources for the basalts (discrete volcanoes or feeder dikes) and to assess the effects of preexisting bathymetry and topography on flow distribution.

DRILLING STRATEGY

LIPs are enormous constructions that present considerable challenges for adequate sampling to address the major questions outlined in the preceding sections. Our knowledge of oceanic Cretaceous LIPs is rudimentary, similar, perhaps, to that of mid-ocean ridges before the general acceptance of the plate tectonics paradigm in the late 1960s. Geophysical surveys and a grid of shallow (100 to 200 m) basement drill holes are necessary to address Cretaceous mantle dynamics, the physical and chemical processes involved in construction of these LIPs, and their environmental consequences. Understanding the temporal and compositional history of the Kerguelen Plateau and Broken Ridge requires a multifaceted drilling strategy (Fig. **F14**), including (1) transects of shallow basement holes across the surface of the LIP; (2) offset drilling in tectonic windows that expose deeper levels of the LIP that are otherwise inaccessible; (3) intermediate (1000–2000 m) and deep (>2000 m) basement holes at carefully chosen locations; and (4) reference holes on older adjacent oceanic crust. Leg 183, complemented by Legs 119 and 120, is part of the fundamental and necessary reconnaissance phase of sampling. To obtain a comprehensive database of eruption ages and lava compositions for the entire LIP, we sampled igneous basement to depths of ~30 to ~230 m at as many morphologically and tectonically distinct regions of the Kerguelen Plateau–Broken Ridge LIP as possible during one drilling leg (Table **T1;** Figs. **F3, F4, F5, F6, F15**). In addition, the sedimentary section immediately overlying the basement provides estimates of minimum ages for extrusive basement, important information regarding eruption and weathering in a subaerial vs. submarine environment, and evidence for tectonic events in the plateau's history. Neogene to Cretaceous sediments overlying basement also provided significant paleoceanographic information for high southern latitudes. At some sites, tephra horizons of various ages provide information on explosive eruptions at nearby islands (McDonald, Heard, and Kerguelen Archipelago) and perhaps more distant volcanoes.

F14. LIP drilling strategies, **p. 65.**

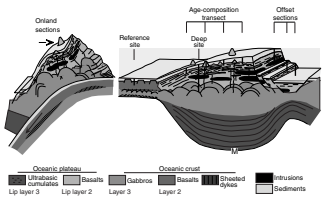

T1. Leg 183 drill sites, locations, water depths, subseafloor penetration, recovery, and age, **p. 101**.

F15. Summary of drill sites on the Kerguelen Plateau and Broken Ridge that recovered volcanic rocks, **p. 66.**

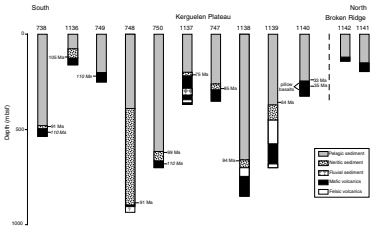

PRINCIPAL RESULTS

Sites 1135 and 1136

Sites 1135 and 1136 (water depths of 1567 and 1931 m, respectively) are on the southern Kerguelen Plateau, approximately midway between two ODP Sites (738 and 750) where basaltic basement has previously been recovered. Sites 1135 and 1136 are ~350 km north of Leg 119 Site 738 and 300 km south of Leg 120 Site 750 (Figs. **F3, F4**). Major objectives of drilling on the southern Kerguelen Plateau were to obtain 150 m of igneous basement to characterize the age, petrography, and compositions of the lavas, the physical characteristics of the lava flows, and

the environment of the eruption (subaerial or submarine). A specific goal was to evaluate the areal extent of the continental lithosphere component that has been recognized in the Site 738 lavas using trace element and isotope geochemistry; such a component is not present in the more northerly Site 750 lavas (Figs. **F9, F10, F11, F12, F13**). Sedimentary objectives at Sites 1135 and 1136 were to determine sequence facies, to define the ages of seismic sequence boundaries, to estimate the duration of possible subaerial and shallow-marine environments, and to obtain minimum estimates for basement age. Hole instability forced us to abandon Site 1135 after drilling to ~70 m above acoustic basement (Fig. **F16**), but we were able to accomplish some of our basement-oriented objectives at Site 1136 (Fig. **F17**), located ~30 km east of Site 1135. In particular, we penetrated 33.3 m of basaltic basement that included three flows; two are apparently inflated pahoehoe flows characterized by massive, relatively unaltered interiors. These rocks provide excellent samples for radiometric dating and geochemical analyses.

The 526-m-thick upper Pliocene to Upper Cretaceous sedimentary sequence recovered at Site 1135 is almost entirely pelagic calcareous ooze and chalk (Fig. **F18**). Compressional wave velocities increase gradually with depth, from 1510 to 1780 m/s in the ooze and from 2000 to 2800 m/s in consolidated chalks. Porosity decreases from 62% to 55% in the ooze and from 55% to 36% in the chalk. Grain density varies little downhole, averaging 2.7 g/cm^3. Chert nodules are common from ~140 m below seafloor (mbsf) to the bottom of the hole. We recovered an expanded (238 m thick) middle Eocene to latest Paleocene nannofossil ooze section, an interval not well represented during previous coring on the Kerguelen Plateau or elsewhere in the Southern Ocean at these high latitudes (~60°S). The study of this section will improve high-latitude biostratigraphic correlations. Furthermore, a Cretaceous/Tertiary boundary section at ~260 mbsf is possibly marked by a bed of light greenish gray calcareous clay with an irregular upper contact and scattered well-rounded clasts of white nannofossil ooze. These features suggest an erosional or mass-wasting event. We have tentatively identified Chron C29n above and Chron C29r below the boundary, respectively. Near the boundary, velocity, magnetic susceptibility, and natural gamma-ray intensity change significantly; in addition, water content, porosity, and carbonate content decrease below the boundary. Sedimentation rates were high in the Paleogene ooze (as much as 15 m/m.y.) and Cretaceous chalks (8–10 m/m.y.); the Paleocene section, however, is abbreviated by hiatuses.

The 128-m-thick sedimentary sequence recovered at Site 1136 (Fig. **F19**) includes an expanded upper lower Eocene to lower middle Eocene section of pelagic calcareous ooze and chalk (Unit II) that is not well represented in other drill holes on the Kerguelen Plateau or in any other southern high-latitude sites. Study of these sediments will refine high-latitude middle Eocene biostratigraphic zonations. Porosity averages 56.2% in Unit II, and compressional wave velocities are typically <1800 m/s. Grain density averages 2.70 g/cm^3. Underlying these pelagic sediments is calcareous zeolitic volcanic clayey sand (Unit IV), probably deposited in a high-energy neritic (shelf) environment, and a carbonate-bearing zeolitic silty clay (Unit V). Fossil debris in Unit V is common and suggests deposition at shallow paleodepths (upper bathyal to outer neritic) in more tranquil conditions than prevailed during deposition of the overlying clayey sand. The sands and clays overlying basement basalt contain sparse but relatively well-preserved micro- and nannofossil faunas of middle Albian age, thereby providing a minimum

F16. *Rig Seismic* RS180/201 multichannel seismic profile across Site 1135, **p. 67.**

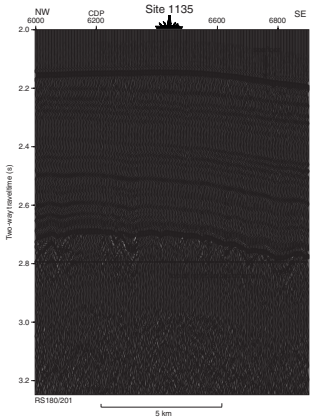

F17. *Marion Dufresne* MD47/10 multichannel seismic profile across Site 1136, **p. 68.**

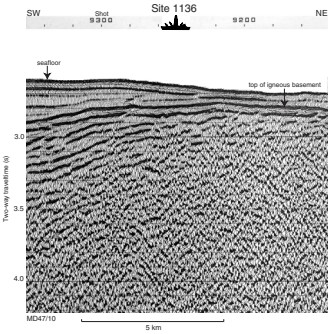

F18. Composite stratigraphic section for Site 1135, **p. 69.**

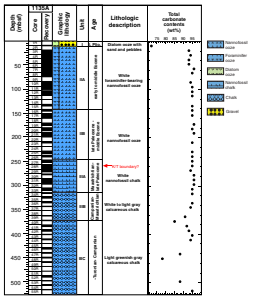

age for the unit and underlying basalts of ~105–107 Ma. Albian marine sediments were not recovered during previous drilling on the Kerguelen Plateau, but microfossils in the sands and clays recovered in Hole 1136A resemble those from Albian sediment drilled on the Falkland Plateau. The sands and clays may correspond to nonmarine, palynomorph-bearing Albian sediment found in silt and claystone cored at Site 750 on the SKP. Albian and Late Cretaceous nannoplankton, foraminifers, and pollen assemblages will provide information on regional paleoceanographic conditions during those times. The epiclastic succession (Units IV and V) and overlying calcareous sediments reflect increasing water depths with time concomitant with a decreasing volcaniclastic component in the sediments. Basaltic volcanic components in the epiclastic sediments at this site are probably derived from erosion of the basaltic plateau.

At Site 1136, from 128.1 to 161.4 mbsf, we cored three normally magnetized tholeiitic basalt flows (55% recovery; Fig. F19). We infer that the vesicular tops of the two upper flows were not recovered. With increasing depth, basalt from the uppermost flow (6.2 m recovered from an ~10-m-thick flow) changes from a moderately altered, massive interior to a fine-grained, vesicle-rich (~10% clay-filled vesicles) and oxidized base. Horizontal vesicle sheets and the distribution of vesicles within the massive interior and lower crust of the upper flow suggest that it formed as an inflated pahoehoe flow. Basalt from the middle flow (13.3 m recovered from an ~20-m-thick flow) varies downward from a massive interior to a fine-grained, vesicle-rich (10%–15%) base. This flow is also probably an inflated, large-volume pahoehoe flow. We only recovered 53 cm of a vesicular basaltic breccia that forms the rubbly flow top of the lower flow. Although we cannot unambiguously determine the eruption environment of these flows, the inference that they are inflated pahoehoe flows and the absence of features indicating submarine volcanism (e.g., pillows and quenched glassy margins) suggest subaerial eruption.

All lavas are sparsely to moderately phyric basalts containing phenocrysts of plagioclase with lesser amounts of clinopyroxene and olivine. Phenocrysts are found as either isolated grains or as two texturally distinct types of glomerocrysts. Corroded plagioclase cores in one glomerocryst type resemble those in small (~1 cm) microgabbro xenoliths. Vesicle-rich segregations (1–2 cm wide) contain 10%–30% vesicles in a nonporphyritic, fine- to medium-grained matrix rich in glass and titanomagnetite. The basaltic rocks are slightly to completely altered to low temperature secondary phases that partly replace primary minerals, completely replace mesostasis, fill veins, and partly to completely fill vesicles. The most common secondary minerals are clays (Mg-saponite and celadonite), calcite, and zeolites. In general, clay minerals abound at all depths, whereas the abundances of calcite and zeolites exhibit more pronounced downhole variations. The wide variation of K and Rb contents in the lavas analyzed by XRF reflects formation of these secondary phases.

The four least altered samples (loss on ignition [LOI] = 0.9 to 2.1 wt%) from the upper and middle flows have 50.0–51.0 wt% SiO_2, 6.4–6.7 wt% MgO, and 1.60–1.76 wt% TiO_2. Both flows are quartz normative tholeiitic basalts (Fig. F20) with relatively low MgO and Ni contents and low Mg numbers; they are similar to basement rocks from other parts of the Kerguelen Plateau. In detail, the upper flow has marginally lower Ti, Nb, Zr, Y, and Ce, distinctly lower V, and higher Cr abundances than the middle flow. Primitive mantle–normalized abun-

F19. Composite stratigraphic section for Site 1136, p. 70.

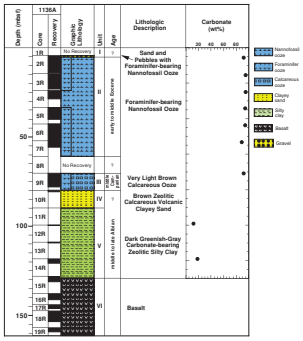

F20. Compositions of volcanic rocks from Sites 1136, 1137, 1138, and 1140, p. 71.

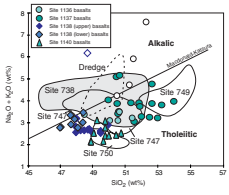

dances of highly incompatible trace elements (Ba, Nb, and Ce) are only slightly greater than those of less incompatible elements (Ti and Y). Site 1136 lavas do not have the anomalously low Nb/Ce and high Zr/Ti ratios that have been used in conjunction with isotope data to infer a continental lithospheric component in basalt from Site 738 on the southern plateau (Fig. F21). In many geochemical characteristics, Site 1136 lavas are similar to the low Al_2O_3 group at Site 749 (Storey et al., 1992). No evidence indicates that these lavas contain a component derived from continental lithosphere.

Major results of drilling at Sites 1135 and 1136 on the SKP include the following:

1. Expanded middle Eocene to uppermost Paleocene (Site 1135) and upper lower Eocene to lower middle Eocene (Site 1136) pelagic calcareous sediment sections not previously recovered at any Southern Ocean sites, which will improve our understanding of high-latitude paleoceanography at critical times of Paleogene cooling as well as aid high-latitude biostratigraphic correlations.
2. Albian and Late Cretaceous nannoplankton, foraminifers, and pollen assemblages, which will provide information on regional paleoceanographic conditions during those times of high relative sea level and high global temperatures.
3. Paleoenvironments of volcanic rock and overlying sediment range from subaerial (basalt) to neritic (clay and sand) to pelagic (chalk and ooze), documenting subsidence of the Kerguelen Plateau since Early Cretaceous time.
4. The >105-Ma basement basalts at Site 1136 are 10- to 20-m-thick inflated pahoehoe flows similar to continental flood basalts, such as the Columbia River Basalt; there is no geochemical evidence for the continental lithosphere component present in Site 738 basalts.

F21. Mantle-normalized $(Nb/Ce)_N$, $(Zr/Ti)_N$, and $(Nb/Zr)_N$ vs. $(Zr/Y)_N$ ratio or Zr content, p. 72.

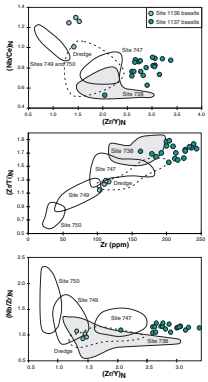

Site 1137

Site 1137 lies on Elan Bank, a large western salient of the main Kerguelen Plateau, at a water depth of 1004 m (Figs. F3, F4). Elan Bank, flanked on three sides by oceanic crust of the Enderby Basin, had not been sampled before our drilling at Site 1137; therefore, the age and geochemistry of its igneous crust, as well as its relationship to the contiguous central and southern Kerguelen Plateau, were completely unknown. Site 1137 lies on the eastern portion of the crest of Elan Bank; we chose the location as representative of the entire Elan Bank on the basis of its relatively simple structural setting, thin sedimentary section, and the presence of intrabasement seismic reflections (Fig. F22). The major objective at Site 1137 was to obtain igneous basement to characterize the age, petrography, and compositions of the lavas, the physical characteristics of the lava flows, and the environment of eruption (subaerial or submarine). We were especially interested in constraining the age of the uppermost igneous basement at Elan Bank for comparison with the proposed ~110 and ~85 Ma volcanic pulses on the southern and central Kerguelen Plateau, respectively (Fig. F7). Sedimentary objectives at Site 1137 were to determine sequence facies, to define the ages of seismic sequence boundaries, to estimate the duration of possible subaerial and shallow-marine environments, to obtain minimum estimates for basement age, and to determine the paleoceanographic his-

F22. *Rig Seismic* RS179/601 multichannel seismic profile across Site 1137, p. 73.

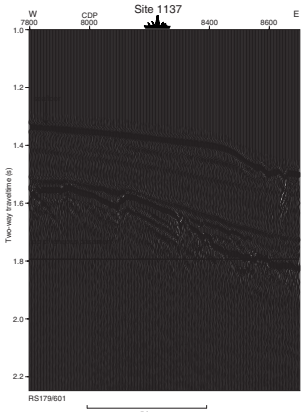

tory of this high-latitude site. As discussed below, we largely achieved our goals at Site 1137. We cored basaltic basement and interbedded sediment from 219.5 to 371.2 mbsf. One of the most significant and unexpected results of the leg was the discovery of garnet gneiss clasts in a fluvial conglomerate interbedded with basaltic basement at this site. This provides unequivocal evidence of continental crust in Elan Bank. In addition, the geochemical characteristics of these basalts clearly indicate a continental crustal component.

We recognize three sedimentary lithologic units (I–III) in the upper 219.5 mbsf (Fig. **F23**). They rest unconformably on basaltic basement (Unit IV). Unit I (0–9.5 mbsf) consists of Pleistocene foraminifer-bearing diatom ooze with interpreted ice-rafted sand and pebbles. Unit II (9.5–199.5 mbsf) is Miocene to uppermost Eocene white nannofossil ooze with rare chert. Some intervals contain diatoms or foraminifers. Units I and II represent marine pelagic deposition and are characterized by compressional wave velocities of 1564 to 1785 m/s that show little scatter. Porosity in the upper two units clusters between 50% and 63%. Unit III (199.5–219.5 mbsf) is a 20-m-thick sequence of glauconite-bearing sandy packstone with abundant shell fragments that was probably deposited in a neritic environment. In the core overlying basaltic basement, the packstone contains well-preserved upper Campanian (72–76 Ma) foraminifers, calcareous nannofossils, and dinoflagellates. Compressional wave velocities in Unit III vary considerably from 3120 and 4340 m/s, and porosity, which ranges between 4.7% and 24.9%, averages 11.7%. Natural gamma-ray intensities are relatively high in the glauconitic sand.

Basalt and interbedded volcaniclastic sediment comprise the 151.7-m basement sequence in Hole 1137A (Unit IV; 219.5–371.2 mbsf), which we subdivide into basement Units 1–10 (Fig. **F23**). The 10 units include seven basaltic lava flows, totaling ~90 m in thickness, and three sedimentary/volcaniclastic units. All basement units are clearly distinguishable in downhole logging data. Relatively good core recovery and high quality logs enable us to constrain true thicknesses of the basement units through core-log integration. All basalts are normally magnetized; in light of biostratigraphic ages in Unit III and thickening of this unit to the east, the basalts likely acquired their magnetization during the long Cretaceous Normal Superchron prior to 83 Ma. Inclinations after thermal demagnetization of basalts from the seven flows range from –55° to –72°, with a mean of –66°. We calculate a paleolatitude of ~48°S, which is 8.5° north of Site 1137. Compressional wave velocities in basement rocks range from 2648 to 6565 m/s, averaging ~4650 m/s. Velocities within lava flows correlate inversely with the degree of alteration estimated from visual inspection.

The excellent core recovery and logging data show that the seven basaltic flows were temporally distinct subaerial eruptions. The flows show oxidation zones and morphologies consistent with subaerial emplacement. The flows are 7 to 27 m thick, and we recovered three flow-top breccias, a pahoehoe surface, and two basal contacts where lava apparently baked the underlying units. Flow-top breccias appear to have formed by breaking up of small pahoehoe-like fingers that are repeatedly intruded into older breccia. This style of autobrecciation is atypical of pahoehoe, aa, or Hawaiian transitional lava flows, but is common in western United States flood basalts. The three (or possibly four) pahoehoe flows in Hole 1137A are inflated; morphologically, they resemble large-volume lava flows forming continental flood basalts. Multiple horizontal vesicular zones within the 27-m-thick flow suggest a compli-

F23. Composite stratigraphic section for Site 1137, **p. 74.**

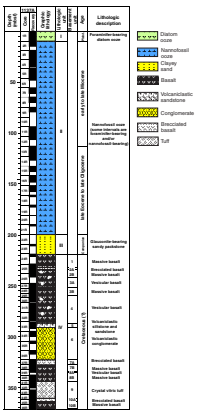

cated inflation history of perhaps four separate pulses of lava. Sediments intercalated with the lowermost flow top breccia indicate that either the lava intruded a small volume of wet sediment or that the flow top was reworked by sedimentary processes.

Basement Units 1–4 are aphyric to moderately plagioclase ± clinopyroxene ± olivine-phyric basalt, whereas Units 7, 8, and 10 are moderately to highly plagioclase ± clinopyroxene-phyric basalt. Like all other Cretaceous basement basalt recovered from the Kerguelen Plateau, Site 1137 basalts are tholeiitic to transitional in composition (Fig. **F20**); they have 50.4 to 52.7 wt% SiO_2 and 4.4 to 7.3 wt% MgO. However, abundances of incompatible minor and trace elements (Fig. **F24**), as well as the ratio of more incompatible to less incompatible elements (e.g., Zr/Y; see Fig. **F21**), are higher than in other Cretaceous basement tholeiites recovered from the plateau. Consequently, Site 1137 basalts form a distinct geochemical group that may reflect a relatively lower extent of melting or a source more enriched in incompatible elements. A continental lithospheric component, probably crust, in Site 1137 basalts is indicated by their relatively low Nb/Ce and high Zr/Ti ratios, as well as their trend in Nb/Y vs. Zr/Y (Figs. **F21, F25**). Such a component is also present in Kerguelen Plateau basalts from Sites 738 and 747, but not in basalts from Sites 749, 750, and 1136 (Figs. **F21, F25**).

Lava flow interiors at Site 1137, as at Site 1136, are relatively unaltered compared to Cretaceous basement lavas previously recovered from the Kerguelen Plateau. For example, LOI for least-altered samples is <2.2 wt% and averages 1.2 wt%. The mobility of Rb and K during postmagmatic alteration shows in the poor correlation of Rb and Nb abundances (Fig. **F24**) and the wide abundance range of K and Rb compared to other incompatible elements (Fig. **F26**). Basement rocks vary from slightly to completely altered with low-temperature secondary phases replacing primary minerals and mesostasis and filling veins, fractures, and vesicles. Clay minerals are the dominant secondary minerals in all basement units. More permeable horizons (such as brecciated and/or vesicular flow tops and bases, and zones with high vein and fracture densities) exhibit higher degrees of alteration and more diverse secondary phases that include calcite, zeolite, quartz, and amorphous silica. In downhole logs, highly altered flow tops are characterized by higher potassium content caused by the increased abundance of clay minerals. Alteration of Hole 1137A lavas likely results from both weathering and low-temperature alteration. Unlike postmagmatic submarine alteration of typical oceanic crust, subaerial weathering and low-temperature interaction of basalts and interbedded sediments with groundwater at Site 1137 preceded submarine alteration.

Basement Units 5, 6, and 9 consist of volcaniclastic sedimentary rocks. Basement Unit 5 (286.7–291.0 mbsf) is a succession of interbedded crystal-lithic volcanic siltstones and sandstones. Many beds are normally graded, and others show parallel laminations. These sediments overlie the volcanic conglomerate of basement Unit 6 (291.0–317.2 mbsf). Clasts in the conglomerate range from well-rounded granules to small boulders. Most intervals are clast supported, but matrix-supported intervals also are present. The depositional environment of basement Units 5 and 6 appears fluvial, perhaps associated with a braided river. These units represent a significant hiatus of unknown duration between eruptions of basaltic flow Units 1–4 and 7 and 8. Furthermore, fluvial facies of Units 5 and 6 corroborate our interpretation of subaerial lava effusion.

F24. Incompatible trace element compositions of basalts from Sites 1136 and 1137, **p. 75.**

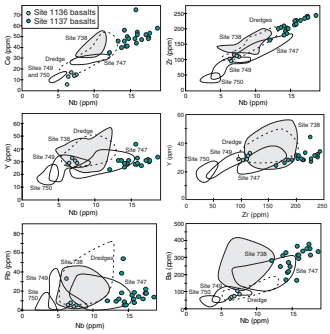

F25. Nb/Y vs. Zr/Y for Kerguelen Plateau basement basalt from Sites 738, 747, 749, 750, 1136, and 1137, **p. 76.**

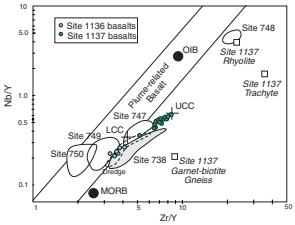

F26. Trace element contents of basalts from Site 1137, **p. 77.**

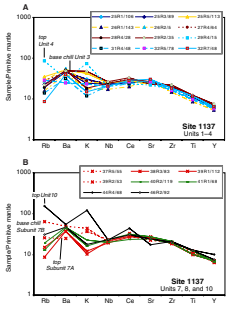

Diverse clasts within the conglomerate (Unit 6), and to a lesser extent similar lithic clasts within the underlying crystal-vitric tuff (Unit 9), constitute a greater variety of rock types than usually recovered from a single drill hole into igneous basement. In particular, the predominant clast lithologies in Units 6 and 9 include porphyritic trachyte, flow-banded rhyolite, plagioclase phyric basalt, and a variety of small, highly altered, sparsely phyric and aphyric basalts. The most unexpected clasts, however, are rounded cobbles of garnet-biotite-gneiss and granitoid. We also find single grains of garnet and perthitic alkali feldspar, presumably weathered from sources similar to those of the gneiss and granitoid cobbles, in the sand fraction of Unit 5 and as xenocrysts in parts of the Unit 9 crystal-vitric tuff. It is difficult to imagine anything but an originally continental source for such material.

Basement Unit 9 (344.0–360.7 mbsf) consists of altered crystal-vitric tuff composed of ~40% coarse (1–2 mm) angular crystals of sanidine and quartz and <5% lithic clasts enclosed within a light to dark green dense matrix. Cuspate and tricuspate glass shards, now partially to completely altered to clay minerals, and sanidine and less abundant quartz phenocrysts (<5 mm) are the principal components of the tuff; minor components include amphibole, plagioclase, and opaques. Broken bubble-wall shards and abundant embayed and broken crystals indicate that the tuff formed in an explosive volcanic eruption. Suspended within the tuff are 1%–2% subangular to rounded, granule- to pebble-sized lithic clasts of varying lithologies, dominantly basalt. The coarse grain size of both the enclosed pebbles and the primary sanidine and quartz crystals precludes formation of this unit as a primary air-fall deposit. Although a pyroclastic flow is a possible emplacement mechanism, we infer that the material was reworked because of the absence of (1) internal stratification, (2) a basal breccia or fine flow top, or (3) normal grading of lithics and crystals. The even distribution of crystals and pebbles throughout the tuff and the massive internal texture of the deposit strongly suggest mass flow redeposition of these sediments to their present locations. Small fault zones with offsets of ≤5 cm are highly altered and contain locally abundant (≤5%) pyrite and possibly chlorite. Native copper surrounds lithic fragments in more intense alteration zones (<1 cm wide).

In summary, significant results bearing on the origin and evolution of Elan Bank include the following:

1. Subsidence of the Kerguelen Plateau is recorded by the paleoenvironments of volcanic rocks and sediment that range from subaerial or fluvial (basalt and interbedded sediment) to neritic (packstone) to pelagic (ooze).
2. The volcanic conglomerate contains clasts of trachyte, rhyolite, granitoid, and garnet-biotite gneiss; the garnet-biotite gneiss, in particular, indicates continental crust at this south Indian Ocean location.
3. The sanidine-quartz-bearing crystal-vitric tuff, as well as the trachyte and rhyolite clasts in the conglomerate, indicates that highly evolved magmas erupted, in some cases explosively, during the final stages of the volcanism that formed Elan Bank.
4. The seven basement flows erupted in a subaerial environment. These inflated pahoehoe and transitional rubbly flows are typical of continental flood basalts, such as the Columbia River Basalt.

5. Like other Cretaceous igneous basement rocks of the Kerguelen Plateau, the seven basement lava flows are tholeiitic to transitional basalts; however, Site 1137 basalts are more enriched in incompatible elements, perhaps a result of lower extents of partial melting or derivation from a source more enriched in incompatible elements. Also, we infer a continental crust component in Site 1137 basalts from their less-than-primitive mantle ratios of Nb/Ce and Zr/Ti and their Nb/Y vs. Zr/Y trends.

Site 1138

Site 1138 lies on the CKP ~150 km north-northwest of Site 747 (Leg 120) and 180 km east-southeast of Heard Island (Figs. F3, F4). In the vicinity of Site 1138, geological structure and seismic stratigraphy are relatively simple, and interpreted igneous basement contains some internal reflections (Fig. F27). Basalts at Site 747 erupted at ~85–88 Ma, as determined from $^{40}Ar/^{39}Ar$ data and from the biostratigraphy of the overlying sediments. In contrast, Heard Island is dominated by Quaternary volcanism. A major objective at Site 1138 was to determine if the uppermost basaltic crust of the CKP is ~85 Ma at more than one location. Also, geochemical characteristics of Site 747 basalts indicate a continental crust component, possibly Archean granulite, which differs from the continental component in basalt from the SKP at Site 738. During continental breakup, continental lithosphere along the conjugate Antarctic and Indian margins may have been fragmented and incorporated into embryonic Indian Ocean mantle. Subsequently, in localized areas this continental material may have interacted with basaltic magmas forming the Kerguelen Plateau. Therefore, we were especially interested in comparing the petrology and geochemistry of basaltic basement from this second CKP drill site with basalt from the southern, northern, and Elan Bank domains, as well as Heard Island and the Kerguelen Archipelago. Additional basement objectives were to determine the physical characteristics of the lava flows and the environment of the eruption (subaerial or submarine). The sedimentary objectives at Site 1138 were to determine sequence facies, to define the ages of seismic sequence boundaries, to estimate the duration of possible subaerial and shallow-marine environments, to obtain minimum estimates for basement age, and to determine the paleoceanographic history of the CKP. At Site 1138 our objectives were achieved by coring ~144 m of volcanic basement and ~698 m of overlying sediment.

We recovered Upper Cretaceous through Pleistocene sediment from the upper 698 mbsf of Hole 1138A, whereas the lower 144 m of the hole yielded multiple ~5-m-thick basalt flows overlain by volcaniclastic and minor sedimentary rocks (Fig. F28). We recognized seven lithologic units in Hole 1138A; Units I–VI are sedimentary rocks resting unconformably on the volcanic basement (Unit VII). The upper 650 m of sediment is biosiliceous and carbonate pelagic ooze, of which the top 110-m section comprises a relatively complete and expanded sequence of Quaternary and Pliocene biosiliceous sediments. The lower ~50 m of the sedimentary section consists of Upper Cretaceous shallow-marine and terrestrial sediments.

Unit I (0–112.0 mbsf) consists of foraminifer-bearing diatom clay with interbedded foraminifer-bearing diatom ooze in the upper portion. We found a few thin volcanic ash layers in this upper Pleistocene to upper Miocene unit. Grain density averages 2.38 g/cm^3; porosity, 77%; and compressional wave velocity, 1568 m/s in Unit I.

F27. *Rig Seismic* RS179/101 multichannel seismic profile across Site 1138, p. 78.

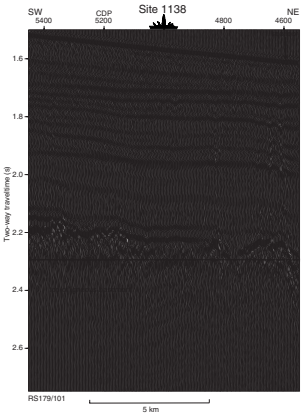

F28. Composite stratigraphic section for Site 1138, p. 79.

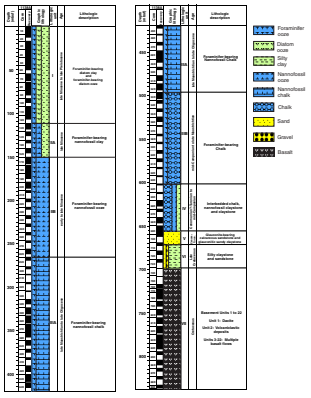

Unit II (112.0–265.9 mbsf) is composed of foraminifer-bearing nannofossil clay (Subunit IIA) that overlies foraminifer-bearing nannofossil ooze (Subunit IIB). The carbonate/silica ratio of the 153.9-m-thick Miocene Unit II is much higher than that of Unit I. Volcanic material is disseminated in the sediment as well as in rare distinct tephra layers. In Unit II, grain density averages 2.61 g/cm^3, porosity 60%, and compressional wave velocity 1672 m/s. Unit III (265.9–601.8 mbsf) is late Oligocene to mid-Campanian in age. It consists of foraminifer-bearing chalk and contains scattered chert nodules in its lower part. Cyclic color variations (white to greenish gray) are common. The Cretaceous/Tertiary boundary near the base of Subunit IIIA (Core 183-1138A-52R) is possibly complete, but lithologies do not change across it. In Unit III, grain density averages 2.70 g/cm^3, porosity averages 48%, and compressional wave velocity averages 2310 m/s.

Unit IV (601.8–655.6 mbsf), of mid-Campanian to Cenomanian(?) age, consists of cyclic alternations of light gray foraminifer-bearing chalk with gray through greenish gray to black intervals of nannofossil claystone. The dark gray to black beds become prominent and increase in clay content in the lower portion. Chert nodules are present in the upper part of the unit. Grain density averages 2.67 g/cm^3, porosity 35%, and compressional wave velocity 2665 m/s. A bed of black, faintly laminated (unburrowed) claystone with high organic carbon content (2.22%) is at the base of Unit IV. Units I through IV represent deep-marine pelagic sedimentation; however, the relatively high clay content of sediments in Unit I and Subunit IIA suggests terrigenous input from overbank flow of turbidity currents moving down a submarine canyon ~45 km west-northwest of Site 1138. The black claystone at the base of Unit IV reflects an oxygen-starved environment that may be the oceanic anoxic event marking the Cenomanian/Turonian boundary.

Unit V (655.57–671.88 mbsf) consists predominantly of glauconitic calcareous sandstone of Turonian–Cenomanian age deposited in a neritic environment. Serpulid worm tubes and large bivalve fragments are common. Grain density averages 2.71 g/cm^3, porosity averages 42%, and compressional wave velocity averages 2719 m/s in Unit V. The gradual transition from neritic oxidized sediment (Unit V) to interbedded black claystone and chalk (Unit IV) to pelagic sediments (Unit III) supports the postulated major transgression causing the Cenomanian–Turonian oceanic anoxic event. This hypothesis will be tested by shore-based studies.

Unit VI (671.88–698.23 mbsf) consists of Upper Cretaceous fossil-rich, dark brown silty claystone with interbedded sandstone of fluvial or shallow-marine origin. The silty claystone contains many wood fragments, possible sporangias, a seed, and fossil spores and pollen. The sandstone beds contain well-rounded pebbles and sand grains of volcanic material. At the bottom of Unit VI, silty claystone rests upon volcanic basement rocks (Unit VII). Large rounded pebbles of weathered basalt close to the base of Unit VI suggest a regolith formed by weathering of volcanic basement. In Unit VI, grain density averages 2.72 g/cm^3, porosity averages 37%, and compressional wave velocity averages 2328 m/s, the latter defining a pronounced velocity inversion from overlying Unit V. The seismic sequence containing the deepest marine sediments cored at Site 1138 thickens to the northeast, suggesting that basaltic basement rocks could be significantly older than the minimum age indicated by biostratigraphy.

We recognize 22 units within the 144 m of igneous basement (Unit VII) drilled at Site 1138 (Fig. **F28**). Basement Unit 1 includes rounded

cobbles of flow-banded, aphyric to sparsely sanidine-phyric dacite. Unit 2 is a complex succession of volcaniclastic rocks overlying basalt lava flows—Units 3 through 22. The 20-m-thick volcaniclastic succession comprising Unit 2 includes six variably oxidized and altered pumice lithic breccias. Our preferred interpretation is that these are minimally reworked and unwelded, subaerial pyroclastic flow deposits. The pumice clasts are typically aphyric, and the bulk composition of a pumice-rich sample is trachytic (Fig. F29). The volcaniclastic sequence also includes pumice beds, reworked volcaniclastic sediments, and highly altered ash deposits that contain accretionary lapilli.

Basement Units 3–22 are ~5-m-thick subaerial basaltic lava flows that range from inflated pahoehoe to classic aa. Several boundaries are oxidized, suggesting subaerial weathering between eruptions. The relatively thin flows at Site 1138 resemble Hawaiian lavas and contrast with the generally thicker flows drilled at Sites 1136 and 1137. Most flows have flow-top breccias that are not easily classified. Some breccias contain slabs of pahoehoe mixed with aa clinker; others are a jumble of pahoehoe lobes. The breccias contain varying amounts of sediment; some appear reworked, most likely in a fluvial environment. Most flows probably erupted on a moderate slope (1° to 4°) under conditions of high shear resulting from a high eruption rate or topographic confinement. Several observations indicate that these are near vent flows: (1) aa and slab pahoehoe flows rarely travel more than a few tens of kilometers from vents; (2) abundant small vesicles indicate that the lavas did not flow far enough for vesicles, which formed at vents, to coalesce; and (3) clasts in some of the welded basal breccias appear to be spatter, which only forms close to vents. There are also suggestions of explosive interaction between the lava and groundwater. The complex relationships between the flows at Site 1138 do not allow us to identify the products of individual eruptions, but the flows and the eruptions that fed them were considerably smaller than for typical continental flood basalts.

All basalts show normal magnetic inclinations. We calculated a mean inclination of –60.8°, which corresponds to a paleolatitude of 46.4°S, assuming a geocentric dipole field. The paleolatitude is thus 7° north of Site 1138. This southward shift in latitude since Late Cretaceous time is consistent with the 8.5° difference we found at Site 1137 on Elan Bank. The basalts have average grain densities of 2.90 g/cm³ (range of 2.44–3.1 g/cm³), porosities of 25% (range of 9%–55%), and compressional wave velocities of 4014 m/s (range of 1884–7491 m/s).

The massive parts of flow Units 3–22 are slightly to locally highly altered, whereas alteration ranges from high to complete in the brecciated zones. Rubbly flow tops are partly to completely altered to clay minerals, and abundant euhedral zeolites form the matrix, fill veins, and partially fill vesicles and large voids. Lava clasts are commonly completely altered to brown clay minerals. Multiple generations of zeolite (clinoptilolite) exhibit many crystal shapes, predominantly equant and prismatic, but fluffy forms frequently fill fissures. Sediment filling breccia void space is variably indurated, perhaps caused by silicification. Calcium carbonate is absent except from the uppermost basalts directly underlying the volcaniclastic sequence.

Most of the basalts are moderately to highly vesicular and aphyric to sparsely plagioclase-phyric tholeiites (Fig. F21, F29). Units 9 and 19 contain clinopyroxene phenocrysts, and Units 5–16 and 19 contain 1%–5% olivine microphenocrysts, now completely replaced by secondary clays. The relatively unaltered (LOI of only 0.5 to 2 wt%) massive parts of these basaltic flows have similar major element compositions

F29. Site 1138 igneous rock compositions in the $Na_2O + K_2O$ vs. SiO_2 classification diagram, p. 80.

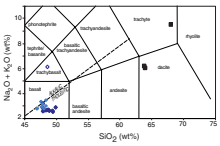

(e.g., MgO contents vary only from 4.5 to 7 wt%). However, with increasing depth, Mg/Fe, Ni, and Cr contents decrease, and abundances of most incompatible elements (Sr is an exception) increase by nearly a factor of two (Fig. F30), thereby defining a trend to Fe- and Ti-rich basalt. This systematic downhole trend is consistent with extensive fractionation of the phenocryst phases, plagioclase, olivine, and clinopyroxene. Basalts from the two drill sites on the CKP (Sites 747 and 1138) overlap in a Nb/Y vs. Zr/Y plot (Fig. F31).

The major results of drilling at Site 1138 on the CKP include

1. Paleoenvironments of the Cenomanian/Turonian boundary event appear to be preserved in the transition from oxidized neritic sediment to black claystone (shale) to pelagic sediment, which may enable testing of the hypothesis that a major transgression caused this oceanic anoxic event.
2. The sedimentary sequence overlying basement contains Upper Cretaceous shallow-marine and terrestrial sediments. Turonian (and older?) silty claystone contains well-preserved wood fragments, a seed, spores, and pollen, documenting for the first time that the CKP was subaerial after volcanism ceased.
3. The inferred minimum basement age, Turonian (89–93 Ma), is older than the 85–88 Ma proposed for Site 747, only 150 km to the southeast.
4. Volcanic growth of the Kerguelen Plateau at this site on the CKP terminated with eruptions of highly evolved magma that include dacitic lavas and pyroclastic flow deposits of trachytic composition.
5. Basaltic basement underlying evolved rocks is represented by ~20 thin, Hawaiian-scale subaerial flows that erupted onto moderate slopes of 1° to 4°. These are tholeiitic basalt flows whose compositions define a systematic downhole trend to Fe- and Ti-rich basalt. Such highly evolved basalts have not been recovered previously from the Kerguelen Plateau; incompatible element abundance ratios, such as Nb/Zr and Nb/Y, of Site 1138 basalts, however, overlap with the field defined by basalts from Site 747, the other drill site on the CKP.

F30. Downhole variations in trace element abundances and abundance ratios for Site 1138 basalts, p. 81.

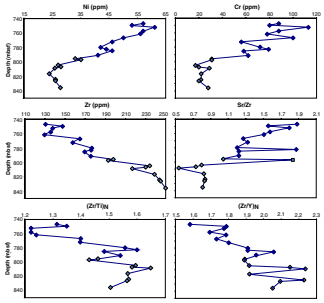

F31. Comparison of Nb/Y vs. Zr/Y plots, p. 82.

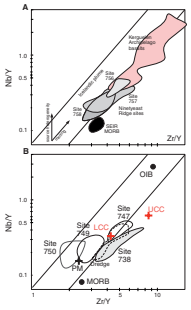

Site 1139

Site 1139 lies on Skiff Bank (Leclaire Rise), a bathymetric and gravimetric high ~350 km west-southwest of the Kerguelen Archipelago (Figs. F3, F4). Flanked to the south and west by Cretaceous oceanic crust of the Enderby Basin, Skiff Bank appears to be structurally related to, and bathymetrically continuous with, the NKP. At least two major faults, however, offset interpreted igneous basement between Skiff Bank and the large massif containing the Kerguelen Archipelago. Skiff Bank has been proposed to be the current site of the Kerguelen hot spot (Figs. F1, F2), but hundreds of meters of sediment on parts of the elevated feature argue against Skiff Bank originating entirely by recent volcanism. Both Skiff Bank and Elan Bank trend east-west, approximately perpendicular to the trends of fracture zones in the Enderby Basin and thus parallel to the axis of breakup between Antarctica and India. The free-air gravity signatures of the two features are also similar; pronounced negative anomalies flank their southern margins, but not their northern margins (Fig. F4). Many rock types, including both aphyric basalt and plutonic rocks such as alkali granite, were recovered in a single

dredge haul from Skiff Bank, quite close to Site 1139 (Weis et al., 1998a). The plutonic rocks were interpreted as ice-rafted debris. Hence, the age and composition of Skiff Bank's igneous crust and its relationship to the contiguous northern Kerguelen Plateau are not established. The NKP is commonly believed to have formed since ~40 Ma, when the SEIR separated Broken Ridge and the CKP (Fig. **F2**), but submarine igneous basement of the NKP has never been drilled.

Site 1139 lies at a depth of 1415 m on Skiff Bank's southwestern terrace, which is >1000 m lower than the crest, located <50 km to the northeast (Fig. **F3**). The top of acoustic basement is flat lying, and basement is overlain by a sediment sequence ~500 m thick (Fig. **F32**). The fault scarp marking the boundary between Skiff Bank and the Enderby Basin lies ~20 km southwest of Site 1139 and offsets the basement by more than 2700 m.

The major objectives at Site 1139 were to obtain igneous basement to characterize the ages, petrography, and compositions of lavas, the physical characteristics of the lava flows, and the environments of eruption (subaerial or submarine). We were especially interested in testing the hypothesis that the age of the uppermost igneous basement at Skiff Bank is <40 Ma. The sedimentary objectives at Site 1139 were to determine sequence facies, to define the ages of seismic sequence boundaries, to estimate the duration of possible subaerial and shallow-marine environments, to obtain minimum estimates for basement age, and to determine the paleoceanographic history of this high latitude site. As discussed below, we largely achieved our goals at Site 1139. We drilled 233 m into igneous basement that is overlain by lower Oligocene shallow-marine sediments.

Sediments were recovered from the upper 462 mbsf of Hole 1139A, whereas extensively altered felsic volcaniclastic rocks and mafic to intermediate composition lava flows were recovered from the lower 233 m of the hole (Fig. **F33**). We recognize six lithologic units. Units I–V are sediment and sedimentary rock resting on volcanic basement (Unit VI). Unit I (0 to 47.5 mbsf) consists of foraminifer-bearing diatom-bearing nannofossil ooze (Subunit IA) of Quaternary age and foraminifer-bearing nannofossil ooze (Subunit IB). Scattered basaltic sand grains and rare pebbles as well as traces of pumice are present in Subunit IA. Unit II (47.5 to 380.7 mbsf) consists of nannofossil-bearing clay and claystone with interbedded nannofossil-bearing ooze and chalk of early late Miocene to mid-Oligocene age. Trace fossils are very common. Unit II records a substantial influx of terrigenous clay from an adjacent volcanic landmass. In Subunit IB and the upper portion of Unit II (to ~107 mbsf) compressional wave velocity averages 1822 m/s, bulk density ranges from 1.5 g/cm^3 to 1.7 g/ cm^3, grain density ranges between 2.6 and 2.8 g/cm^3, and porosity changes from 60% to 74%. Sediments become semilithified by 100–110 mbsf. An unusual nannofossil (*Braarudosphaera*) bloom in late Oligocene time, reported previously on the SKP, may have been synchronous with other occurrences in the Atlantic and Indian Oceans. Minimum sedimentation rates were ~16 m/m.y. in the Miocene and ~20 m/m.y. in the Oligocene. We observed very rare tephra layers and disseminated volcanic ash, locally concentrated in burrows. Chert nodules appear only at the base of Unit II. We correlate normal and reverse magnetic polarities between ~100 and ~380 mbsf to early Miocene to early Oligocene geomagnetic Chrons C5D to C12 (or C13). From 108.9 mbsf to the base of Unit II at 380.7 mbsf, velocities increase linearly with depth, from 1785 to 4331 m/s. Within this depth interval, three volcanic ash layers have high compressional wave veloc-

F32. *Marion Dufresne* MD109-05 multichannel seismic profile across Site 1139, **p. 85.**

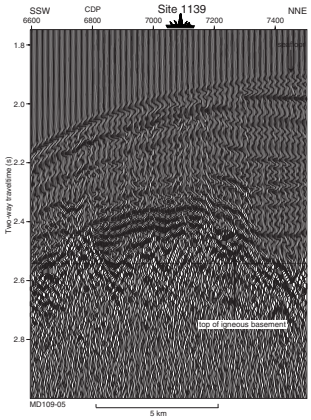

F33. Composite stratigraphic section for Site 1139, **p. 86.**

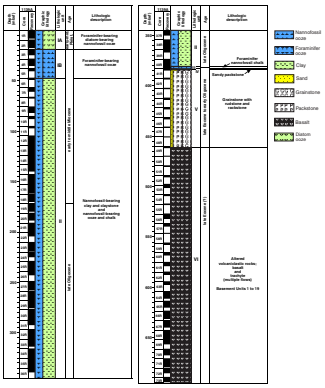

ities. In the same interval, bulk density increases from 1.3 g/cm³ to 2.1 g/cm³ with a mean of 1.7 g/cm³, and porosity decreases from a maximum of 75% to 42%. Grain density maintains a nearly constant value of ~2.8 g/cm³. Unit III (380.7 to 383.5 mbsf) is foraminifer nannofossil chalk of anomalous brownish to reddish yellow color. The compressional wave velocity averages 3616 m/s. Units I–III represent deep-marine pelagic sedimentation. The base of the pelagic section is earliest Oligocene in age.

Unit IV (383.5 to 384.9 mbsf) consists of dusky red to greenish pink sandy packstone with rare planktonic foraminifers and bivalve shell fragments (Fig. F33). Index properties change significantly near the boundary between Units III and IV, from 381.4 to 384.4 mbsf. The bulk density in this zone averages 2.0 g/cm³, grain density averages 2.8 g/cm³, and porosity ranges between ~50% and ~31%. Grains are predominantly highly altered volcanic lithic fragments. Compressional wave velocity averages 3616 m/s. Unit V (384.9 to 461.7 mbsf) consists of interlaminated grainstone and sandstone with some thin interbeds of rudstone and cross-bedded intervals. Bryozoans, bivalves, and echinoids are the major biogenic components. Units IV and V were deposited in a shallow-marine neritic environment in low-energy and very high energy (near shore) settings, respectively. Well-rounded cobbles at the top of the basement suggest a beach deposit at the base of the sedimentary succession.

At Site 1139, we drilled 232.5 m into igneous basement with 37.4% recovery (Fig. F34). We identify 19 basement units; an upper succession of variably welded trachytic to rhyolitic volcanic and volcaniclastic rocks (Units 1–5) is underlain by a series of 14 lava flows (Units 6–19). All basement units are highly altered and fractured. The high degree of alteration and poor core recovery in Units 1–5 make it difficult to identify physical volcanic features and interpret modes of emplacement. However, these units can be distinguished in the natural gamma-ray logs. Rocks in Units 1–5 have compressional wave velocities varying from 2577 to 4770 m/s, with a mean value of 3616 m/s. Their bulk densities average 2.3 g/cm³, grain densities range from 2.6 to 2.9 g/cm³, and porosities average ~25%. The underlying 14 subaerial lava units (Units 6–19) have compressional wave velocities that are typically >3000 m/s, with a mean of 4416 m/s. Bulk densities vary widely, with a mean of 2.4 g/cm³; mean grain density is 2.8 g/cm³ and decreases slightly with depth; and porosity varies widely, from 65% to 3%. All basement units have positive magnetic inclinations, corresponding to reversed polarity.

Unit 1, which had poor recovery (57 m thick; 5.3 m recovered), contains a variety of felsic volcanic and volcaniclastic rocks (Figs. F34). Subunit 1A consists of rounded, massive to flow-banded rhyolite cobbles. Subunit 1B is a thin lens of bioclastic sandstone that resembles the grainstone at the base of the sedimentary section. Beneath this, a thin felsic pumice breccia (Subunit 1C) overlies a zone of altered, perlitic felsic glass that contains lithic fragments (Subunit 1D). We interpret the glassy zone to be the densely welded core of a pyroclastic flow deposit. The base of Subunit 1D is a silicified basal breccia with lithic fragments and pumice. Beneath this are highly sheared and altered, clay-rich volcaniclastic sediments (Subunit 1E) that we interpret as a fault zone. Within Subunits 1C through 1E, both clasts and the matrix commonly display cataclastic fabrics, and slickensides are ubiquitous on broken clay-rich surfaces. Unit 2 (10.5 m thick; 1.35 m recovered) consists of dark red (oxidized) rhyolite with ~10% sanidine and minor quartz phe-

F34. Interpretative summary diagram for Site 1139, p. 87.

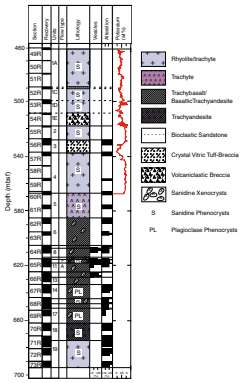

nocrysts. Flattening and agglutination textures suggest that this is a welded pyroclastic flow deposit. Unit 3 (9.7 m thick; 4.6 m recovered) is a green, highly altered crystal-vitric tuff. It contains abundant sanidine phenocrysts, minor quartz, and lithic clasts, in a perlitic glassy matrix that is locally banded. As with Subunit 1C, we interpret Unit 3 to be the densely welded core of a pyroclastic flow deposit. Unit 4 (30.1 m thick; 5.9 m recovered) contains massive to brecciated, dark red (oxidized) rhyolite that is similar to Unit 2. Unit 5 (17.4 m thick; 4.2 m recovered) is highly altered sanidine-phyric trachyte that consists of a massive central zone bounded by a brecciated top and base; this unit is probably a lava flow.

Basement Units 6–17 (65.7 m drilled; 41.4 m recovered) consist of aphyric to sparsely plagioclase-phyric volcanic rocks ranging in composition from trachybasalt to trachyandesite (Fig. F35). We subdivide this sequence on the basis of brecciated zones and vesicularity patterns, but intense alteration commonly precludes identifying contacts between flows. Although defined flow units vary widely in thickness, most flows are ~5 m thick. Unit 10 consists of small pahoehoe lobes, Unit 11 is an aa flow, and the other flow units have brecciated margins of indeterminate character. The breccias are highly altered and sheared, with both matrix and clasts nearly completely altered to clay minerals. Breccia clasts are oxidized and cemented by calcite and siderite(?) as well as clay minerals. The relatively thin massive portions of the flows have many moderately to steeply dipping fractures and pronounced streaks of mesostasis, now altered to green clay minerals. Thin veins, commonly containing carbonate, pervade the basalt units. Rarely, the rock has a pale gray hue, and the groundmass is bleached because of the replacement of igneous minerals by secondary calcite.

Basement Units 18 and 19 are highly to completely altered highly sanidine-phyric trachyandesite and trachyte, respectively. Alteration consists of either intense red hematitic staining or white/pink bleaching. The minerals in the bleached rocks include quartz, sanidine, and siderite. The latter mineral is a common phase that cements groundmass, replaces primary phases, and fills veins and vesicles. The veins within the bleached intervals have prominent red alteration halos (hematite) and are filled with hematite, quartz, siderite, and calcite. The alteration of these rocks probably results from interaction of felsic igneous rocks with large volumes of CO_2-rich fluids in a hydrothermal (subaerial?) system.

Although their compositions were affected by posteruption alteration, the major element compositions of the volcanic and volcaniclastic rocks comprising the basement at Site 1139 clearly form a series from trachybasalt to trachyte and quartz-bearing rhyolite (Fig. F35A). These lavas are significantly more alkaline than the dominantly transitional to tholeiitic basement lavas recovered from all other Kerguelen Plateau drill sites (Fig. F35B). However, with the exception of the rhyolites, the alkaline Skiff Bank lavas are quite similar to alkaline lava series erupted in the Southeast Province of the Kerguelen Archipelago in the early Miocene and again in the Pliocene and Pleistocene (cf. Figs. F8A, F35A).

In summary, significant results bearing on the origin and evolution of Skiff Bank (Site 1139) are

1. Subsidence of the NKP is recorded by the paleoenvironments of volcanic rocks and overlying sediments; since Eocene time, environments have changed from subaerial (volcanic and volcani-

F35. Igneous rock compositions for Site 1139, p. 88.

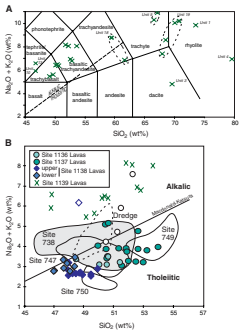

clastic rocks) to intertidal (beach deposits) to very high energy, nearshore (grainstone and sandstone) to low-energy, offshore (packstone) to bathyal pelagic (ooze).
2. The oldest sediments overlying igneous basement are earliest Oligocene; this minimum age for basement is consistent with a <40-Ma age for the uppermost igneous basement of Skiff Bank.
3. The 233 m of igneous basement consists of an uppermost 124-m succession of variably welded trachytic to rhyolitic volcanic and volcaniclastic rocks; in addition, the two lowermost lava flow units comprise 33 m of sanidine-phyric trachyandesite and rhyolite. As at Elan Bank (Site 1137), highly evolved magmas erupted, in some cases explosively, during the final stages of volcanism that formed Skiff Bank.
4. The volcanic basement at Skiff Bank, with a minimum age of earliest Oligocene, includes an alkaline lava series ranging from trachybasalt to trachyte and rhyolite. Similar alkaline lavas have erupted in the Kerguelen Archipelago in Miocene and Pliocene/Pleistocene time; therefore, Skiff Bank, which crests <500 m below sea level, may have been a somewhat older island analogous to the Kerguelen Archipelago 350 km to the east-northeast.

Site 1140

Site 1140 lies on the northernmost Kerguelen Plateau ~270 km north of the Kerguelen Archipelago (Figs. **F3, F4**). Flanked to the north and east by Eocene and younger oceanic crust of the Australian-Antarctic Basin, and to the west by Cretaceous oceanic crust of the Crozet and Enderby basins, the NKP is believed to have formed since 40 Ma via Kerguelen hot spot magmatism (Royer and Sandwell, 1989; Royer and Coffin, 1992). The boundary between the northern Kerguelen Plateau and the Australia-Antarctic Basin lies ~5 km north of Site 1140 and offsets basement by ~400 m.

The Kerguelen Archipelago is part of the NKP; its igneous rocks yield dates from 39 Ma to recent (Nicolaysen et al., 1996, in press). However, submarine igneous basement of the NKP has never been sampled, so its age and composition, as well as its relationship to the central and southern plateau sectors and to Skiff and Elan banks, are unknown. Site 1140 lies at a depth of 2394 m on the northern flank of the NKP. We chose this location as representative of the NKP on the basis of its relatively simple structural setting and thin sedimentary section (Fig. **F36**). The top of acoustic basement is flat lying, and the overlying basement is a sediment sequence ~350 m thick.

The major objectives at Site 1140 were to obtain igneous basement to characterize the ages, petrography, and compositions of the lavas and the environments of eruption (subaerial or submarine). We were especially interested in (1) testing the hypothesis that at least the uppermost igneous basement of the NKP is <40 Ma and (2) comparing the submarine NKP lavas with the subaerial lavas forming the Kerguelen Archipelago. The sedimentary objectives at Site 1140 were to determine sequence facies, to define the ages of seismic sequence boundaries, to estimate the duration of possible subaerial and shallow-marine environments, to obtain minimum estimates for basement age, and to determine the paleoceanographic history of this moderate latitude site. As discussed below, we largely achieved our goals at Site 1140. We drilled 88 m into pillow basalt flows that are intercalated with thin chalk beds containing late Eocene nannofossils and foraminifers.

F36. *Marion Dufresne* MD109-06 multichannel seismic profile across Site 1140, **p. 89.**

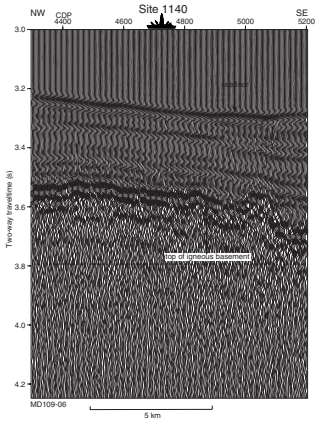

The sedimentary section above igneous basement consists entirely of pelagic ooze and chalk and appears to rest unconformably on the underlying submarine basalt flows. We recognize only one sedimentary unit (lithologic Unit I) overlying volcanic basement rocks (Fig. F37). Unit I (0 to 234.5 mbsf) consists predominantly of light greenish gray foraminifer-bearing nannofossil ooze and nannofossil chalk. Biostratigraphic data, as well as preliminary interpretation of reversed and normal magnetic Chrons, indicate that lithologic Unit I is middle Miocene to early Oligocene or latest Eocene in age. We divide this unit into two subunits (IA and IB) based on the presence of diatom ooze in the uppermost part of the unit. Subunit IA (0 to 10.0 mbsf) consists of white diatom nannofossil ooze with interbeds of dark brown silty diatom ooze, light brown silty foraminifer-bearing diatom ooze, and yellowish brown nannofossil-bearing diatom ooze. Subunit IB (10.0 to 234.5 mbsf) comprises most of the sedimentary section and is predominantly light greenish gray foraminifer-bearing nannofossil ooze, which contains middle Miocene nannofossil and planktonic foraminifer species of warm-water affinity not found elsewhere on the Kerguelen Plateau. Physical properties in Subunit IA and the upper part of Subunit IB (0–180 mbsf) vary only slightly; bulk density ranges from 1.4 to 1.7 g/cm^3, grain densities range between 2.1 and 2.8 g/cm^3, and porosity changes from 57% to 76%. Compressional wave velocities show little scatter, ranging from 1491 to 1852 m/s. As the ooze becomes semilithifed nannofossil chalk downhole (~180–234 mbsf), bulk density gradually increases from 1.5 to 2.0 g/cm^3 (mean = 1.7 g/cm^3), with porosity decreasing from a maximum value of 74% to 44% (mean = 60%). Grain density is nearly constant at ~2.7 g/cm^3 throughout this interval, and compressional wave velocities increase from 1578 to 2018 m/s. At the base of Subunit IB, just above igneous basement, transparent rhombic dolomite crystals are disseminated throughout the sediments. Nannofossils and planktonic foraminifers in the ooze directly overlying igneous basement indicate a minimum basement age of early Oligocene (30.0–34.3 Ma). All physical properties change abruptly at the sediment/basalt boundary. From 235 to 250 mbsf, porosity decreases sharply from a mean of 60% in lithologic Subunit IB to 6% in basalt flows, and grain density increases from 2.7 to 2.9 g/cm^3. Compressional wave velocity varies from 5484 to 6859 m/s.

Drilling at Site 1140 penetrated 87.9 m of basement rocks, which we divide into six units, five submarine basaltic flows (Units 1–3, 5, and 6) and an ~1-m-thick layer of dolomitized nannofossil chalk (Unit 4). Two other thin calcareous-dolomitic sedimentary interbeds are between basalt flows at the Unit 2/3 and Unit 5/6 boundaries. We observe a magnetic reversal at the boundary between basement Units 1 and 2, which are separated by two cored intervals from which there was no recovery (Cores 183-1140A-29R and 30R in Fig. F37). Unit 1 is normal polarity, and Units 2 through 6 are reversed. Downhole logs of density, resistivity, and velocity show high values in the interiors of basalt flows and lower values at flow margins and in the interbedded sediments. At the top of basement Unit 3, a thin bed of well-burrowed, greenish white nannofossil chalk is latest Eocene in age. Basement Unit 4 contains a sedimentary bed with a top and bottom composed of rusty orange dolomite separated by a bed of well-burrowed, very pale brown dolomitic nannofossil chalk. Index properties change sharply at the boundary between Units 3 and 4; bulk density decreases from 2.8 to 2.1 g/cm^3, grain density decreases to a mean of 2.8 g/cm^3, and porosity increases to a

F37. Composite stratigraphic section for Site 1140, p. 90.

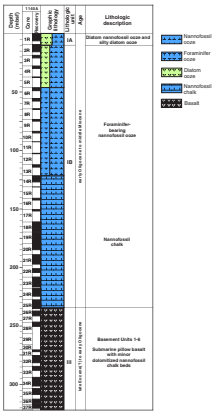

mean of 41%. In Units 5 and 6, bulk density ranges from 2.5 to 3.0 g/cm³, porosity changes from 4% to 24%, grain density varies between 2.9 and 3.1 g/cm³, and compressional wave velocity ranges from 5099 to 6829 m/s (mean = 6055 m/s). The top interval of basement Unit 6 is rusty brown dolomite resembling that of basement Unit 4. The interbedded sediments indicate bathyal water depths during late Eocene to early Oligocene extrusion of the lava flows. Pelagic deposition in a bathyal environment continued uninterrupted until at least middle Miocene time.

Basement Units 1 and 6 each contain a ~5-m-thick massive lobe in addition to ~30 small (50 to 100 cm) basaltic pillows. Only <1-m-diameter pillows were recovered from Units 2 and 3. Unit 5 contains similar pillows and an ~10-m-thick massive lobe. Comparison between cores and logging data indicate that these flow units are 4.4 to 23.4 m thick. The thick massive lobes are probably sheet flows. Thick sheet flows and absence of rubbly talus suggest low to moderate slopes. Although small pillows cannot advance far before freezing, the larger sheets could efficiently transport magma from a distant vent. The flows are cryptocrystalline to fine grained and generally only sparsely vesicular. Vesicles are largely restricted to chilled margins. Vesicularity varies within the units but is consistently low, suggesting the deep water corroborated by bathyal sediments.

Pillow margins are fine grained with 1- to 2-cm-wide unaltered glassy rims (Fig. **F38**). Calcareous sediment or carbonate veins commonly fill sutures between pillows. The fine-grained pillow margins consist of moderately plagioclase ± olivine ± clinopyroxene-phyric basalt, whereas pillow interiors range from plagioclase-phyric to aphanitic. Olivine is a minor phenocryst and groundmass phase in Units 1 and 2 (Fig. **F39**), but it is rare to absent in the lower basaltic units, in which clinopyroxene is a phenocryst phase. Units 4 and 6 are moderately plagioclase-phyric, whereas the others are essentially aphanitic with <1% phenocrysts in the massive portions of the flows. Groundmass phases are calcic ($An_{60–70}$) plagioclase (20%–40%), augite (25%–40%), olivine (0%–5%), titanomagnetite (1%–2%), and altered glass. Textures range from ophitic, intergranular, or intersertal in pillow interiors to glassy at pillow margins.

Alteration of Site 1140 lavas strongly resembles that of young mid-ocean ridge pillows from the uppermost ocean crust (e.g., DSDP/ODP Holes 504B and 896A, located in 5.9-m.y.-old crust in the eastern equatorial Pacific Ocean). Glass at the margins of lava pillows is fresh and isotropic in thin section. These margins are crosscut by numerous calcite and dolomite veins that developed concentrically to the pillow rinds. These veins are generally 2 to 3 mm wide, and the carbonates exhibit dog-tooth, sparry habits. Baked, highly indurated chalk-derived marbles are commonly preserved in the pillow interstices. Rarely, these sediments apparently penetrated the magma, resulting in internal glassy quenched zones in the pillow interiors.

Crystalline interiors of the lavas are slightly to moderately altered. The most common feature of the alteration is development of brown to orange oxidation halos concentric with the pillow rinds, as well as along clay and carbonate veins. Orange brown clays and iron oxyhydroxides pseudomorphically replace groundmass mafic minerals. The gray to greenish gray portions of the basalts are generally fresh, except for the replacement of mesostasis by green clays and the partial filling of rare vesicles with green-blue clay and coarse-grained pyrite. Oxidation halos are less common in the more massive, fine-grained interiors

F38. Close-up photograph of Section 183-1140A-28R-3 (Piece 2, 86–101 cm), **p. 91.**

F39. Photomicrograph of the glass from a chilled pillow margin from Unit 1, **p. 92.**

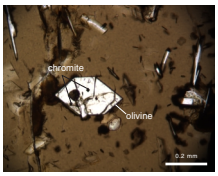

of the thicker lava units, except where these rocks are intercalated with an ~1-m-thick bed of dolomitized and oxidized chalk. The sedimentary rocks may have acted as channels enabling the access of large volumes of seawater-derived fluids into the basement sequences, resulting in the precipitation of abundant, euhedral, colorless dolomite crystals in the chalk and numerous sparry carbonate veins in the pillow lavas.

Compared to other basement basalt recovered from the Kerguelen Plateau during Leg 183, the Site 1140 basalts are distinctive in that they (1) were erupted in a submarine environment, as indicated by their pillowed structure and the intercalated nannofossil-bearing calcareous sediments and (2) are relatively unaltered, as indicated by fresh glass preserved at pillow margins and the lack of alteration in massive interiors of flow units. The five basement flow units at Site 1140 are tholeiitic basalts that are poorer in alkalis than lavas at other locations on the Kerguelen Plateau, except for Site 750 (Fig. **F20**). Basalts from Site 1140 range to higher MgO (8.1 wt%) and Ni (100 ppm) contents than basalts from other Leg 183 drill sites (Fig. **F40**). They form two distinctive geochemical groups. Relative to Units 1, 5, and 6, Units 2 and 3 are enriched in highly incompatible elements, such as P, Zr, and Nb, by factors of 2 to 4 (Fig. **F40**). Units 1, 5, and 6 have near chondritic ratios of Nb/Zr and Zr/Y; in this respect they are similar to the ~110-Ma lavas from Site 749 on the SKP. Despite their eruption in late Eocene time, when the SEIR was <50 km away, Site 1140 lavas are not geochemically similar to depleted MORB. They are geochemically similar to other tholeiitic basalts associated with the Kerguelen plume (Fig. **F31**). Unlike basalts from Elan Bank (Site 1137) and Site 738 on the SKP, basalts from Site 1140 show no evidence for a component derived from continental lithosphere.

Major results of drilling at Site 1140 on the northern flank of the NKP include

1. Miocene nannofossil and planktonic foraminifer species of warm water affinity that had not been recovered previously by drilling on the Kerguelen Plateau.
2. Five submarine basalt flows with intercalated sediments. The ~1-m-thick dolomitized nannofossil chalk and other thinner chalk interbeds within the submarine basaltic flow units indicate episodic eruptions in a bathyal environment. Nannofossils and foraminifers in these chalks indicate a latest Eocene age, confirming that the uppermost igneous basement of the northernmost Kerguelen Plateau formed at <40 Ma. A magnetic reversal at the boundary between Basement Units 1 (normal) and 2–6 (reversed) corroborates nonvolcanic intervals as the uppermost igneous crust of the NKP formed.
3. The ~4- to 23-m-thick basalt flows are dominantly <1-m pillows with a few massive, 5- to 10-m lobes. The ~1-cm-thick quenched pillow margins are fine grained and contain macroscopically unaltered glass that is isotropic in thin section. Basaltic glass has not been recovered at other drill sites on the Kerguelen Plateau; shore-based studies of this glass will provide geochemical data, especially abundances of H_2O, CO_2, and S, that cannot be obtained from studies of altered crystalline rocks.
4. Five pillow lava flow units consist of tholeiitic basalts that form two distinct geochemical groups; both groups have incompatible element abundance ratios within the range of other tholeiitic basalts associated with the Kerguelen plume. Unlike basalts from

F40. Nb, $(Zr/Ti)_N$, and Ni vs. Zr, p. 93.

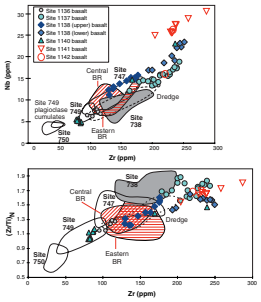

Elan Bank (Site 1137), there is no evidence for a continental lithosphere component.

Sites 1141 and 1142

Sites 1141 and 1142 are situated near the crest of Broken Ridge ~350 km east of DSDP/ODP Sites 255, 752, 753, 754, and 755 (Figs. F5, F6). Flanked to the south by Eocene and younger oceanic crust of the Australia-Antarctic Basin and to the north by Cretaceous oceanic crust of the Wharton Basin, Broken Ridge appears to have formed during Late Cretaceous time as a result of Kerguelen hot spot magmatism (Duncan, 1991; Duncan and Storey, 1992). Subsequently, Broken Ridge and the Kerguelen Plateau began to separate along the westward-propagating SEIR at ~40 Ma. Igneous basement of Broken Ridge had not been sampled previously by drilling; dredge samples from three locations along the feature's southern, faulted boundary yield dates of ~62, ~83, and 88–89 Ma (Duncan, 1991). Because of the scatter in ages of the dredged rocks and the absence of in situ basement samples from Broken Ridge, knowledge of Broken Ridge's age and composition remains extremely limited. We located Sites 1141 and 1142 on the *JOIDES Resolution* single-channel seismic Line JR183-101. Sites 1141 and 1142 lie at depths of 1197 m and 1201 m, respectively, ~3–4 km north of the crest of Broken Ridge. We chose this location primarily on the basis of its thin sedimentary section (Fig. F41). The top of acoustic basement has an apparent dip to the north-northeast of 0° at Site 1141 and 2.5° at Site 1142. An ~100-m-thick sediment sequence overlies igneous basement. Since basement of Broken Ridge had never been drilled, our major objective at Sites 1141 and 1142 was to determine its age and composition. Additional basement objectives were to determine the physical characteristics of the lava flows and the environment of eruption (subaerial or submarine). The sedimentary objectives at Site 1141 were to determine sequence facies, to define the ages of seismic sequence boundaries, to estimate the duration of possible subaerial and shallow-marine environments, to obtain minimum estimates for basement age, and to determine the paleoceanographic history of Broken Ridge. At Sites 1141 and 1142, these objectives were achieved by coring 71 and 51 m of volcanic basement, respectively, and ~113 m of overlying sediment at Site 1141 (Figs. F42, F43). The abrupt termination of Hole 1141A led to an unanticipated experiment whereby we compared two basement sections separated by only 800 m.

At Site 1141, sediments were recovered from 0 to 103.8 mbsf (Fig. F42). We recognize only one sedimentary unit, lithologic Unit I. The basement volcanic rocks are designated lithologic Unit II. Unit I (0–113.5 mbsf) consists of white foraminifer nannofossil ooze of Pleistocene to early Miocene age. Core 183-1141A-1R consists of nannofossil-bearing foraminifer ooze that is predominantly composed of sand-sized foraminifers and displays slight normal size-grading. Traces of aragonite are present in Core 183-1141A-1R. Temperate calcareous microfaunas and floras characterize the current-winnowed Neogene calcareous ooze recovered at Site 1141. They are joined by subtropical index taxa in the Pliocene–Pleistocene section, a result of northward movement of Broken Ridge into warmer, lower latitude waters. The average sedimentation rate of 6 m/m.y. for the entire carbonate ooze section is the lowest Neogene rate for Leg 183. In Cores 183-1141A-8R and 9R, we obtained reliable remanent magnetization and correlated normal and reversed polarities with middle Miocene Chrons C5 to C5AD.

F41. *JOIDES Resolution* JR183-101 single-channel seismic profile across Sites 1141 and 1142, p. 95.

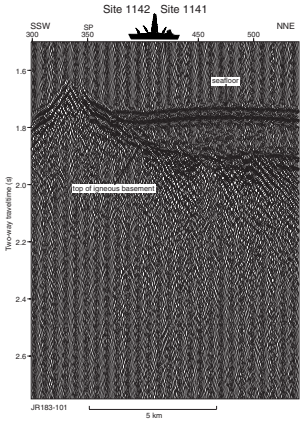

F42. Composite stratigraphic section for Site 1141, p. 96.

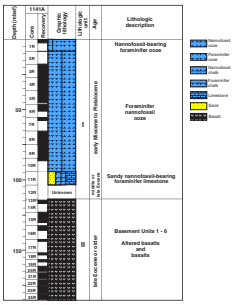

F43. Composite stratigraphic section for Site 1142, p. 97.

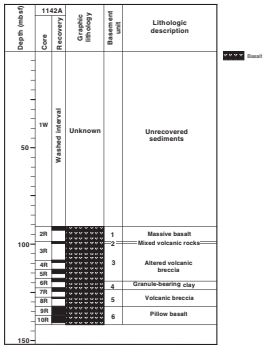

Bulk densities in Unit I vary from 1.6 to 1.8 g/cm^3, and porosity ranges from 54% to 65%, with a mean of 62%. Compressional wave velocities in Unit I show very little scatter, with a mean value of ~1860 m/s. The base of Unit I consists of a layer of sandy foraminifer limestone with abundant sand- to pebble-sized rock fragments and mineral grains. The limestone, late middle to late Eocene in age (35–38 Ma), postdates rifting and separation of Broken Ridge and the CKP. The pebbles include basalt with ferromanganese crusts. The thickness of this basal layer is uncertain as only two small fragments were recovered. The pelagic sedimentary succession at Site 1141 indicates that Broken Ridge has been at bathyal water depths since at least early Miocene time. Neritic fossils in the basal limestone indicate redeposition from shallow-water areas to a bathyal environment during the Eocene or later. Unit II consists of basalts, which are highly altered in the upper portion of the section. It is subdivided into six basement units. Near the top of Unit II (~114 mbsf), index properties change abruptly. From 115.8 to 116.7 mbsf in the upper part of basement Unit 2, bulk densities increase to a mean value ~2.0 g/cm^3, grain densities increase to 2.9 g/cm^3, and porosities decrease to 48%.

At Site 1142 (Fig. **F43**) no sediments were recovered from the drilled interval (0–91 mbsf; Core 183-1142A-1W, except for some small fragments of sandy pebbly foraminifer limestone with Oligocene or Eocene nannofossils.

The six basement units at Site 1141 represent 72.1 m of basement penetration and consist of five mafic lava flows overlain by a poorly sampled, coarse-grained sedimentary deposit consisting of three pebbles of moderately altered, medium-grained, plagioclase-clinopyroxene-olivine gabbro. The lava flows appear to have been erupted subaerially. The tops of most volcanic units in Hole 1141A have been highly to completely altered to clay; in some cases this intense alteration affects entire units. Red flow tops and green to gray flow interiors suggest decreasing oxidation with depth. In many intervals, traces of native copper are in the groundmass, and abundant native copper lines some fracture surfaces. Vesicles are filled with dark green clay, calcite, zeolite, amorphous silica, and quartz and have well-developed colloform textures. Slickensides are present along some fractured surfaces. Perhaps the most noteworthy alteration within Hole 1141A is the spectacular alteration halos associated with quartz veins. In some instances, a single quartz vein extends for >120 cm with multiple, symmetrical alteration halos progressively altering the surrounding wall rock. Common calcite veins are generally <0.5 mm wide and crosscut the quartz-filled veins.

Basement Unit 2 (20 m thick) is fine-grained, aphyric basalt. The least-altered portion of basement Unit 3 (8 m thick) is fine- to medium-grained, sparsely plagioclase-phyric basalt. Basement Unit 4 (20 m thick) is aphyric to moderately plagioclase- or plagioclase-olivine-phyric basalt. Basement Unit 5 (8 m thick) is sparsely olivine-phyric. Basement Unit 6 (15 m thick) ranges from aphyric to moderately olivine-plagioclase-phyric basalt. In addition to olivine phenocrysts, groundmass olivine and minor apatite in the lower part of basement Unit 4, and throughout basement Units 5 and 6, suggest that these basalts are alkalic. Thin sections show that carbonate, clay, and iron oxides completely replace the mafic phases and groundmass glass from the top of Unit 1 to the upper part of Unit 6; the bottom part of Unit 6 retains a large proportion of relatively fresh phenocryst and groundmass olivine. All index properties change markedly near the boundary between basement Units 2 and 3 and reach extremes in basement Unit 6, where bulk

densities vary from 2.6 to 2.9 g/cm³ with a mean of 2.7 g/cm³, grain density approaches a mean of 2.8 g/cm³, and porosity varies from 16% to 3%. Compressional wave velocities in basement Unit 6 increase gradually with depth, from 4276 to 6902 m/s.

At Site 1142, 50.9 m of basement penetration recovered six units (Fig. F43). They include a diverse range of lithologies, including olivine-phyric basalt lava flows, possible pillow basalts, subaerial deeply weathered (felsic?) lavas, and volcaniclastic sediments. Alteration and weathering of these basement rocks suggest subaerial exposure. The lithologies and alteration intensity within Hole 1142A are heterogeneous. Some units are relatively massive, slightly altered basalt, whereas other volcanic units are variably brecciated by both volcanic and tectonic processes and have been completely altered to clay. Primary igneous textures are still visible in most units and are typically accentuated by the replacement of feldspar by light green clay and mafic minerals by red-brown clay.

Basement Unit 1 (2 m thick) is a slightly to moderately altered, massive, fine-grained, aphyric to sparsely olivine-plagioclase-phyric basalt; the upper portion has prominent oxidation halos, suggesting a period of exposure and weathering, possibly related to Eocene rifting and breakup between Broken Ridge and the CKP. Basement Unit 2 (1 m thick) consists of a single section containing 20 moderately to completely altered cobble-sized pieces of genetically unrelated rock types, including volcanic breccia, clinopyroxene-phyric, plagioclase-phyric, olivine-phyric, and aphyric basalt, and feldspar- and feldspar-quartz-phyric felsic volcanic rocks. Some of the pieces have abraded, slightly weathered surfaces, suggesting that the unit may be a near-source debris flow or a talus pile. Basement Unit 3 (20 m thick) is a completely altered, aphanitic, aphyric to moderately olivine-plagioclase-phyric basaltic breccia with three subunits defined on the basis of textural characteristics. Basement Unit 4 is a 4-m-thick, well-indurated, normally graded claystone or mudstone with very highly to completely altered, very coarse sand-sized to small granule-sized lithic clasts and crystals of quartz and altered feldspar in a red clay matrix. We interpret this unit to be a mudflow deposit. Basement Unit 5 (9 m thick) is a very highly to completely altered, aphanitic, aphyric volcanic breccia. The only hint of the original rock type is provided by very rare quartz crystals, which suggest an evolved composition. Basement Unit 6 is composed of ≥10 m of aphyric, nonvesicular, fine-grained to aphanitic basalt. Several alteration features indicate that this unit may be a pillow basalt; specifically, semicircular, red-brown oxidation halos and narrow dark green to black intervals associated with carbonate veins that may be altered pillow margins. However, grain size does not decrease toward these highly altered zones. Thus, evidence is equivocal as to whether these are pillow basalts. The numerous sinuous and semicircular oxidation halos may represent subaerial weathering after the uplift of Broken Ridge that accompanied its breakup with the CKP.

Most of the basement lavas from Sites 1141 and 1142 have slightly alkalic compositions, but the youngest lava analyzed at Site 1141 is highly alkalic (trachybasalt in Fig. F44). Flow Unit 1 from Hole 1142A has geochemical characteristics similar to flow Unit 6 from Hole 1141A. Unlike some of the lavas dredged from Broken Ridge, most lavas from Sites 1141 and 1142 have $(Nb/Ce)_N > 1$; the lowermost flow unit at Site 1142 is an exception. It is tholeiitic and has $(Nb/Ce)_N < 1$ like dredged tholeiitic basalts from Broken Ridge (Mahoney et al., 1995). Therefore,

F44. Compositions of volcanic rocks from all Leg 183 basement recovery sites, p. 98.

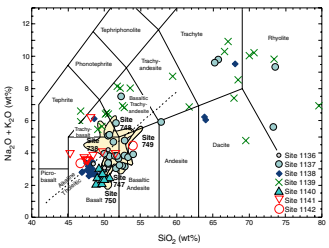

only one of the 11 Site 1141 and 1142 lavas analyzed has a composition reflecting the possible influence of a continental crust component. Compared to basement lavas from the Kerguelen Plateau, 10 of the 11 Site 1141 and 1142 lavas analyzed have relatively high contents of incompatible elements such as P, Ti, Zr, and Nb and the compatible elements Ni and Cr (Fig. F40). These characteristics are consistent with derivation of their parental magmas by relatively low extents of melting coupled with limited fractionation of olivine and pyroxene. We infer that the alkalic nature of most Site 1141 and 1142 basalts shows that the extent of melting decreased during the final stage of volcanism.

All basement rocks in Holes 1141A and 1142A are normally magnetized. Despite a lateral separation of only 800 m, macroscopic observations do not enable correlation between the basement units at Sites 1141 and 1142. Seismic reflection data collected over the sites during Leg 183, as well as seismic reflection data and drilling results from Sites 752–755 lying ~350 km to the west, indicate that to the north of the bathymetric crest of Broken Ridge, prebreakup sediment and presumably igneous basement dip consistently to the north. Therefore, Site 1142 may have penetrated a deeper stratigraphic section than Site 1141. This interpretation is consistent with the geochemical similarity of the uppermost basement flow unit at Site 1142 with the lowermost basement flow unit at Site 1141, and the tholeiitic composition of the oldest flow unit at Site 1142.

The major results of drilling at Sites 1141 and 1142 include

1. Six basement units at Site 1141 include five mafic flows that appear to have been erupted subaerially.
2. Several of these ~10- to 20-m-thick lava flows contain phenocryst and groundmass plagioclase and olivine.
3. Six basement units at Site 1142 range from olivine-phyric basaltic flows to subaerial deeply weathered (felsic?) lavas and volcaniclastic sediments. A surprising result is that basement Unit 6 may be a pillow basalt that was subsequently oxidized in a subaerial environment, perhaps after the ~40-Ma uplift of Broken Ridge that accompanied its breakup with the CKP.
4. Differences between igneous basement sections at Sites 1141 and 1142 may result from penetration of different stratigraphic levels or from considerable, unanticipated lateral variability in volcanism.
5. Unlike many of the dredged basalts from Broken Ridge, most of the basaltic lavas at Sites 1141 and 1142 provide no evidence for a continental lithosphere component. In contrast, the lowermost flow unit at Site 1142 is geochemically similar to dredged basalts from Broken Ridge.
6. Compared to basaltic lavas from the CKP and SKP, basaltic lavas from Sites 1141 and 1142 have relatively high abundances of incompatible and compatible elements, characteristics that are consistent with relatively lower extents of melting coupled with limited fractionation of olivine and pyroxene.

SUMMARY

Coring Summary

During Leg 183, we drilled eight widely spaced holes in different domains of the Kerguelen Plateau–Broken Ridge LIP (Figs. F3, F5, F15): the SKP (Sites 1135 and 1136), Elan Bank (Site 1137), CKP (Site 1138), Skiff Bank on the NKP (Site 1139), northern NKP (Site 1140) and Broken Ridge (Sites 1141 and 1142). Except at Site 1135, igneous basement rocks were recovered with penetrations ranging from 33 to 233 m (Fig. F15; Table T1).

Chronology of Kerguelen Plateau–Broken Ridge Magmatism

Biostratigraphic studies of sediment directly overlying igneous basement at Leg 183 sites provide minimum ages for the volcanic and volcaniclastic rock. Middle Albian (~104.5–106.5 Ma) shallow-water sands and clays overlie inflated pahoehoe flows at Site 1136, suggesting that the age of the lavas is close to the ~110 Ma age of all other basalt samples recovered to date from the SKP. Site 1138 on the CKP yielded undifferentiated Upper Cretaceous claystone and sandstone on top of igneous basement; these sediments are overlain by Cenomanian–Turonian (~93.5 Ma) sandstone. This age is older than, but close to, the ~85 Ma date for basalt at Site 747 (Pringle et al., 1994; Storey et al., 1996). Drilling at the conjugate Broken Ridge region (Site 1141 and 1142; see Fig. F2) did not provide useful minimum ages because the oldest sediment is Miocene, postdating Eocene separation of Broken Ridge and the CKP and, therefore, much younger than the formation age of Broken Ridge.

The first igneous basement ever recovered from Elan Bank at Site 1137 is overlain by upper Campanian (73.5–74.6 Ma) packstone. The lavas and volcaniclastic sediments forming basement are likely to be somewhat older, as the packstone is at the top of a basal sedimentary sequence that thickens significantly to the east of Site 1137. Submarine igneous basement of the NKP was cored for the first time at Site 1139 on Skiff Bank and Site 1140 on the northernmost Kerguelen massif (Fig. F3). On Skiff Bank, chalk at the base of the pelagic sedimentary section is earliest Oligocene (32.8–34.3 Ma) in age. Igneous basement is probably older, as grainstone, packstone, and sandstone lie between it and the overlying pelagic section. Nevertheless, the minimum age is not inconsistent with the oldest rocks from the Kerguelen Archipelago (Giret and Beaux, 1984; Nicolaysen et al., 1996, in press). At Site 1140, lowermost Oligocene (34.3 Ma) pelagic sediment directly overlies basement, and pelagic sediment of late Eocene age (~35 Ma) is intercalated within basalt flows that form the uppermost basement.

Petrogenesis of Basement Igneous Rocks

At 10 of the 11 drill sites on the Kerguelen Plateau–Broken Ridge LIP, the oldest recovered basement rocks are basalt with slightly alkalic to slightly tholeiitic compositions; the basement alkalic lavas from Site 1139 (Skiff Bank on the NKP) are the exception (Fig. F44). All of the basement basalts have relatively low MgO and Ni contents (typically, MgO < 8 wt% and Ni < 100 ppm, except for basalts from Broken Ridge

Sites 1141 and 1142, which have similarly low MgO contents but 100–200 ppm Ni), and their compositions are not similar to primary melts of peridotite (BVSP, 1981). An example of the important role of fractional crystallization in controlling the compositions of these lavas are basalts from Site 1138, which show a systematic downhole trend to Fe-Ti-rich basalt reaching TiO_2 and total Fe_2O_3 contents of 3.2 wt% and 19.2 wt%, respectively. In general, evolved basalt compositions are typical of many flood basalts. The likely explanation is that the youngest magmas in a LIP, like Kerguelen Plateau–Broken Ridge, must ascend through relatively thick lithosphere, thereby promoting cooling and partial crystallization of the magma. Subsequent segregation of olivine- and pyroxene-rich cumulates then forms the high-velocity lower crust that is typical of oceanic plateaus such as the Kerguelen Plateau (Charvis et al., 1993, 1995; Operto and Charvis, 1995, 1996; Farnetani et al., 1996; Könnecke et al., 1998; Charvis and Operto, 1999) and leads to the complementary evolved residual melts. In regard to this scenario, it is important to realize that we have only sampled the upper 30–200 m of a ~20-km-thick mafic crust. In contrast to basalts from all other sites, basement lavas at Site 1139 (Skiff Bank on the NKP) form an alkaline lava series ranging from trachybasalt to trachyte and rhyolite; the lowermost flow at Site 1139 is a rhyolite (Figs. **F34, F35**). Similar alkaline lava series erupted in early Miocene and Pliocene/Pleistocene time in the Southeast Province of the Kerguelen Archipelago (Fig. **F8**) (Weis et al., 1993, 1998b; Frey et al., in press). The simplest interpretation is that Skiff Bank, which reaches <500 m water depth, is a submerged island analogous to but slightly older than the Kerguelen Archipelago, also on the NKP but 350 km to the east-northeast (Fig. **F3**). Alkalic lavas had not been previously recovered from the basement of the Kerguelen Plateau. At Site 748 on the SKP, however, alkalic basalt was recovered from ~200 m above basement.

An important objective of Leg 183 was to evaluate the role of continental crust in constructing the Kerguelen Plateau–Broken Ridge LIP. Previous evidence pointing to a significant role for continental crust in diverse parts of the LIP includes isotope and trace element abundance data for basalts from the SKP (Site 738), CKP (Site 747), and basalts dredged from the SKP and eastern Broken Ridge (Figs. **F11, F12, F13;** Storey et al., 1989, 1992; Mahoney et al., 1995) and the seismic structure of the crust in the northern part of the SKP (Operto and Charvis, 1995, 1996). Some mantle xenoliths in the Kerguelen Archipelago lavas also show evidence for a continental lithosphere component (Hassler and Shimizu, 1998; Mattielli et. al., 1999), as does a trachyte from Heard Island (Barling et al., 1994). Drilling at Site 1137, however, recovered the strongest evidence to date for a component of continental crust in the Kerguelen Plateau. A ~26-m-thick fluvial conglomerate (Fig. **F45**) intercalated with basaltic basement contains clasts of trachyte, rhyolite, granitoid, and garnet-biotite gneiss (Fig. **F46**); the garnet-biotite gneiss, in particular, indicates that continental crustal rocks were once exposed at Elan Bank. Furthermore, although it is difficult to use shipboard geochemical data to identify continental material in mantle-derived basaltic rocks, our study of Site 1137 cores builds a compelling case. The basement basalts at Site 1137 are geochemically distinctive; they have atypically high Zr/Y and Zr/Ti (Figs. **F21, F40**) and a slight relative depletion in Nb abundance (Figs. **F21, F25**)—both characteristics are consistent with a component derived from continental crust.

A Nb/Y vs. Zr/Y plot has been used to distinguish between lavas derived from the Icelandic plume and North Atlantic MORB (Fitton et al.,

F45. Color close-up photograph of Site 1137 conglomerate, **p. 99.**

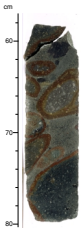

F46. Photomicrographs of garnet gneiss, **p. 100.**

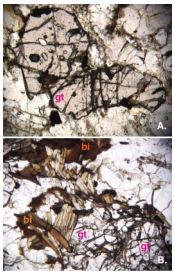

1997, 1998b). In this plot (Fig. F31), it is important to realize that different plumes are geochemically distinct; in particular, lavas of varying age, from ~82 Ma to Pliocene–Pleistocene, associated with the Kerguelen plume define a Nb/Y-Zr/Y trajectory along the lower boundary for the Icelandic plume (Fig. F31). We conclude that the Kerguelen plume plots on this line in the lower left portion of the plot. Basement basalts from several locations on the Kerguelen Plateau and Broken Ridge also lie along this trend (namely, Sites 747, 1136, 1138, 1140, 1141, and 1142). Two other locations are in the Icelandic field (Sites 749 and 750), and two others lie in the MORB field (Sites 738 and 1137); however, basalts from these latter two sites do not have MORB geochemical characteristics (Figs. F9, F25). We infer that basalts from Sites 738 and 1137 are in the MORB field because they are plume-derived basalts that have been contaminated by continental crust (Figs. F25, F31). The effects of crustal contamination are obvious in the Sr, Nd, and Pb isotope characteristics of Site 738 basalts (Figs. F9, F10). Isotope data are not yet available for Site 1137 basalts, but the clasts of garnet-biotite gneiss in a conglomerate intercalated with these basalts (Fig. F46) unambiguously show that continental crust is present in the oceanic environment of Elan Bank.

Continental material, whether derived from continental crust or subcrustal continental lithosphere, is occasionally incorporated into oceanic lithosphere. At one end of the spectrum are microcontinents such as Seychelles and Jan Mayen, which maintain normal continental crustal thicknesses when isolated in ocean basins by jumps of seafloor spreading centers, with or without involvement of mantle plumes. At the other end of the spectrum are subtle geochemical signatures in otherwise typical mid-ocean ridge basalts that have been interpreted to represent the influence of deeply recycled continental material or subcrustal continental lithosphere (e.g., Mahoney et al., 1996). As described above, interpreted continental components of the Kerguelen Plateau and Broken Ridge encompass a range of petrologic, geochemical, and geophysical signatures and, therefore, may be accounted for by more than one process. However, the simplest mechanism for incorporating continental material into the Kerguelen Plateau–Broken Ridge LIP is a ridge jump postdating the breakup and initial seafloor spreading between India and Antarctica. One or more ridge jumps to the north would have transferred continental parts of the Indian plate to oceanic portions of the Antarctic plate, accounting for features like Elan Bank and the portion of the SKP characterized by continental crustal velocities. Published plate motion models (e.g., Fig. F2) do not show any ridge jumps because the oceanic crust between Antarctic and Kerguelen Plateau formed during the long Cretaceous Normal Superchron and, therefore, is not datable using the usual technique of marine magnetic anomaly identification. Nevertheless, the unambiguously continental garnet-biotite gneiss recovered as clasts in a conglomerate intercalated with basement basalt at Site 1137 on Elan Bank strongly suggests that at least one northward ridge jump transferred a continental fragment (Elan Bank) from the Indian to the Antarctic plate.

Environmental Impact of Kerguelen LIP Volcanism

Evidence from basalts and overlying sediments at Sites 738, 747, 748, 749, and 750 (Figs. F1, F15), combined with results of subsidence modeling (Coffin, 1992), shows that much of the igneous crust of the SKP and CKP was erupted in a subaerial environment. Portions of the SKP

remained subaerial for as much as 50 m.y. after volcanism ceased. Leg 183 drilling results corroborate, extend, and add detail to those previous results. On the SKP (Site 1136), we cored upper bathyal to neritic sediment overlying inflated pahoehoe lavas up to 20 m thick. The basalts lack features of submarine volcanism (e.g., pillows and quenched glassy margins) suggesting subaerial eruption. The CKP (Site 1138) was above sea level during the final stages of construction; subaerial pyroclastic flow deposits overlie ~5-m-thick subaerial lava flows ranging from inflated pahoehoe to classic aa. Terrestrial and shallow-marine sediment containing wood fragments, a seed, spores, and pollen overlies igneous basement, documenting for the first time that the CKP was subaerial after volcanism ceased. In a conjugate position to the CKP, Broken Ridge basaltic lavas were erupted in subaerial (Site 1141) and possibly submarine (Site 1142) environments.

The igneous basement complex of Elan Bank at Site 1137 consists of seven basaltic lava flows and three sedimentary units. The seven 7- to 27-m-thick lava flows were erupted subaerially, as indicated by oxidation zones, inflated pahoehoe characteristics, and the morphology of flow-top breccias. Some of the interbedded volcaniclastic sedimentary rocks were deposited in a fluvial environment (braided river), consistent with subaerial eruption of the basalts. Neritic packstones overlying the igneous basement complex, in turn succeeded by pelagic oozes, indicate gradual subsidence of Elan Bank.

Skiff Bank (Site 1139) was also subaerial during its final stages of formation, as indicated by a succession of volcanic and volcaniclastic rocks (some of which are oxidized) underlain by lava flows, including both pahoehoe and aa types. After volcanism ceased, paleoenvironments of the overlying sediments changed intertidal (beach deposits) to very high-energy, nearshore (grainstone and sandstone) to low-energy, offshore (packstone) to bathyal pelagic (ooze). In contrast, igneous basement Site 1140 at the northernmost tip of the NKP consists entirely of pillow basalts and intercalated pelagic sediment. However, seafloor depths at all six other basement sites drilled during Leg 183 are between 1000 and 2000 m, whereas Site 1140 is situated at a water depth of 2394 m.

An unexpected result of Leg 183 drilling was the discovery that highly evolved, felsic magmas were erupted explosively during the final stages of magmatism over extensive regions of the Kerguelen Plateau (Fig. **F15**). Igneous basement recovered from four previous ODP sites on the SKP and CKP did not include felsic lavas, but at four Leg 183 drill sites we recovered pyroclastic flow deposits and dense lava samples of trachyte, dacite, and quartz-bearing peralkaline rhyolite (Fig. **F44**). At Site 1137 on Elan Bank, a 15-m-thick sanidine-rich vitric tuff is intercalated between basaltic lava flows. Well-preserved bubble-wall glass shards in part of the tuff together with abundant broken crystals indicate that the tuff formed in an explosive volcanic eruption. Higher in the stratigraphic sequence at Elan Bank, a fluvial conglomerate contains clasts of rhyolitic and trachytic lavas. At Site 1138 on the CKP, we recovered a 20-m-thick volcaniclastic succession containing six trachytic pumice lithic breccias that were deposited by pyroclastic flows. This volcaniclastic sequence also includes highly altered ash fall deposits that contain accretionary lapilli. Above this sequence we recovered a reworked deposit of rounded cobbles of flow-banded dacite. At Site 1139 on Skiff Bank, which forms part of the NKP, the uppermost basement contains a variety of felsic volcanic and volcaniclastic rocks. In contrast to the CKP and Elan Bank sites, biostratigraphic ages of sedi-

ments directly overlying this basement suggest that this episode of felsic volcanism is Cenozoic in age. The Skiff Bank section includes densely welded pyroclastic flow deposits of quartz-bearing rhyolite, in addition to lava flows and reworked cobbles of volcanic rock ranging from sanidine-rich trachyte to rhyolite.

Evolved magmas (e.g., trachyte, phonolite, and rhyolite) are erupted during plume-related volcanism at oceanic islands and in some continental flood basalt provinces (e.g., Parana, Etendeka, Karoo, and Siberian Traps). Typically these eruptions occur near the end of voluminous, basaltic magmatism. Two alternative modes of formation for highly evolved magmas are partial melting of lower crustal rocks or as residual magmas created as the supply of mantle-derived basaltic magma wanes, leading to formation of crustal-level magma chambers in which highly evolved magma forms through crystal fractionation of basalt (±wallrock assimilation).

The eruption of enormous volumes of basaltic magma during formation of the Kerguelen Plateau–Broken Ridge LIP probably had significant environmental consequences because of the release of volatiles such as CO_2, SO_2, HCl, and HF. A key factor in the magnitude of volatile release is whether the eruptions were subaerial or submarine; hydrostatic pressure inhibits vesiculation and degassing of magma during submarine eruptions, whereas subaerial eruptions directly input volatiles into the atmosphere. Results of Leg 183 drilling complement earlier results from Legs 119 and 120 in demonstrating that subaerial basaltic eruptions occurred during the final constructional stages of the plateau.

Another important factor that would have increased the environmental consequences of Kerguelen Plateau–Broken Ridge LIP volcanism is the high latitude at which the plateau formed. In most basaltic eruptions, released volatiles remain in the troposphere. However, at high latitudes, the tropopause is relatively low, allowing large mass flux basaltic fissure eruption plumes to transport SO_2 and other volatiles into the stratosphere (Strothers et al., 1986; Self et al., 1998). The sulfuric acid aerosol particles that form in the stratosphere after such eruptions have a longer residence time and greater global dispersal than if the SO_2 remains in the troposphere; therefore, they have greater effects on climate and atmospheric chemistry. The large volume, high eruption rates (e.g., at Site 1137), and long duration of subaerial basaltic volcanism on the Kerguelen Plateau–Broken Ridge LIP, combined with the high latitude of most of the plateau, would all have contributed to potential environmental effects.

Highly explosive felsic eruptions, such as those that formed the pyroclastic deposits on Elan Bank, Skiff Bank, and the CKP can also inject both particulate material and volatiles (SO_2, CO_2, possibly HCl) directly into the stratosphere (McCormick et al., 1995). The significant volume of subaerial and explosive felsic volcanism that was discovered at several Leg 183 drill sites (Fig. **F15**) may have affected global climate and environment significantly. The total volume of felsic volcanic rocks and the magnitude of individual eruptions are poorly constrained, but our results indicate that felsic rocks account for a significant fraction of the volcanic deposits erupted during the final stages of magmatism at several locations on the Kerguelen Plateau.

Tectonic History

The uppermost volcanic basement of the Kerguelen Plateau was mostly erupted in a subaerial environment (Leg 183 Sites 1136, 1137, 1138, 1139, and 1141; Leg 119 Site 738; Leg 120 Sites 747, 749, and 750), although bathymetrically deeper basalts on the NKP (Site 1140) formed under water (Figs. F36, F38). Sediments overlying basaltic basement at Leg 183 drill sites record the vertical tectonic history of the Kerguelen Plateau through changing facies. At Site 1136 on the SKP, neritic clay and sand overlie basement, which are in turn overlain by pelagic chalk and ooze. This sedimentary succession documents subsidence of the SKP since Early Cretaceous time. On the CKP (Site 1138), terrestrial and shallow-marine sediment overlie basement. In particular, the transition from oxidized neritic sediment to black claystone to pelagic sediment likely records both thermal subsidence and eustatic sea level rise. At Site 1137 on Elan Bank, fluvial sediment is interbedded with basalt, and neritic packstone succeeded by pelagic ooze overlies volcanic basement. Despite a component of continental crust in Elan Bank, its subsidence behavior appears to resemble that of oceanic crust. The subsidence of Skiff Bank (Site 1139), part of the NKP, is recorded by a transition from subaerial (volcanic and volcaniclastic rocks) to intertidal (beach deposits) to very high energy, nearshore (grainstone and sandstone) to low-energy offshore (packstone) to bathyal pelagic (ooze). In summary, during Leg 183 we recovered sediments that record subsidence of the SKP, CKP, Elan Bank, and Skiff Bank; for the latter three domains, these constitute the first such records.

Postcruise Research

The basement rocks will be the focus of several shore-based studies; for example:

1. The chronology of basement rocks will be principally determined by $^{40}Ar/^{39}Ar$ studies of relatively unaltered whole rock samples and potassium-bearing phases such as plagioclase and sanidine.
2. The composition (major and trace element abundances) and isotope ratios (Sr, Nd, and perhaps others) of unaltered phenocrysts (such as plagioclase and clinopyroxene) will provide information on parental magma composition and the role of crustal processes such as fractional crystallization, magma mixing, and assimilation of wallrocks.
3. The composition (major and trace element abundances) and isotope ratios of (O, Sr, and perhaps others) in secondary phases formed as the lavas interacted with the surficial environment will be used to understand the postmagmatic processes in subaerial and submarine environments.
4. The composition (major and trace element abundances) and isotope ratios (O, Sr, Nd, Pb, Hf, and Os) of whole rocks will be used to understand both magmatic and postmagmatic processes and the role of geochemically distinct mantle and crustal components in these rocks.
5. The magnetic inclination of basement rocks will be determined, providing paleolatitude information necessary for plate kinematic and paleoceanographic studies.

6. The range of lava flow morphology and eruption style will be used to understand the physical volcanological processes that created the Kerguelen Plateau–Broken Ridge LIP.
7. Shore-based research will also focus on unique core samples that bear particularly on narrowly focused problems; for example:
   a. Both the chemical and physical characteristics of the felsic volcanic units will be used to understand the environmental effects of such volcanism, especially the units that reflect explosive eruption of presumably volatile-rich magmas.
   b. The diverse array of clasts (basalt, rhyolite, trachyte, granitoid, and garnet-biotite gneiss) in the 26 m of conglomerate within the basement at Site 1137 will be used to define the depositional environment and geologic terrain, in terms of geochemistry and age, at Elan Bank near the end of its volcanic history; this research will include U-Pb dating of zircons in the gneiss clasts and volcaniclastic units.
   c. The glassy pillow rinds at Site 1140 will be studied to determine the composition of the basaltic melts; such samples are particularly important for determining the volatile contents of the magmas at this NKP location.
8. Tectonic studies will incorporate new age constraints on basement rocks and the existence of continental material in developing new, improved regional plate reconstructions.
9. Seismic volcanostratigraphy will extend borehole results from basement drilling regionally to interpret different types of volcanism and relationships between magmatism and tectonism.
10. Downhole logging data, the Formation MicroScanner (FMS) in particular, will be used to determine true lava flow thicknesses and structure in intervals of low core recovery.
11. Physical properties and downhole logging data will be used to better understand the effects of intrabasement velocity inversions on seismic reflection data.

Several shore-based studies will also focus on the sediments; for example:

1. The Turonian–Coniacian black shale at Site 1138 will be the focus of several studies including analyses for a wide range of metals to evaluate abundance anomalies of metals that may have been introduced into seawater by hydrothermal activity associated with LIP formation, C and N isotope analyses of the organic carbon fraction, which can be used as proxies for source and productivity followed by biomarker molecule extractions and analyses.
2. The expanded sections (e.g., middle Eocene to uppermost Paleocene at Site 1135 and lower to middle Eocene at Site 1136) will be used to understand high-latitude paleoceanographic conditions and improve biostratigraphic resolution.
3. Paleomagnetic studies will be used to establish magnetostratigraphy in sedimentary sections.
4. Palynological studies will help date terrestrial and terrigenous sediment and determine vegetation types and paleoclimates when the Kerguelen Plateau and Broken Ridge were subaerial.
5. Exploratory research on isotope variations of Li and first-series transition elements in the sedimentary environment.

6. Seismic stratigraphy will use borehole results to interpret key seismic reflections regionally, enabling dating of tectonic and paleoceanographic events.
7. Subsidence analyses will model the Kerguelen Plateau's vertical tectonic history, taking different magmatic and deformational events into account.

REFERENCES

Alibert, C., 1991. Mineralogy and geochemistry of a basalt from Site 738: implications for the tectonic history of the southernmost part of the Kerguelen Plateau. *In* Barron, J., Larsen, B., et al., *Proc. ODP, Sci. Results,* 119: College Station, TX (Ocean Drilling Program), 293–298.

Angoulvant-Coulon, M.-P., and Schlich, R., 1994. Mise en évidence d'une nouvelle direction tectonique sur le plateau de Kerguelen. *C.R. Acad. Sci. Paris Ser. 2,* 319:929–935.

Barling, J., Goldstein, S.L., and Nicholls, I.A., 1994. Geochemistry of Heard Island (Southern Indian Ocean): characterization of an enriched mantle component and implications for enrichment of the sub-Indian Ocean Mantle. *J. Petrol.,* 35:1017–1053.

Barron, J., Larsen, B., et al., 1989. *Proc. ODP, Init. Repts.,* 119: College Station, TX (Ocean Drilling Program).

Basaltic Volcanism Study Project (BSVP), 1981.Characteristics of primary basaltic magmas. In *Basaltic Volcanism on the Terrestrial Planets:* New York (Pergamon Press), 409–432.

Bralower, T.J., Fullagar, P.D., Paull, C.K., Dwyer, G.S., and Leckie, R.M., 1997. Mid-Cretaceous strontium-isotope stratigraphy of deep-sea sections. *Geol. Soc. Am. Bull.,* 109:1421–1442.

Cande, S.C., and Kent, D.V., 1995. Revised calibration of the geomagnetic polarity timescale for the Late Cretaceous and Cenozoic. *J. Geophys. Res.,* 100:6093–6095.

Charvis, P., and Operto, S., 1999. Structure of the Cretaceous Kerguelen volcanic province (southern Indian Ocean) from wide-angle seismic data. *J. Geodyn.,* 28:51–71.

Charvis, P., Operto, S., Könnecke, L.K., Recq, M., Hello, Y., Houdry, F., Lebellegard, P., Louat, R., and Sage, F., 1993. Structure profonde du domaine nord du plateau de Kerguelen (océan Indien austral): résultats préliminaires de la campagne MD66/KeOBS. *C.R. Acad. Sci. Ser. 2,* 316:341–347.

Charvis, P., Recq, M., Operto, S., and Brefort, D., 1995. Deep structure of the northern Kerguelen Plateau and hot spot related activity. *Geophys. J. Int.,* 122:899–924.

Chen, C.-Y., and Frey, F.A., 1985. Trace element and isotopic geochemistry of lavas from Haleakala Volcano, East Maui, Hawaii: implications for the origin of Hawaiian basalts. *J. Geophys. Res.,* 90:8743–8768.

Clarke, I., McDougall, I., and Whitford, D.J., 1983. Volcanic evolution of Heard and McDonald Islands, southern Indian Ocean. *In* Oliver, R.L., James, P.R., and Jago, J.B. (Eds.), *Antarctic Earth Science:* Cambridge (Cambridge Univ. Press), 631–635.

Coffin, M.F., 1992. Emplacement and subsidence of Indian Ocean Plateaus and submarine ridges. *In* Duncan, R.A., Rea, D.K., Kidd, R.B., von Rad, U., and Weissel, J.K. (Eds.), Synthesis of results from scientific drilling in the Indian Ocean. *Geophys. Monogr., Am. Geophys. Union,* 70:115–125.

Coffin, M.F., Davies, H.L., and Haxby, W.F., 1986. Structure of the Kerguelen Plateau province from SEASAT altimetry and seismic reflection data. *Nature,* 324:134–136.

Coffin, M.F., and Eldholm, O., 1994. Large igneous provinces: crustal structure, dimensions, and external consequences. *Rev. Geophys.,* 32:1–36.

Coffin, M.F., and Gahagan, L.M., 1995. Ontong Java and Kerguelen Plateau: Cretaceous Islands? *J. Geol. Soc. Spec. Publ. London,* 152:1047–1052.

Coffin, M.F., Munschy, M., Colwell, J.B., Schlich, R., Davies, H.L., and Li, Z.-G., 1990. Seismic stratigraphy of the Raggatt Basin, Southern Kerguelen Plateau: tectonic and paleoceanographic implications. *Geol. Soc. Am. Bull.,* 102:563–579.

Davies, H., Sun, S.S., Frey, F.A., Gautier, I., McCulloch, M.T., Price, R.C., Bassias, Y., Klootwijk, C.T., and Leclaire, L., 1989. Basalt basement from the Kerguelen Plateau and the trail of a Dupal plume. *Contrib. Mineral. Petrol.,* 103:457–469.

Dosso, L., Bougault, H., Beuzart, P., Calvez, J.-Y., and Joron, J.-L., 1988. The geochemical structure of the South-East Indian Ridge. *Earth Planet. Sci. Lett.,* 88:47–49.

Duncan, R.A., 1991. Age distribution of volcanism along aseismic ridges in the eastern Indian Ocean. *In* Weissel, J., Peirce, J., Taylor, E., Alt, J., et al., *Proc. ODP, Sci. Results,* 121: College Station, TX (Ocean Drilling Program), 507–517.

Duncan, R.A., and Storey, M., 1992. The life cycle of Indian Ocean hotspots. *In* Duncan, R.A., Rea, D.K., Kidd, R.B., von Rad, U., and Weissel, J.K. (Eds.), *Synthesis of Results from Scientific Drilling in the Indian Ocean.* Geophys. Monogr., Am. Geophys. Union, 70:91–103.

Farnetani, C.G., Richards, M.A., and Ghiorso, M.S., 1996. Petrological models of magma evolution and deep crustal structure beneath hotspots and flood basalt provinces. *Earth Planet. Sci. Lett.,* 143:81–94.

Fitton, J.G., Hardarson, B.S., Ellam, R.M., Rogers, G., 1998a. Sr-, Nd-, and Pb-isotopic composition of volcanic rocks from the southeast Greenland Margin at 63°N: temporal variation in crustal contamination during continental breakup. *In* Saunders, A.D., Larsen, H.C., and Wise, S.W., Jr. (Eds.), *Proc. ODP, Sci. Results,* 152: College Station, TX (Ocean Drilling Program), 351–357.

Fitton, J.G., Saunders, A.D., Larsen, L.M., Hardarson, B.S., and Norry, M.J., 1998b. Volcanic rocks from the southeast Greenland Margin at 63°N: composition, petrogenesis, and mantle sources. *In* Saunders, A.D., Larsen, H.C., and Wise, S.W., Jr. (Eds.), *Proc. ODP, Sci. Results,* 152: College Station, TX (Ocean Drilling Program), 331–350.

Fitton, J.G., Saunders, A.D. Norry, M.J., Hardarson, B.S., and Taylor, R., 1997. Thermal and chemical structure of the Iceland plume. *Earth Planet. Sci. Lett.,* 153:97–208.

Frey, F.A., Jones, W.B., Davies, H., and Weis, D., 1991. Geochemical and petrologic data for basalts from Sites 756, 757, and 758: implications for the origin and evolution of the Ninetyeast Ridge. *In* Weissel, J., Peirce, J., Taylor, E., Alt, J., et al., *Proc. ODP, Sci. Results,* 121: College Station, TX (Ocean Drilling Program), 611–659.

Frey, F.A., McNaughton, N.J., Nelson, D.R., deLaeter, J.R., and Duncan, R.A., 1996. Petrogenesis of the Bunbury Basalt, Western Australia: interaction between the Kerguelen plume and Gondwana lithosphere? *Earth Planet. Sci. Lett.,* 144:163–183.

Frey, F.A., and Weis, D., 1995. Temporal evolution of the Kerguelen plume: geochemical evidence from ~38 to 82 Ma lavas forming the Ninetyeast Ridge. *Contrib. Mineral. Petrol.,* 121:12–28.

————, 1996. Reply to Class et al. discussion of "Temporal evolution of the Kerguelen plume: geochemical evidence from ~38 to 82 Ma lavas forming the Ninetyeast Ridge." *Contrib. Mineral. Petrol.,* 124:104–110.

Frey, F.A,. Weis, D., Yang H.-J., Nicolaysen, K., Leyrit, H., and Giret, A., in press. Temporal geochemical trends in the Kerguelen Archipelago: evidence for decreasing magma supply from the Kerguelen plume. *Chem. Geol.*

Fritsch, B., Schlich, R., Munschy, M., Fezga, F., and Coffin, M.F., 1992. Evolution of the southern Kerguelen Plateau deduced from seismic stratigraphic studies and drilling at Sites 748 and 750. *In* Wise, S.W., Jr., Schlich, R., et al., *Proc. ODP, Sci. Results,* 120: College Station, TX (Ocean Drilling Program), 895–906.

Fröhlich, F., and Wicquart, E., 1989. Upper Cretaceous and Paleogene sediments from the northern Kerguelen Plateau. *Geo-Mar. Lett.,* 9:127–133.

Gautier, I., Weis, D., Mennessier, J.-P., Vidal, P., Giret, A., and Loubet, M., 1990. Petrology and geochemistry of the Kerguelen Archipelago basalts (South Indian Ocean): evolution of the mantle sources from ridge to intraplate position. *Earth Planet. Sci. Lett.,* 100:59–76.

Giret, A., and Beaux, J.-F., 1984. The plutonic massif of Val Gabbro (Kerguelen Islands), a tholeiitic complex related to the activity of the East-Indian paleo-ridge. *C. R. Acad. Sci. Ser. 2,* 299:965–970.

Gladczenko, T.P., Coffin, M.F., Eldholm, O., and Symonds, P., 1997. Kerguelen Plateau tectonic fabric and crustal structure. *Eos,* 78:712.

Hamelin, B., Dupré, B., and Allègre, C.-J., 1985/1986. Pb-Sr-Nd isotopic data of Indian Ocean ridges: new evidence for large-scale mapping of mantle heterogeneities. *Earth Planet. Sci. Lett.,* 76:288–298.

Hassler, D.R., and Shimizu, N., 1998. Osmium isotopic evidence for ancient subcontinental lithosphere mantle beneath the Kerguelen Islands, Southern Indian Ocean. *Science,* 280:416–421.

Head, J.W., III, and Coffin, M.F., 1997. Large igneous provinces: a planetary perspective. *In* Mahoney, J.J., and Coffin, M.F. (Eds.), *Large Igneous Provinces: Continental, Oceanic, and Planetary Flood Volcanism*. Geophys. Monogr., Am. Geophys. Union, 100:411–438.

Hofmann A.W., 1997. Mantle geochemistry: the message from oceanic volcanism. *Nature,* 385:219–229.

Houtz, R.E., Hayes, D.E., and Markl, R.G., 1977. Kerguelen Plateau bathymetry, sediment distribution and crustal structure. *Mar. Geol.,* 25:95–130.

Ingram, B.L., Coccioni, R., Montanari, A., and Richter, F.M., 1994. Strontium isotopic composition of Mid-Cretaceous seawater. *Science,* 264:546–550.

Jones, C.E., Jenkyns, H.C., Coe, A.L., and Hesselbo, S.P., 1994. Strontium isotopic variations in Jurassic and Cretaceous seawater. *Geochim. Cosmochim. Acta.,* 58:3063–3074.

Kent, R.W., and McKenzie, D., 1994. Rare earth element inversion models for basalts associated with the Kerguelen mantle plume. *Mineral. Mag.,* 58:471–472.

Kent, W., Saunders, A.D., Kempton, P.D., and Ghose, N.C., 1997. Rajmahal Basalts, eastern India: mantle sources and melt distribution at a volcanic rifted margin. *In* Mahoney, J.J., and Coffin, M.F. (Eds.), *Large Igneous Provinces: Continental, Oceanic and Planetary Flood Volcanism.* Geophys. Monogr., Am. Geophys. Union, 100:145–182.

Könnecke, L., and Coffin, M.F., 1994. Tectonics of the Kerguelen Plateau, Southern Indian Ocean. *Eos,* 75:154.

Könnecke, L., Coffin, M.L., and Charvis, P., 1998. Early development of the Southern Kerguelen Plateau (Indian Ocean) from ocean bottom seismograph and multichannel seismic reflection data. *J. Geophys. Res.,* 103:24085–24108.

Könnecke, L.K., Coffin, M.F., Charvis, P., Symonds, P.A., Ramsay, D., and Bernadel, G., 1997. Crustal structure of Elan Bank, Kerguelen Plateau. *Eos,* 78:712.

Larson, R.L., 1991. Geological consequences of superplumes. *Geology,* 19:963–966.

Le Bas, M.J., Le Maitre, R.W., Streckeisen, A., and Zanettin, B., 1986. A chemical classification of volcanic rocks based on the total alkali-silica diagram. *J. Petrol.,* 27:745–750.

Leclaire, L., Bassias, Y., Denis-Clochiatti, M., Davies, H.L., Gautier, I., Gensous, B., Giannesini, P.-J., Patriat, P., Ségoufin, J., Tesson, M., and Wannesson, J., 1987. Lower Cretaceous basalt and sediments from the Kerguelen Plateau. *Geo-Mar. Lett.,* 7:169–176.

Li, Z.G., 1988. Structure, origin et évolution du plateau de Kerguelen [These de Doctorat]. Univ. Louis Pasteur, Strasbourg, France.

Macdonald, G.A., and Katsura, T., 1964. Chemical composition of Hawaiian lavas. *J. Petrol.,* 5:82–133.

Mahoney, J., Jones, W., Frey, F.A., Salters, V., Pyle, D., and Davies, H., 1995. Geochemical characteristics of lavas from Broken Ridge, the Naturaliste Plateau and southernmost Kerguelen Plateau: early volcanism of the Kerguelen hotspot. *Chem. Geol.,* 120:315–345.

Mahoney, J.J., and Coffin, M.F. (Eds.), 1997. *Large Igneous Provinces: Continental, Oceanic, and Planetary Flood Volcanism.* Am. Geophys. Union, Geophys. Monogr., 100.

Mahoney, J.J., Macdougall, J.D., Lugmair, G.W., and Gopalan, K., 1983. Kerguelen hotspot source for Rajmahal Traps and Ninetyeast Ridge? *Nature,* 303:385–389.

Mahoney, J.J., White, W.M., Upton, B.G.J., Neal, C.R., and Scrutton, R.A., 1996. Beyond EM-1: lavas from Afanasy-Nikitin rise and the Crozet archipelago, Indian Ocean. *Geology,* 24:615–618.

Mattielli, N., Weis, D., Scoates, J.S., Shimizu, N., Mennessier, J.-P., Gregoire, M., Cottin, J-Y., and Giret, A., in press. Evolution of heterogeneous lithospheric mantle in a plume environment beneath the Kerguelen Archipelago. *J. Petrol.*

Mehl, K.W., Bitschene, P. R., Schminke, H.-U., and Hertogen, J., 1991. Composition, alteration, and origin of the basement lavas and volcaniclastic rocks at Site 738, southern Kerguelen Plateau. *In* Barron, J., Larsen, B., et al., *Proc. ODP, Sci. Results,* 119: College Station, TX (Ocean Drilling Program), 299–322.

Michard, A., Montigny, R., and Schlich, R., 1986. Geochemistry of the mantle beneath the Rodriguez Triple Junction and the South-East Indian Ridge. *Earth Planet. Sci. Lett.,* 78:104–114.

Montigny, R., Karpoff, A.-M., and Hofmann, C., 1993. Résultats d'un dragage par 55°18′S–83°04′E dans le Bassin de Labuan (campagne MD 67, océan Indien méridional): implications géodynamiques. *Geol. Fr.,* 83.

Morgan, W.J., 1971. Convection plumes in lower mantle. *Nature,* 230:42–43.

Morgan, W.J., 1981. Hotspot tracks and the opening of the Atlantic and Indian Oceans. *In* Emiliani, C. (Ed.), *The Sea* (Vol. 7): New York (Wiley), 443–487.

Müller R.D., Royer J.Y., and Lawver L.A., 1993. Revised plate motions relative to the hotspots from combined Atlantic and Indian-Ocean hotspot tracks. *Geology,* 21:275–278.

Munschy, M., Dyment, J., Boulanger, M.O., Boulanger, D., Tissot, J.D., Schlich, R., Rotstein, Y., and Coffin, M.F., 1992. Breakup and seafloor spreading between the Kerguelen Plateau-Labuan Basin and the Broken Ridge-Diamantina Zone. *In* Wise, S.W., Jr., Schlich, R., et al., *Proc. ODP, Sci. Results,* 120: College Station, TX (Ocean Drilling Program), 931–944.

Munschy, M., Fritsch, B., Schlich, R., and Rotstein, Y., 1994. Tectonique extensive sur le Plateau de Kerguelen. *Mem. Soc. Geol. Fr.,* 166:99–108.

Mutter, J.C., and Cande, S.C., 1983. The early opening between Broken Ridge and Kerguelen Plateau. *Earth Planet. Sci. Lett.,* 65:369–376.

Nicolaysen, K., Frey, F.A., Hodges, K.V., Weis, D., and Giret, A., in press. $^{40}Ar/^{39}Ar$ geochronology of flood basalts from the Kerguelen Archipelago, southern Indian Ocean: implication for Cenozoic eruption rates of the Kerguelen plume. *Earth Planet. Sci. Lett.*

Nicolaysen, K., Frey, F.A., Hodges, K., Weis, D., Giret, A., and Leyrit, H., 1996. $^{40}Ar/^{39}Ar$ geochronology of flood basalts forming the Kerguelen Archipelago. *Eos,* 77:824.

Nogi, Y., Seama, N., Isezaki, N., and Fukuda, Y., 1996. Magnetic anomaly lineations and fracture zones deduced from vector magnetic anomalies in the West Enderby Basin. *In* Storey, B.C., King, E.C., and Livermore, R.A. (Eds.), *Weddell Sea Tectonics and Gondwana Break-up.* Geol. Soc. Spec. Publ. London, 108:265–273.

Operto, S., and Charvis, P., 1995. Kerguelen Plateau: a volcanic passive margin fragment? *Geology,* 23:137–140.

————, 1996. Deep structure of the southern Kerguelen Plateau (southern Indian Ocean) from ocean bottom seismometer wide-angle seismic data. *J. Geophys. Rev.,* 101:25077–25103.

Peirce, J., Weissel, J., et al., 1989. *Proc. ODP, Init. Repts.,* 121: College Station, TX (Ocean Drilling Program).

Peng, Z.X., and Mahoney, J.J., 1995. Drill hole lavas from the northwestern Deccan Traps, and the evolution of the Réunion hotspot mantle. *Earth Planet. Sci. Lett.,* 134:169–185.

Plank, T., and Langmuir, C.H., 1998. The chemical composition of subducting sediment and its consequences for the crust and mantle. *Chem. Geol.,* 145:325–494.

Pratson, E.L., Broglia, C., and Castillo, D., 1992. Geochemical well logs from the Argo Abyssal Plain and Exmouth Plateau, northeast Indian Ocean, Sites 765 and 766 of Leg 123. *In* Gradstein, F.M., Ludden, J.N., et al., *Proc. ODP, Sci. Results,* 123: College Station, TX (Ocean Drilling Program), 637–656.

Pringle, M.S., Storey, M., and Wijbrans, J., 1994. $^{40}Ar/^{39}Ar$ geochronology of mid-Cretaceous Indian ocean basalts: constraints on the origin of large flood basalt. *Eos,* 75:728.

Quilty, P.G., Shafik, S., McMinn, A., Brady, H., and Clarke, I., 1983. Microfossil evidence for the age and environment of deposition of sediments of Heard and McDonald islands. *In* Oliver, R.L., James, P.R., and Jago, J.B. (Eds.), *Antarctic Earth Science:* Cambridge (Cambridge Univ. Press), 636–639.

Recq, M., Bréfort, D., Malod, J., and Veinante, J.-L., 1990. The Kerguelen Isles (southern Indian Ocean): new results on deep structure from refraction profiles. *Tectonophysics,* 182:227–248.

Recq, M., and Charvis, P., 1986. A seismic refraction survey in the Kerguelen isles, Southern Indian Ocean. *Geophys. J. R. Astron. Soc.,* 84:529–559.

Recq, M., Le Roy, I., Charvis, P., Goslin, J., and Bréfort, D., 1994. Structure profonde du mont Ross d'après la réfraction sismique (les Kerguelen, océan Indien austral). *Can. J. Earth Sci.,* 31:1806–1821.

Rotstein, Y., Munschy, M., Schlich, R., and Hill, P.J., 1991. Structure and early history of the Labuan Basin, South Indian Ocean. *J. Geophys. Res.,* 96:3887–3904.

Rotstein, Y., Schlich, R., Munschy, M., and Coffin, M.F., 1992. Structure and tectonic history of the southern Kerguelen Plateau (Indian Ocean) deduced from seismic reflection data. *Tectonics,* 11:1332–1347.

Royer, J.-Y., and Coffin, M.P., 1992. Jurassic to Eocene plate tectonic reconstructions in the Kerguelen Plateau region. *In* Wise, S.W., Jr., Schlich, R., et al., *Proc. ODP, Sci. Results,* 120: College Station, TX (Ocean Drilling Program), 917–928.

Royer, J.-Y., Peirce, J.W., and Weissel, J.K., 1991. Tectonic constraints on the hotspot formation of the Ninetyeast Ridge. *In* Weissel, J., Peirce, J., Taylor, E., Alt, J., et al., *Proc. ODP, Sci. Results,* 121: College Station, TX (Ocean Drilling Program), 763–776.

Royer, J.Y., and Rollet, N., 1997. Plate-tectonic setting of the Tasmanian region. *In* Exon, N.F., and Crawford, A.J., (Eds.), *Aust. J. Earth Sci.*, 44:543–560.

Royer, J.-Y., and Sandwell, D.T., 1989. Evolution of the eastern Indian Ocean since the Late Cretaceous: constraints from GEOSAT altimetry. *J. Geophys. Res.,* 94:13755–13782.

Rudnick, R.L., and Fountain, D.M., 1995. Nature and composition of the continental crust: a lower crustal perspective. *Rev. Geophys.*, 33:267–309.

Salters, V.J.M., Storey, M., Sevigny, J.H., and Whitechurch, H., 1992. Trace element and isotopic characteristics of Kerguelen-Heard Plateau basalts. *In* Wise, S.W., Jr., Schlich, R., et al., *Proc. ODP, Sci. Results,* 120: College Station, TX (Ocean Drilling Program), 55–62.

Sandwell, D.T., and Smith, W.H.F., 1997. Marine gravity anomaly from Geosat and ERS-1 satellite altimetry. *J. Geophys. Res.,* 102:10039–10054.

Saunders, A.D., Larsen, H.C., and Fitton, J.G., 1998. Magmatic development of the southeast Greenland Margin and evolution of the Iceland Plume: geochemical constraints from Leg 152. *In* Saunders, A.D., Larsen, H.C., and Wise, S.W., Jr. (Eds.), *Proc. ODP, Sci. Results,* 152: College Station, TX (Ocean Drilling Program), 479–501.

Saunders, A.D., Storey, M., Gibson, I.L., Leat, P., Hergt, J., and Thompson, R.N., 1991. Chemical and isotopic constraints on the origin of basalts from Ninetyeast Ridge, Indian Ocean: results from DSDP Legs 22 and 26 and ODP Leg 121. *In* Weissel, J., Peirce, J., Taylor, E., Alt, J., et al., *Proc. ODP, Sci. Results,* 121: College Station, TX (Ocean Drilling Program), 559–590.

Schaming, M., and Rotstein, Y., 1990. Basement reflectors in the Kerguelen Plateau, South Indian Ocean: indications for the structure and early history of the plateau. *Geol. Soc. Am. Bull.,* 102:580–592.

Schlich, R., 1975. Structure et âge de l'océan Indien occidental. *Mem. Hors-Ser. Soc. Geol. Fr.,* 6:1–103.

Schlich, R., Coffin, M.F., Munschy, M., Stagg, H.M.J., Li, Z.G., and Revill, K., 1987. *Bathymetric Chart of the Kerguelen Plateau.* Jointly edited by Bureau of Mineral Resources, Geology and Geophysics, Canberra, Australia, Institut de Physique du

Globe, Strasbourg, France, and Terres Australes et Antarctiques Francaises, Paris, France, 1:5,000,000.

Schlich, R., Rotstein, Y., and Schaming, M., 1993. Dipping basement reflectors along volcanic passive margins—new insight using data from the Kerguelen Plateau. *Terra Nova,* 5:157–163.

Schlich, R., and Wise, S.W., Jr., 1992. The geologic and tectonic evolution of the Kerguelen Plateau: an introduction to the scientific results of Leg 120. *In* Wise, S.W., Jr., Schlich, R., et al., *Proc. ODP, Sci. Results,* 120: College Station, TX (Ocean Drilling Program), 5–30.

Schlich, R., Wise, S.W., Jr., et al., 1989. *Proc. ODP, Init. Repts.,* 120: College Station, TX (Ocean Drilling Program).

Sevigny, J.H., Whitechurch, H., Storey, M., and Salters, V.J.M., 1992. Zeolite-facies metamorphism of central Kerguelen Plateau basalts. *In* Wise, S.W., Jr., Schlich, R., et al., *Proc. ODP, Sci. Results,* 120: College Station, TX (Ocean Drilling Program), 63–69.

Stein, M., and Hofmann, A.W., 1994. Mantle plumes and episodic crustal growth. *Nature,* 373:63–68.

Storey, M., Kent, R.W., Saunders, A.D., Salters, V.J., Hergt, J., Whitechurch, H., Sevigny, J.H., Thirlwall, M.F., Leat, P., Ghose, N.C., and Gifford, M., 1992. Lower Cretaceous volcanic rocks on continental margins and their relationship to the Kerguelen Plateau. *In* Wise, S.W., Jr., Schlich, R., et al., *Proc. ODP, Sci. Results,* 120: College Station, TX (Ocean Drilling Program), 33–53.

Storey, M., Mahoney, J.J., Kroenke, L., and Saunders, A.D., 1991. Are oceanic plateaus sites of komatiite formation? *Geology,* 19:376–379.

Storey, M., Pringle, M.S., Coffin, M.F., and Wijbrans, J., 1996. Geochemistry and geochronology of Kerguelen Plateau basalts: results from ODP Legs 119 and 120. *Eos,* 77:123.

Storey, M., Saunders, A.D., Tarney, J., Gibson, I.L., Norry, M.J., Thirlwall, M.F., Leat, P., Thompson, R.N., and Menzies, M.A., 1989. Contamination of Indian Ocean asthenosphere by the Kerguelen-Heard mantle plume. *Nature,* 338:574–576.

Sun, S.-S., and McDonough, W.F., 1989. Chemical and isotopic systematics of oceanic basalts: implications for mantle composition and processes. *In* Saunders, A.D., and Norry, M.J. (Eds.), *Magmatism in the Ocean Basins.* Geol. Soc. Spec. Publ. London, 42:313–345.

Thompson, R.N., Morrison, M.A., Hendry, G.L., and Parry, S.J., 1984. An assessment of the relative roles of crust and mantle in magma genesis: an elemental approach. *Philos. Trans. R. Soc. London A,* 310:549–590.

Weaver, S.D., and Tarney, J., 1984. Empirical approach to estimating the composition of continental crust. *Nature,* 310:575–577.

Weis, D., Bassias, Y., Gautier, I., and Mennesier, J.-P., 1989. DUPAL anomaly in existence 115 Ma ago: evidence from isotopic study of the Kerguelen Plateau (South Indian Ocean). *Geochim. Cosmochim. Acta,* 53:2125–2131.

Weis, D., Damasceno, D., Scoates, J.S., Schlich, R., Schaming, M., Montigny, R., and Frey, F.A., 1998a. Submarine alkali lavas (14–10 Ma) erupted between Heard Island and the Kerguelen Archipelago, Indian Ocean. *Eos,* 79:944.

Weis, D., and Frey, F.A., 1991. Isotope geochemistry of Ninetyeast Ridge basement basalts: Sr, Nd, and Pb evidence for involvement of the Kerguelen hot spot. *In* Weissel, J., Peirce, J., Taylor, E., Alt, J., et al., *Proc. ODP, Sci. Results,* 121: College Station, TX (Ocean Drilling Program), 591–610.

Weis, D., Frey, F.A., Giret, A., and Cantagrel, J.M., 1998b. Geochemical characteristics of the youngest volcano (Mount Ross) in the Kerguelen Archipelago: inferences for magma flux and composition of the Kerguelen plume. *J. Petrol.,* 39:973–994.

Weis, D., Frey, F.A., Leyrit, H., and Gautier, I., 1993. Kerguelen Archipelago revisited: geochemical and isotopic study of the Southeast Province lavas. *Earth Planet. Sci. Lett.,* 118:101–119.

Weis, D., White, W.M., Frey, F.A., Duncan, B., Dehn, J., Fisk, M., Ludden, J., Saunders, A., and Storey, M., 1992. The influence of mantle plumes in generation of Indian Ocean crust. *In* Duncan, R.A., Rea, D.K., Kidd, R.B., von Rad, U., and Weissel, J.K. (Eds.), *The Indian Ocean: A Synthesis of Results from the Ocean Drilling Program*. Geophys. Monogr., Am. Geophys. Union, 70:57–89.

Weissel, J.K., and Karner, G.D., 1989. Flexural uplift of rift flanks due to mechanical unloading of the lithosphere during extension. *J. Geophys. Res.,* 94:13919–13950.

White, W.M., McBirney, A.R., and Duncan, R.A., 1993. Petrology and geochemistry of the Galápagos Islands: portrait of a pathological mantle plume. *J. Geophys. Res.,* 98:19533–19563.

Whitechurch, H., Montigny, R., Sevigny, J., Storey, M., and Salters, V.J.M., 1992. K-Ar and ^{40}Ar ages of central Kerguelen Plateau basalts. *In* Wise, S.W., Jr., Schlich, R., et al., *Proc. ODP, Sci. Results,* 120: College Station, TX (Ocean Drilling Program), 71–77.

Yang, H.-J., Frey, F.A., Weis, D., Giret, A., Pyle, D., and Michon, G., 1998. Petrogenesis of the flood basalts forming the northern Kerguelen Archipelago: implications for the Kerguelen plume. *J. Petrol.,* 39:711–748.

Figure F1. Map of the eastern Indian Ocean showing major physiographic features and pre-Leg 183 sites where igneous basement was recovered from the Ninetyeast Ridge, Broken Ridge, and Kerguelen Plateau by DSDP and ODP drilling (circles) and dredging (squares). Rajmahal Traps, lamprophyres, and Bunbury Basalt (BB) are continental volcanics that have been postulated to be related to the Kerguelen plume. Star indicates a proposed location (Skiff Bank) for the Kerguelen hot spot (Müller et al., 1993).

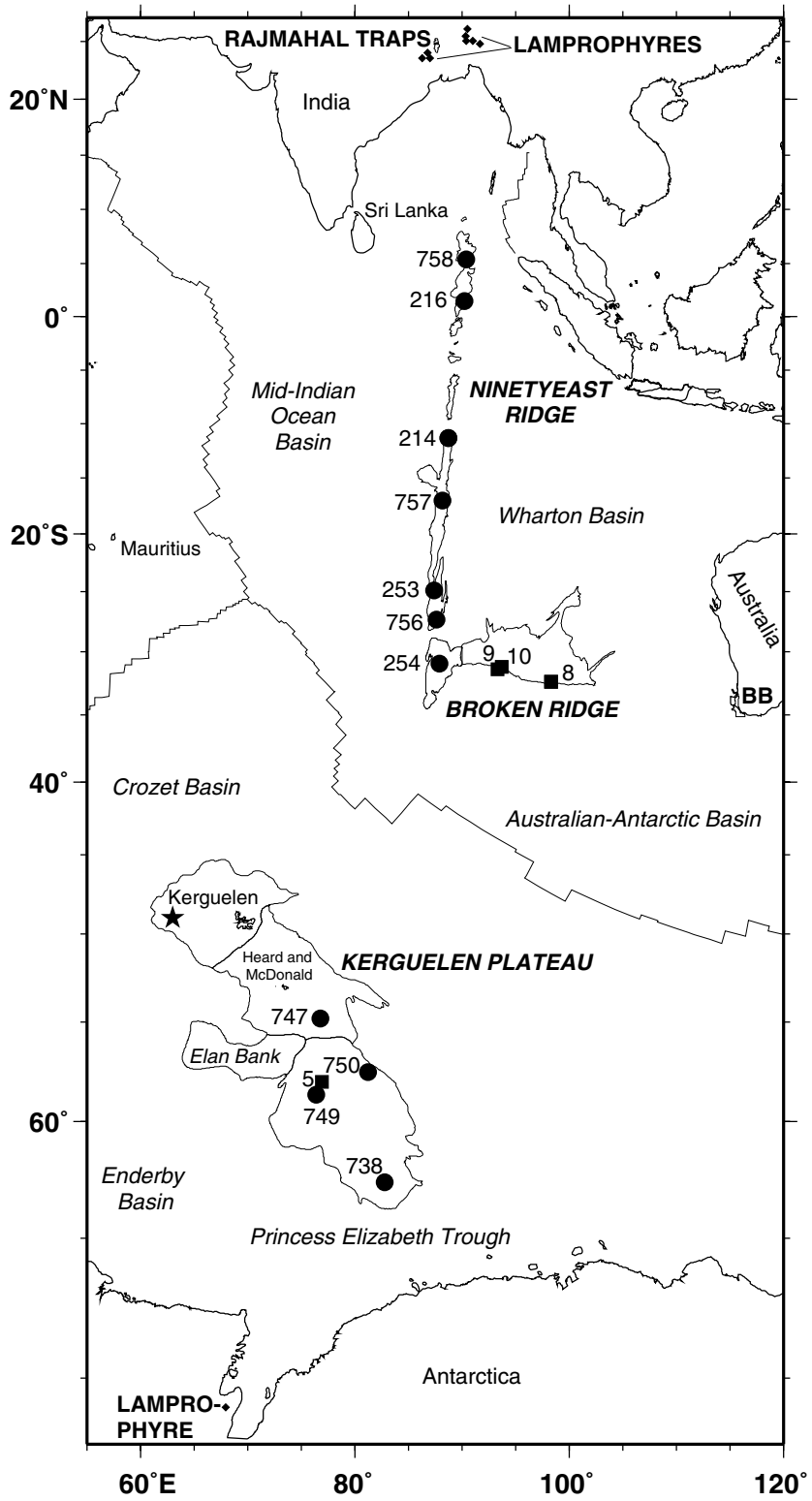

Figure F2. Plate reconstructions of the southern Indian Ocean region (after Royer and Coffin, 1992; Royer and Sandwell, 1989) using a hot spot reference frame (Müller et al., 1993) and keeping Antarctica fixed. Reconstructed position of the Kerguelen hot spot (after Müller et al., 1993) is indicated by stars. Volcanic rocks associated with the Kerguelen plume, as it has appeared through geologic time, are indicated in red shading, and lamprophyres (southeast India and Antarctica) (at 110 Ma) are indicated as diamonds. Dashed line denotes a possible northern boundary for Greater India. IND = India; ANT= Antarctica; AUS = Australia. 130.9 (M1O [o]) and 118.7 (MO [y]) Ma: Seafloor spreading initiates during Chron M11 (~133 Ma) between Western Australia and Greater India. The Bunbury Basalt (BB) of southwest Australia is erupted close to these breakup events in both time and space. Of the two Bunbury Basalt types, the Casuarina may be related to the breakup of Australia and India, influenced by the Kerguelen hot spot, and the Gosselin may represent magmatism associated with the breakup of Australia and Antarctica. Between 130.9 and 118.7 Ma, Antarctica migrates to the southeast relative to the Kerguelen hot spot. 110 and 100 Ma: Seafloor spreading continues among India, Antarctica, and Australia. Rajmahal (RAJ) volcanic rocks postdate breakup of India and Australia by ~15 m.y. (Markl, 1974, 1978) and the breakup of India and Antarctica by ~15–40 m.y. Indian and Antarctic lamprophyres (diamonds) also postdate major breakup events. The first massive pulse of Kerguelen magmatism creates the southern Kerguelen Plateau (SKP) (Figs. **F3,** p. 52, **F4,** p. 53) at ~110 Ma, as Indian Ocean lithosphere migrates southeast relative to the Kerguelen hot spot. 83 (C34n [y]) and 63.6 (C28n [o]) Ma: India continues its northward drift relative to Antarctica, and the Kerguelen hot spot is predicted to have remained close to the northeast edge of the central Kerguelen Plateau (CKP) (Figs. **F3,** p. 52, **F4,** p. 53) and Broken Ridge (BR) (Figs. **F5,** p. 55, **F6,** p. 56), which form at ~85 Ma. Subsequently, the hot spot generates the Ninetyeast Ridge (NER). 40.1 (C18n.2n [o]) and 23.4 (C6cn.1n [y]) Ma: At ~40 Ma, seafloor spreading commences between the CKP and BR. The hot spot generates the northern Kerguelen Plateau (NKP) (Figs. **F3,** p. 52, **F4,** p. 53), and since 40 Ma, as BR and the Kerguelen Plateau continue to separate, produces the Kerguelen Archipelago (KA), Heard and McDonald Islands (Figs. **F3,** p. 52, **F4,** p. 53), and the chain of volcanoes between Kerguelen Archipelago and Heard (Figs. **F3,** p. 52, **F4,** p. 53). (**Figure shown on next page.**)

Figure F2 (continued). (Caption shown on previous page.)

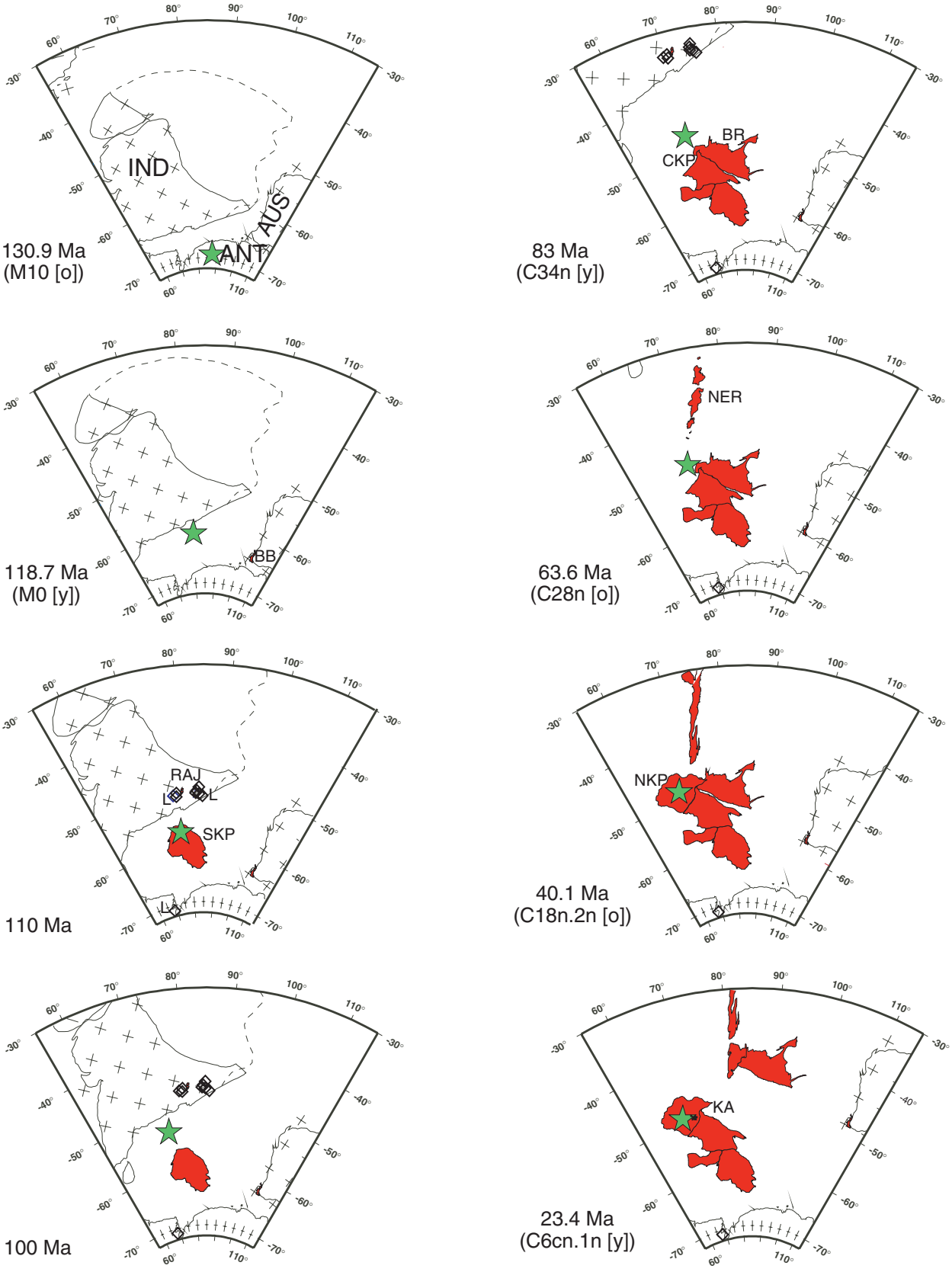

Figure F3. Bathymetry of the Kerguelen Plateau. Leg 119, 120, and 183 drill sites that recovered igneous basement are indicated by filled stars; sites that bottomed in sediment are shown as open stars. Contour interval = 500 m.

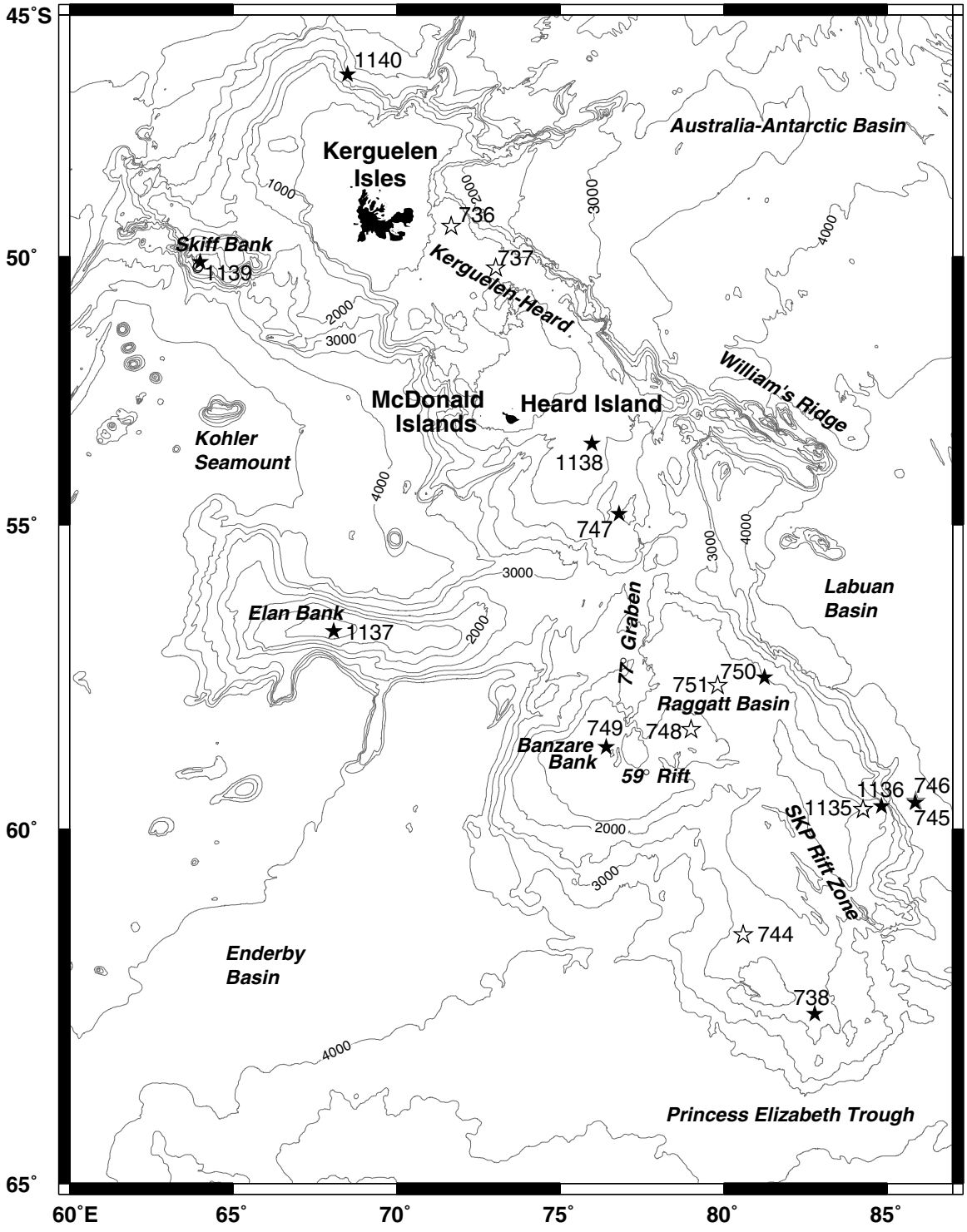

Figure F4. A. Satellite-derived free-air gravity map of the Kerguelen Plateau (after Sandwell and Smith, 1997). The plateau consists of five sectors: northern, central, southern, Elan Bank, and Labuan Basin (outlined in white). Current (Leg 183) and previous (Legs 119 and 120) sites are indicated by stars and circles, respectively (solid symbols = basement sites; open = sediment sites). Squares indicate dredge and piston core sites where igneous rock (solid squares) and sediment (open squares) were recovered. (**Figure shown on next page.**) **B.** An **oversized figure** that includes site lithologies accompanies this volume.

Figure F4 (continued). (Caption shown on previous page.)

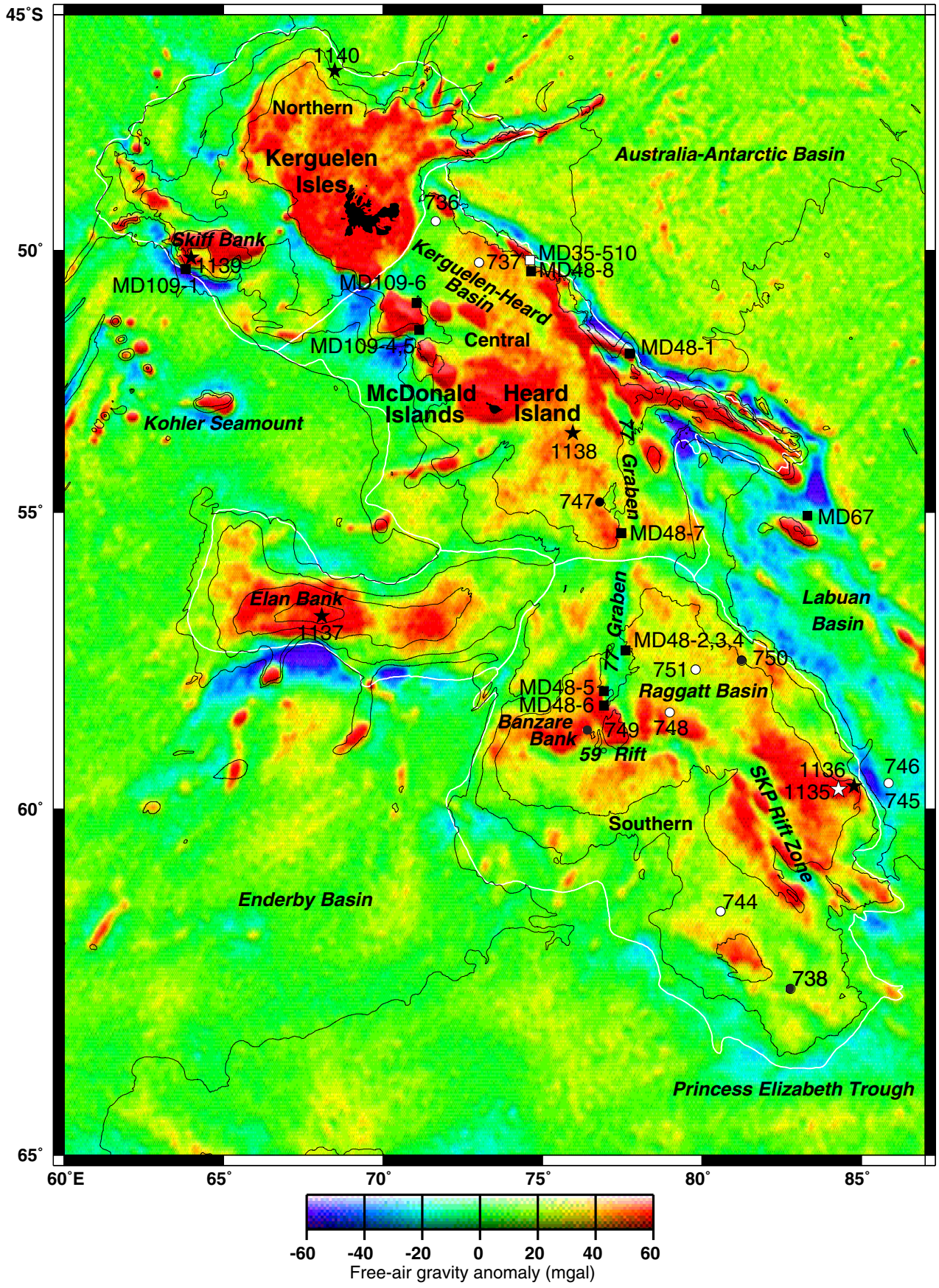

Figure F5. Bathymetry of Broken Ridge. Previous DSDP and ODP drill sites that recovered igneous basement are indicated by solid circles; sites that bottomed in sediment are shown as open circles. Dredge locations (DR-X) that recovered igneous basement are indicated by solid squares. Leg 183 Sites 1141 and 1142 are indicated by a solid star. Contour interval = 500 m.

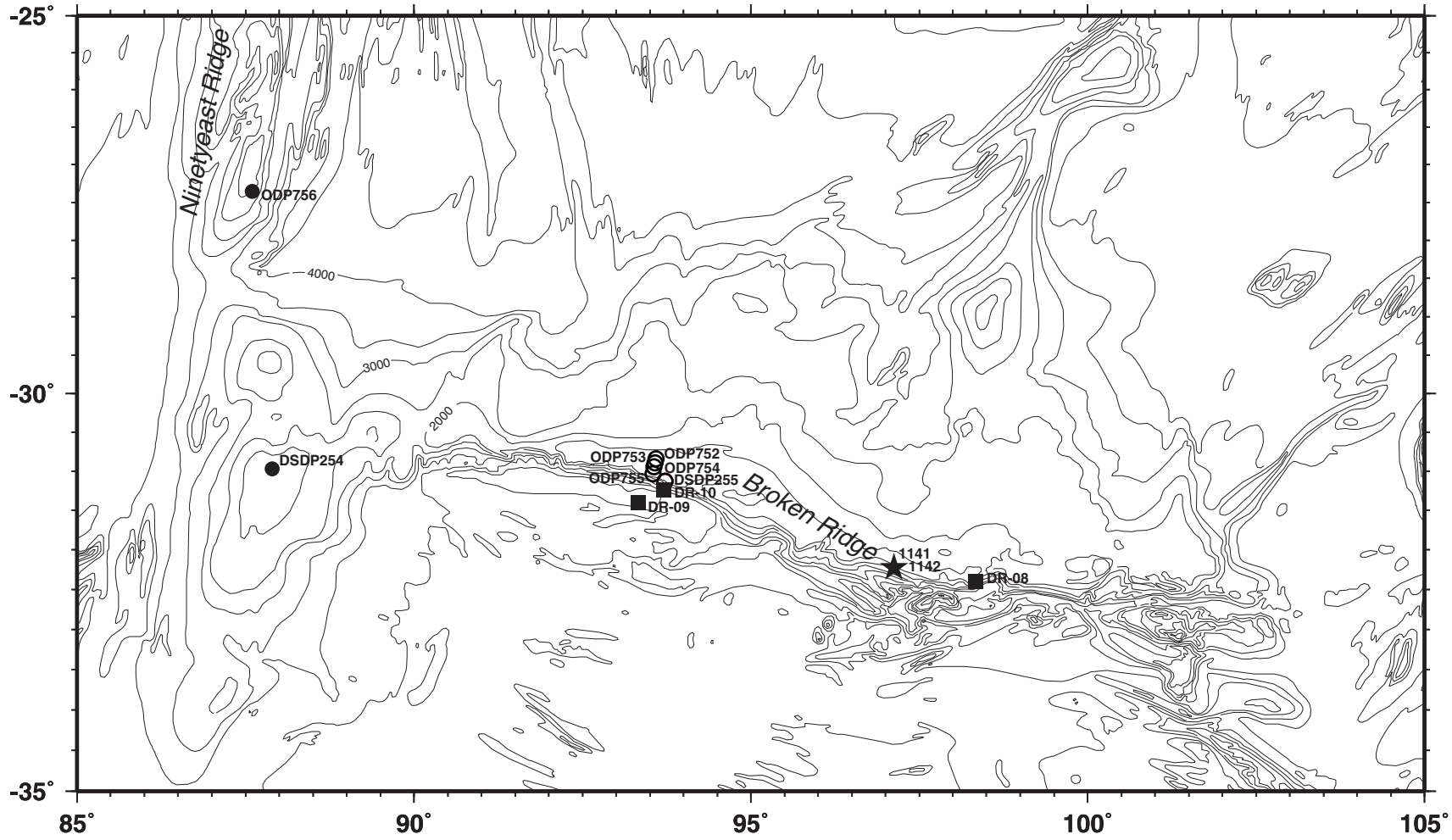

Figure F6. Satellite-derived free-air gravity field for Broken Ridge (after Sandwell and Smith, 1997) showing location of previous ODP/DSDP drill sites (solid circles), locations of the three dredge sites (solid squares), and ODP Leg 183 drill sites (solid star) that recovered basaltic basement. Bathymetric contour interval = 500 m.

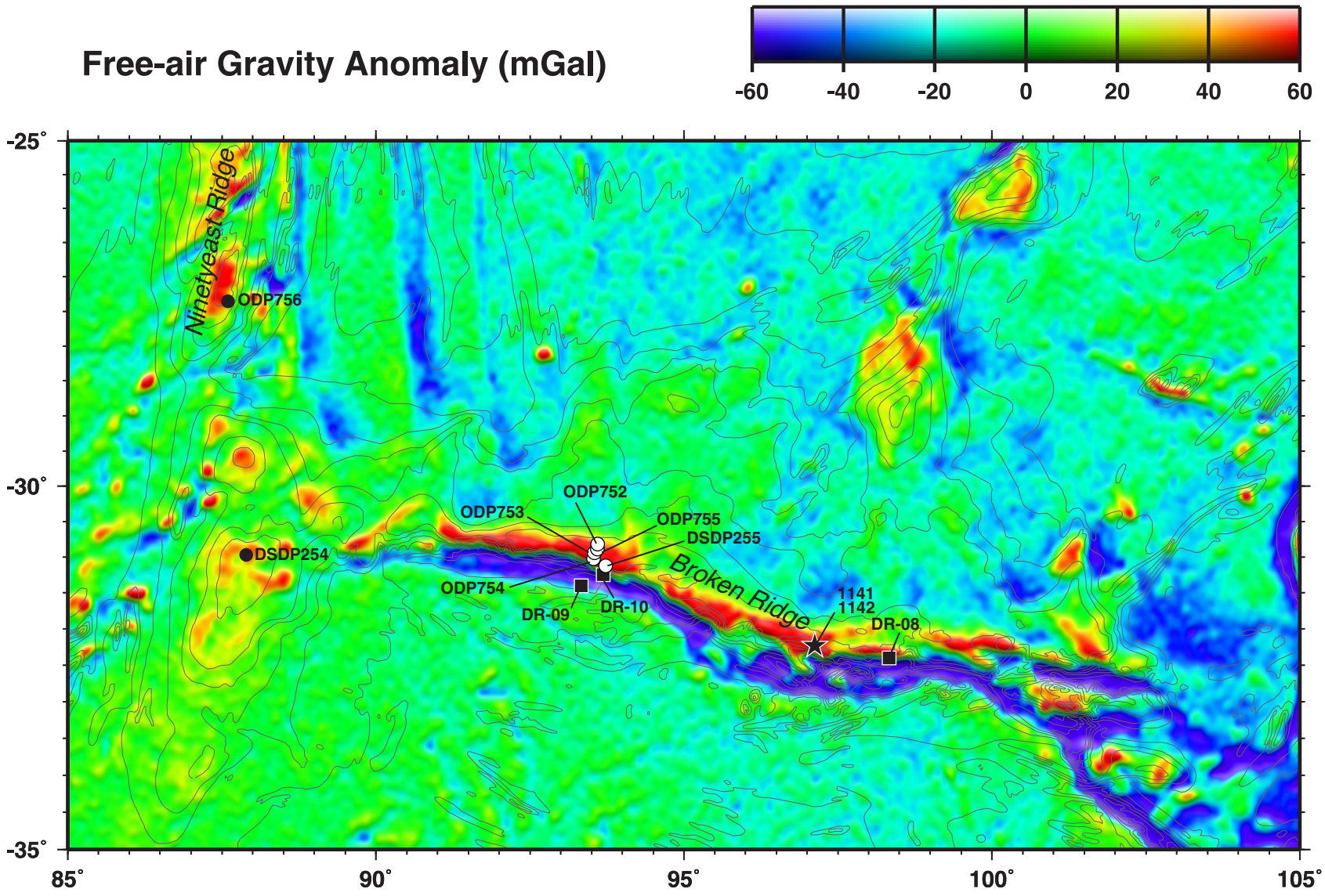

Figure F7. Kerguelen hot spot magma output since ~130 Ma. Volumes for each of the Kerguelen Plateau–Broken Ridge LIP sectors (Coffin and Eldholm, 1994; Coffin and Gahagen, 1995) and radiometric age data (Davies et al., 1989; Whitechurch et al., 1992; Pringle et al., 1994; and Storey et al., 1996) were used to calculate the output; duration of emplacement for each domain was assumed to be equal to ±2 σ values for either single or multiple dates from each domain.

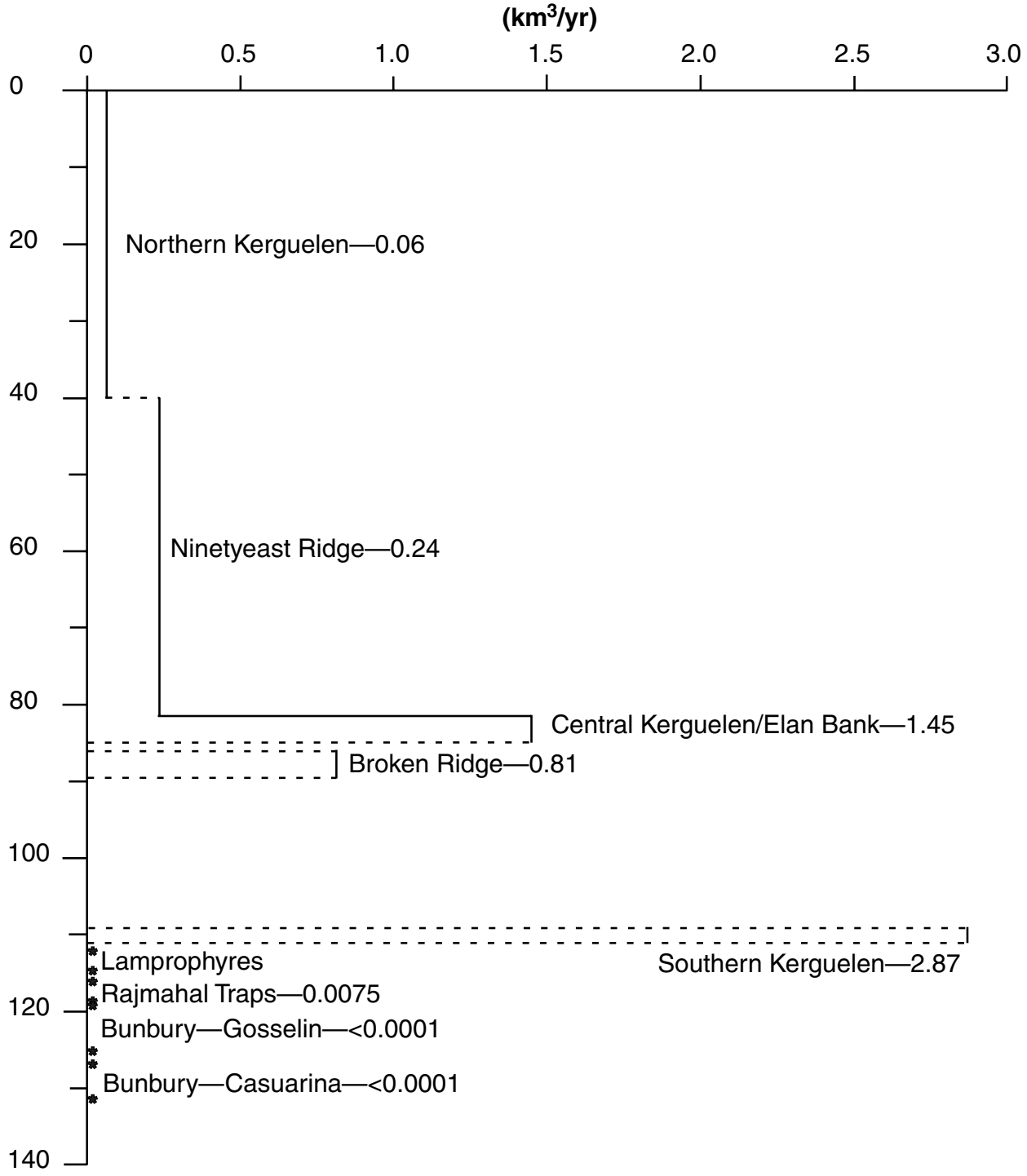

Figure F8. Total alkalis ($Na_2O + K_2O$) vs. SiO_2 plot (wt%) for classifying tholeiitic and alkalic basalts. Boundary line separating alkalic and tholeiitic fields is from Macdonald and Katsura (1964). All analyses are normalized to sum to 100% on an anhydrous basis with FeO adjusted to 80% of total iron. **A.** The open fields show the temporal evolution of Kerguelen Archipelago lavas from the ~30-Ma flood basalts, with compositions transitional between tholeiitic and alkalic lavas (Mts. Bureau and Rabouillère), to the slightly alkalic Southeast Lower Miocene Series (LMS) to the highly alkalic Southeast Upper Miocene Series (UMS). Data sources are Weis et al. (1993, 1998b) and Yang et al. (1998). In contrast, lavas from Kerguelen Plateau ODP Sites 747, 749, and 750 are tholeiitic basalts, except for the above-basement lavas from ODP Site 748, which are alkalic basalts. **B.** Expanded panel showing more detail for basalts drilled and dredged from the Kerguelen Plateau and Broken Ridge. Lavas dredged from the central Kerguelen Plateau and Broken Ridge (open circles) and ODP Site 738 straddle the boundary line, largely because the total alkali contents of these lavas were increased during postmagmatic alteration. As an extreme example, the solid triangle indicates a highly altered sample from ODP Leg 120, Site 750 (Sample 120-750B-19R-1, 47–50 cm). Data from Davies et al. (1989), Storey et al. (1992), and Mahoney et al. (1995).

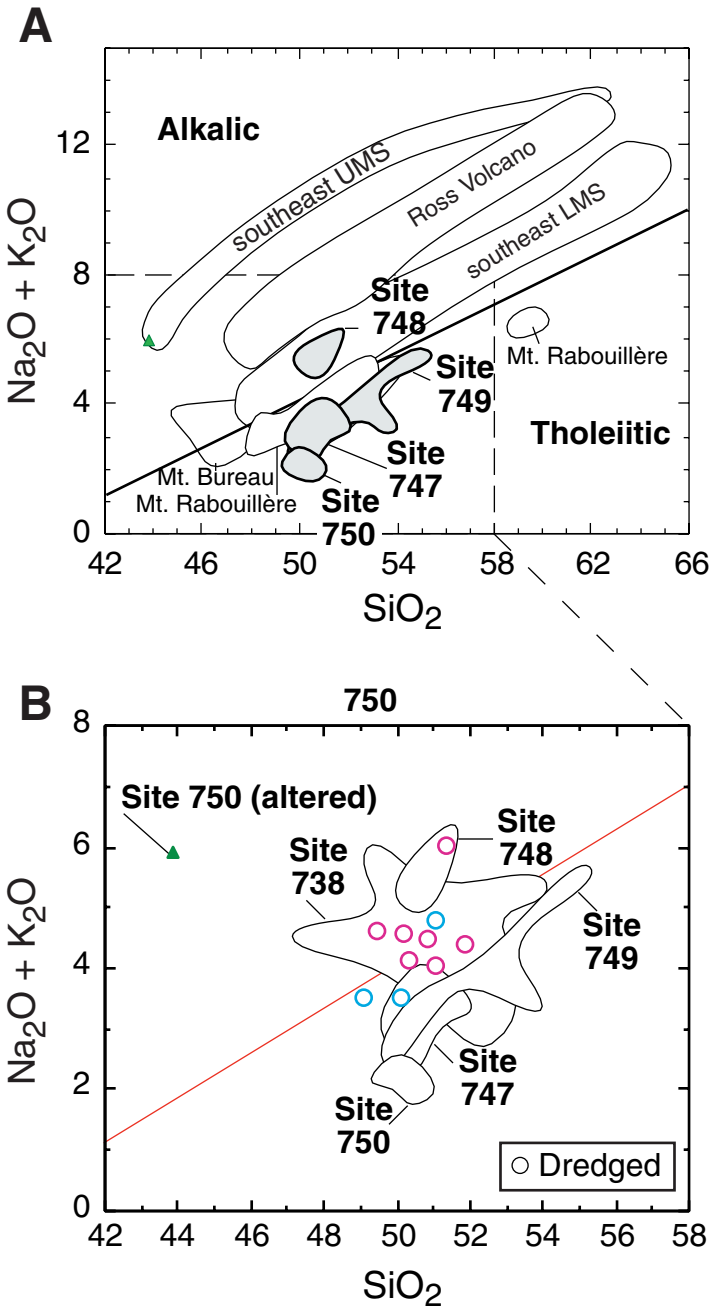

Figure F9. $^{143}Nd/^{144}Nd$ vs. $^{87}Sr/^{86}Sr$ showing data points for basalts recovered from the Kerguelen Plateau and Broken Ridge. The data for Broken Ridge samples are corrected to an eruption age of 88 Ma; the data for dredged Kerguelen Plateau samples are corrected to an eruption age of 115 Ma. The effects of age correction are shown by the two fields (measured and age-corrected) for Site 738 on the southern Kerguelen Plateau. Data for other sites are not age corrected because parent/daughter abundance ratios are not available. Data for Kerguelen Plateau and Broken Ridge samples are from Weis et al. (1989), Salters et al. (1992), and Mahoney et al. (1995). Shown for comparison are fields for Southeast Indian Ridge (Hamelin et al., 1985/1986; Michard et al., 1986; Dosso et al., 1988; J.J. Mahoney, unpubl. data), St. Paul and Heard Islands (Heard data indicated by trajectory of solid line from Barling et al., 1994), the Ninetyeast Ridge (fields labeled NER and NER 216 [DSDP Site 216] from Weis and Frey, 1991, and Frey and Weis, 1995), and the entire Kerguelen Archipelago. Most samples from the Kerguelen Archipelago plot in the subfield labeled "Kerguelen plume?" that Weis et al. (1993, 1998b) interpreted as representative of the Kerguelen plume.

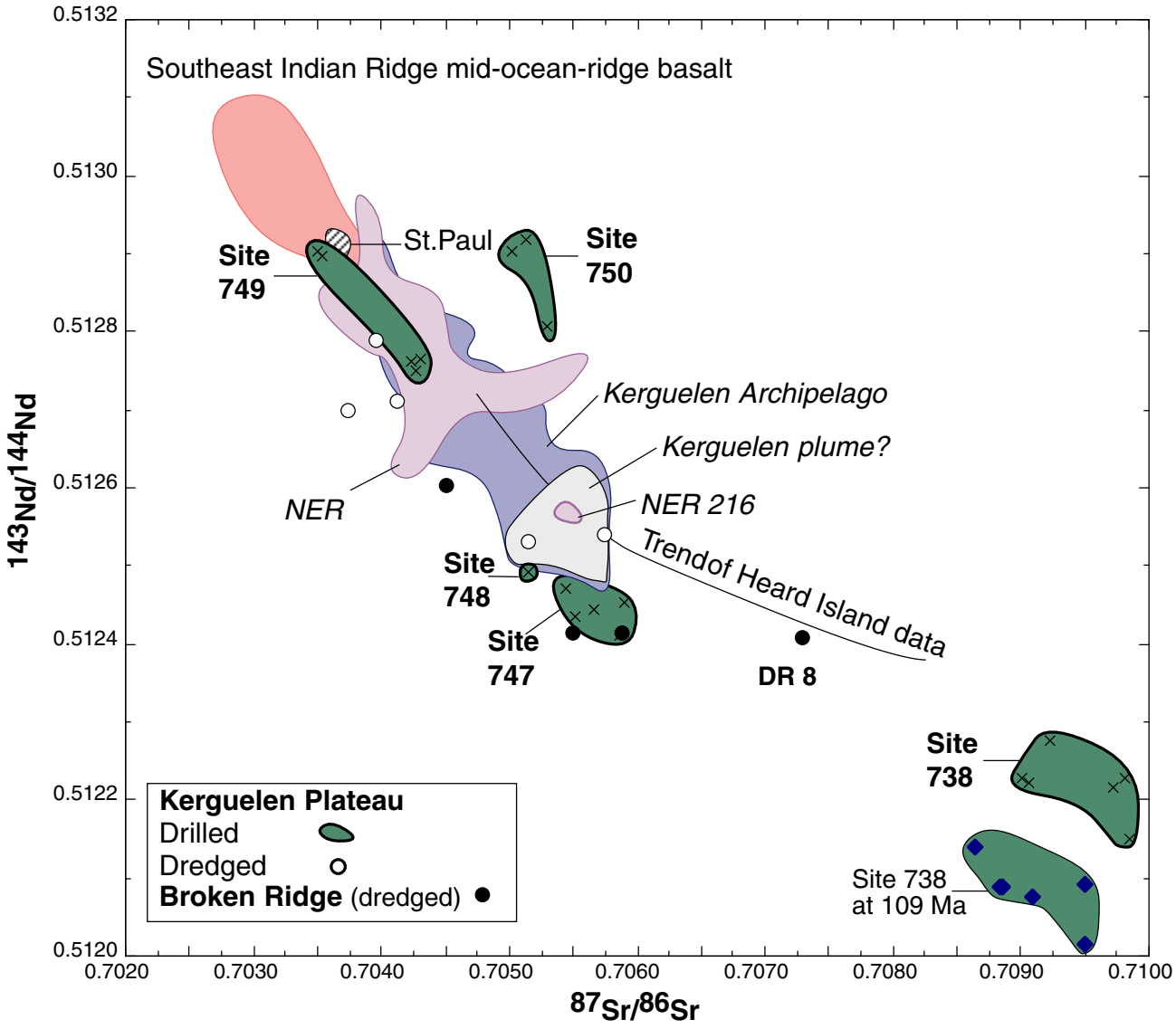

Figure F10. $^{208}Pb/^{204}Pb$ vs. $^{206}Pb/^{204}Pb$ showing measured data points for basalts recovered from the Kerguelen Plateau and Broken Ridge. Shown for comparison are measured fields for Southeast Indian Ridge (two subfields: the field extending to high ratios includes samples near the Amsterdam–St. Paul platform), lavas from St. Paul and Amsterdam Islands (diagonal hatching), and initial ratios for lavas from the Kerguelen Archipelago (shaded area) and the Ninetyeast Ridge (fields labeled NER and NER 216). Data sources are given in Figure F9, p. 59.

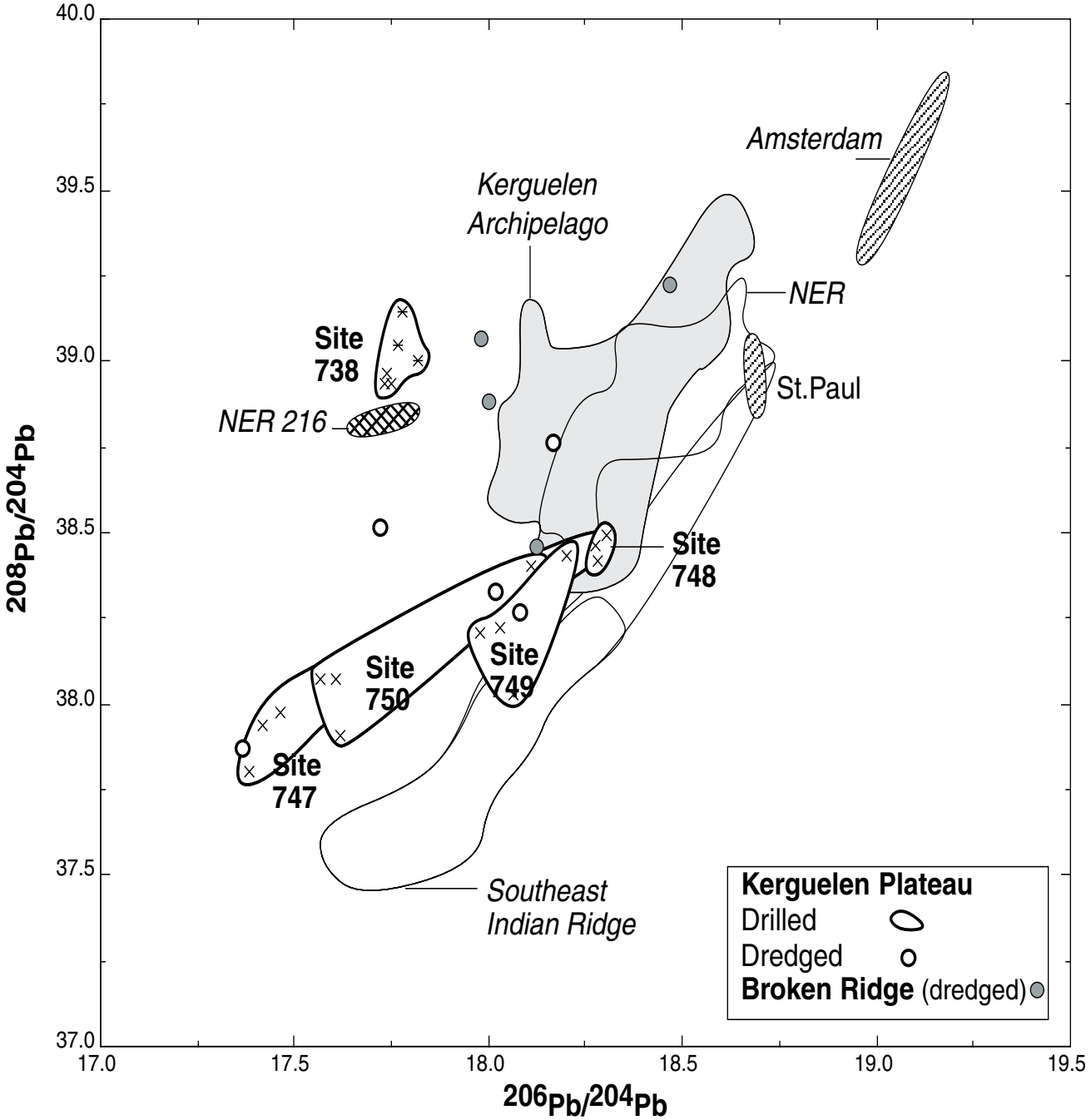

Figure F11. A. Abundance ratios of $(Th/Nb)_N$ vs. $(La/Nb)_N$ (subscript N indicates ratios normalized to primitive mantle values of Sun and McDonough, 1989). Most oceanic island basalts, including ~100 basalts from the Kerguelen Archipelago, have $(Th/Nb)_N < 1$ and $(La/Nb)_N = \sim 1$. In contrast, most continental crust, especially upper crust, is relatively depleted in Nb (and Ta) (e.g., Thompson et. al., 1984) with $(Th/Nb)_N = 5.46$ and $(La/Nb)_N = 2.17$ in average bulk crust (calculated from Rudnick and Fountain, 1995, using revised Nb and Ta values of upper crust from Plank and Langmuir, 1998). As indicated, lower (LC) and upper crustal compositions differ considerably (averages of Rudnick and Fountain, 1995). Furthermore, estimates of lower crustal composition differ significantly; compare LC in the figure (based on Rudnick and Fountain, 1995) with the lower crustal value of Weaver and Tarney (1984) (W&T in figure). Dredge 8 basalts from eastern Broken Ridge and Kerguelen Plateau basalts from Site 738 and dredge basalts from the 77° graben (Kerguelen Plateau Dredges) lie outside the oceanic basalt field, thereby showing that they contain a continental crustal component, an inference consistent with isotope data (Figs. F7, p. 57, F8, p. 58). Also, Kerguelen Plateau samples from Site 747 are offset to high $(La/Nb)_N$, but they have normal $(Th/Nb)_N$; these basalts may have a smaller proportion of a different continental crustal component. Although all Kerguelen Archipelago flood basalts lie within the field for normal oceanic basalts, lavas of the Heard Island–Big Ben basaltic series trend to high $(Th/Nb)_N$. This trend is accompanied by increasing $^{87}Sr/^{86}Sr$ (Fig. F9, p. 59), and it is also a trend reflecting an increasing role for a continental crust component (Barling et al., 1994). Other data sources are Davies et al. (1989); Storey et al. (1992); Mahoney et al. (1995); Yang et al. (1998); Frey et al. (in press). (Continued on next page.)

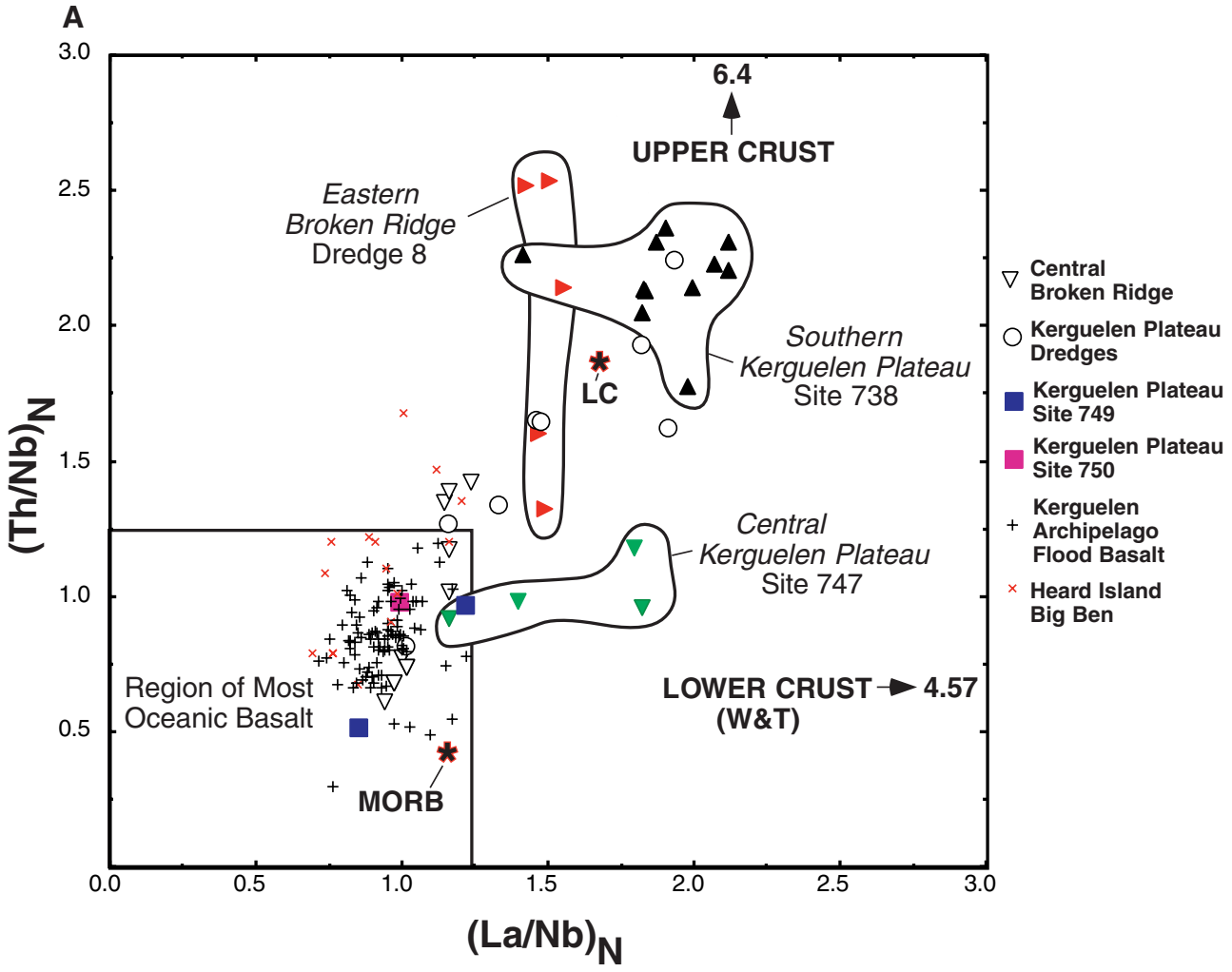

Figure F11 (continued). B. Same plot as in A, but with an enlarged scale to include data for continental basalts that have been attributed to the Kerguelen plume, that is, the Bunbury Basalt (southwest Australia) and Rajmahal Basalt (northeast India). These basalts show a trend of variable contamination by a continental crust component (Frey et al. 1996; Kent et al., 1997). Estimates of average, upper, and lower continental crust are from Rudnick and Fountain (1995) and Weaver and Tarney (1984) and are labeled (R&F) and (W&T) in the figure. Also shown are North Atlantic MORBs recovered during Leg 152 in a transect away from Greenland. The lowermost lavas in Hole 917A, the drill site closest to Greenland, define a trend consistent with variable contamination by lower crustal granulites. In fact, Fitton et al. (1998a, 1998b) concluded that two different crustal components are present in lavas from Hole 917A; the oldest lavas contain a component derived from granulite-facies Archean crust, whereas some of the younger lavas contain a component derived from amphibolite-facies Archean crust. Relative to Kerguelen Plateau basalts, the much stronger continental signature in these North Atlantic MORBs probably reflects the lower abundances of incompatible elements in MORBs relative to plume magmas.

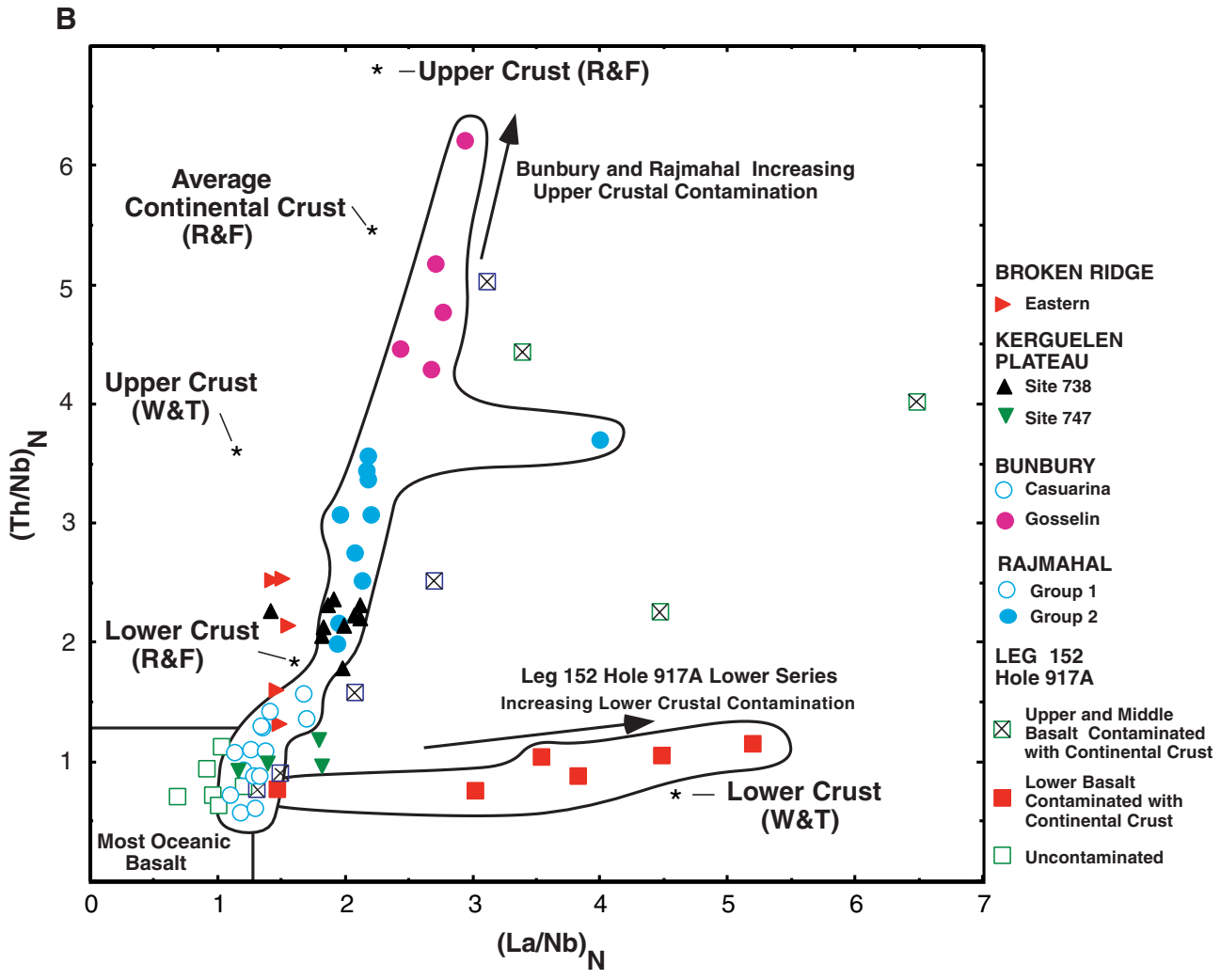

Figure F12. Initial $^{87}Sr/^{86}Sr$ vs. $(La/Nb)_N$ (subscript N indicates ratios normalized to primitive mantle values of Sun and McDonough, 1989), showing the positive correlation that arises from an increasing proportion of a continental crust component in the Bunbury Basalt of southwest Australia (Frey et al., 1996). By analogy, we infer a significant continental crustal component in the Kerguelen Plateau basalts from ODP Site 738 and dredged basalts from the eastern Broken Ridge. In contrast, most oceanic island basalts and all basalts from the Kerguelen Archipelago and Heard Island have $(La/Nb)_{pm} < 1.2$; these lavas are interpreted to be representative of the Kerguelen plume (e.g., Weis et al., 1993, 1998b). Data sources are given in Figure F9, p. 59, and Figure F11, p. 61.

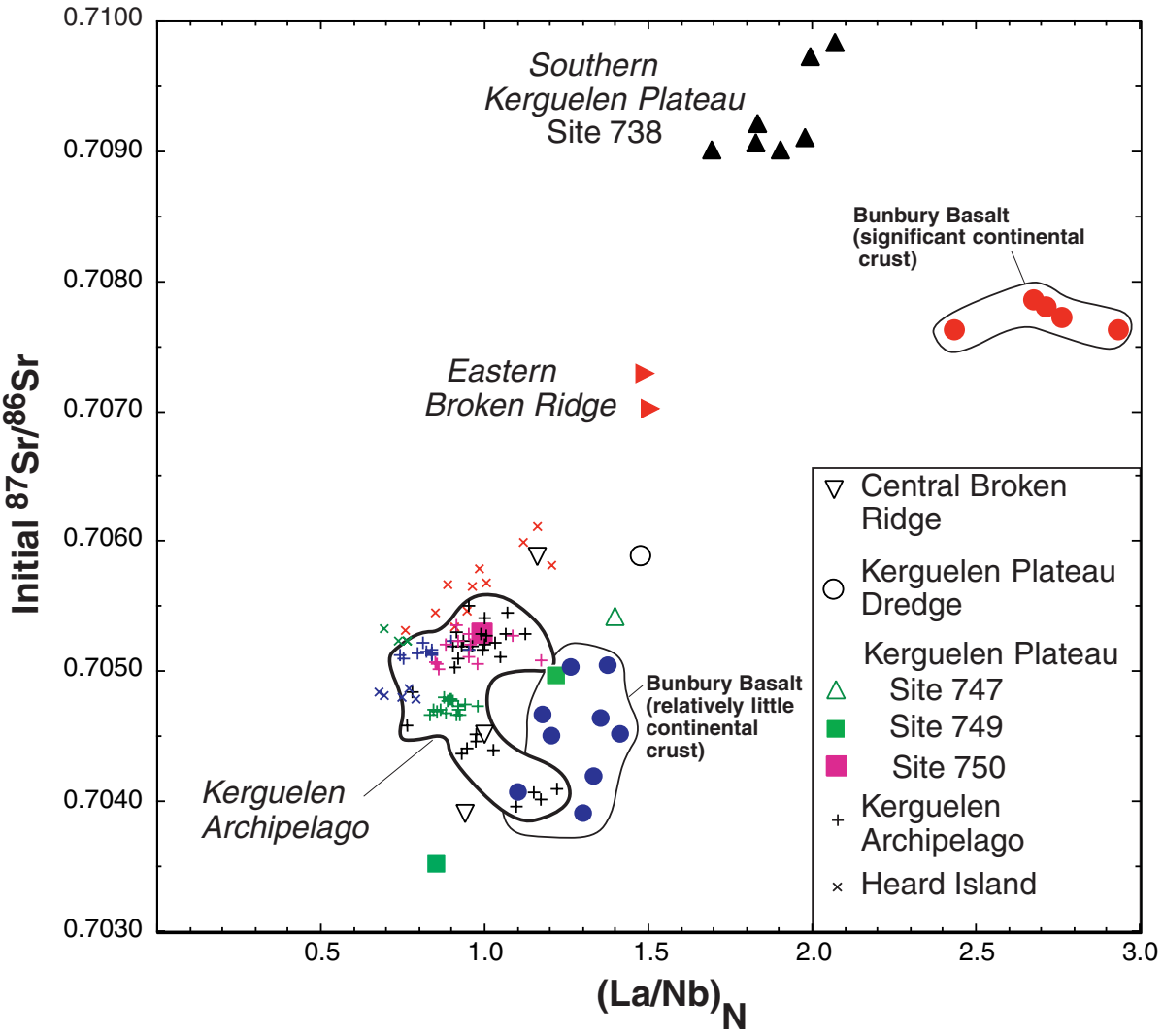

Figure F13. Ti/Zr vs. MgO (in weight percent) for basalts from Broken Ridge and the Kerguelen Plateau. The four Kerguelen Plateau basement drill sites, 738, 747, 749, and 750, have distinctive values ranging from unusually high to low ratios; the primitive mantle and normal MORB ratios are 116 and 103, respectively (Sun and McDonough, 1989). Kerguelen Plateau basalts from Site 738, which have an obvious continental crustal component, also have anomalously low Ti/Zr. Site 747 lavas also have relatively low Ti/Zr and high $^{87}Sr/^{86}Sr$ (Fig. F9, p. 59). In many continental flood basalts, relatively low Ti/Zr results from contamination with continental crust (e.g., Frey et al., 1996; Kent et al., 1997). Abundances of Ti and Zr are precisely determined by shipboard XRF analysis; therefore, Ti/Zr is a useful ratio for shipboard assessment of the role of continental crust in the Kerguelen Plateau and Broken Ridge basalts.

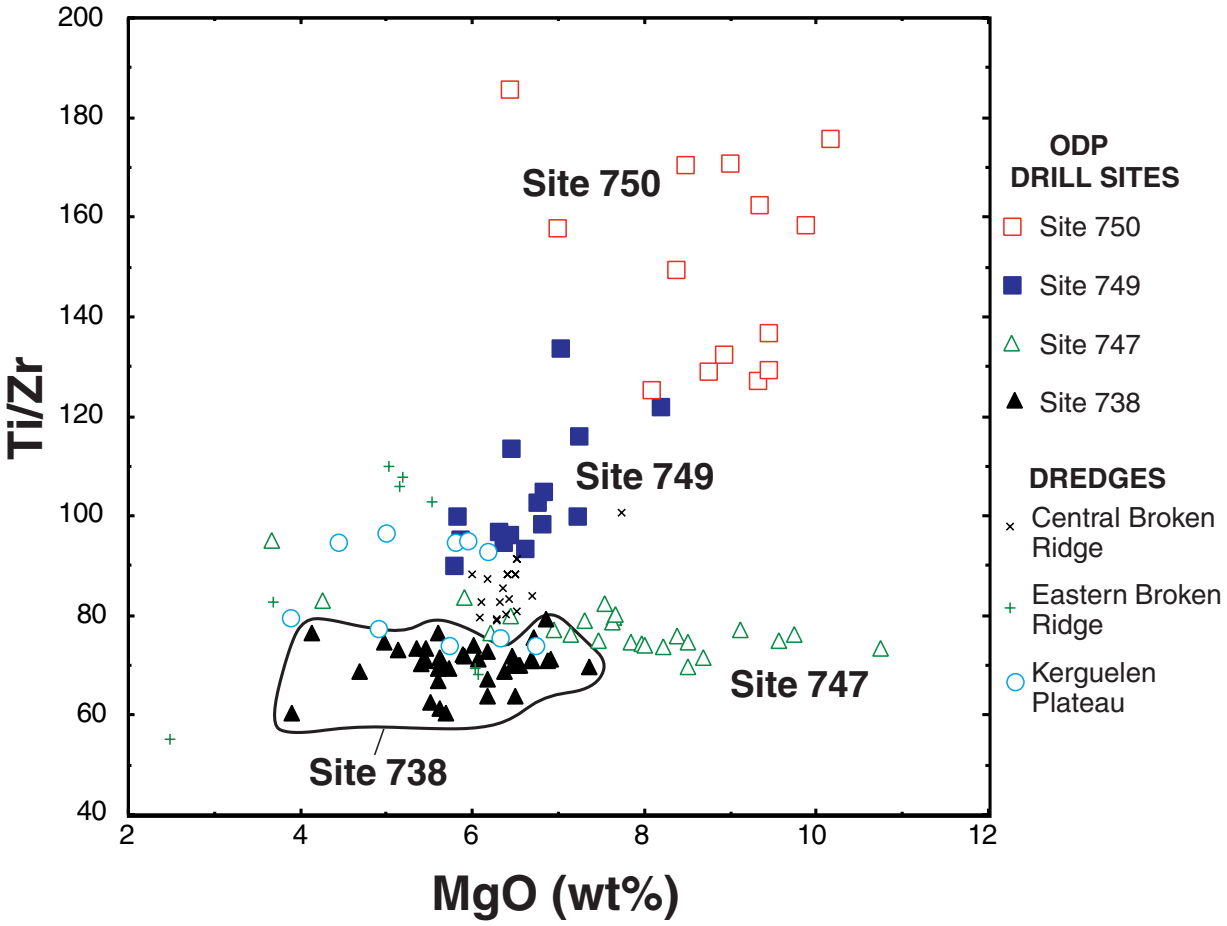

Figure F14. LIP drilling strategies. Age-composition transect sites penetrate ~150 m into volcanic basement, with intermediate and deep sites to be chosen following exploratory drilling. Offset sections provide windows into middle and deep crustal levels. Onland sections permit detailed sampling, albeit of tectonized rocks. Reference sites on older oceanic crust record the volcanic and deformational history of LIP emplacement. M = Moho.

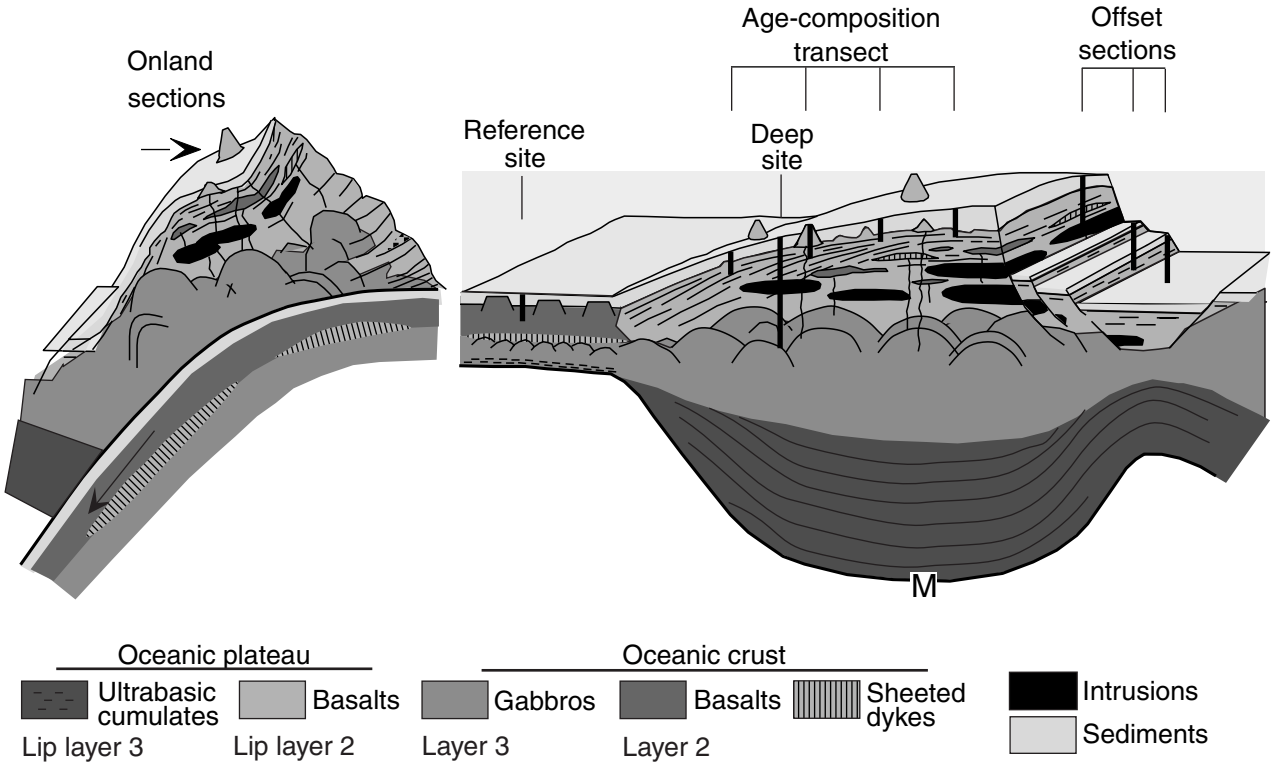

Figure F15. Summary of drill sites on the Kerguelen Plateau and Broken Ridge that recovered volcanic rocks. Data are shown for Sites 738, 747, 748, 749, 750, 1136, 1137, 1138, 1139, 1140, 1141, and 1142. Multichannel seismic reflection profiles indicate that the volcanic rocks at all sites except Site 748 were recovered from the uppermost igneous basement of the plateau, which lies beneath younger sedimentary cover. Basalt at Site 748 was recovered ~200 m above the seismically defined basement and overlies a poorly recovered zone that contains smectitic clay and highly altered basalt. Radiometric ages for basalts are shown in italics. Biostratigraphic ages of sediments overlying basement are also indicated.

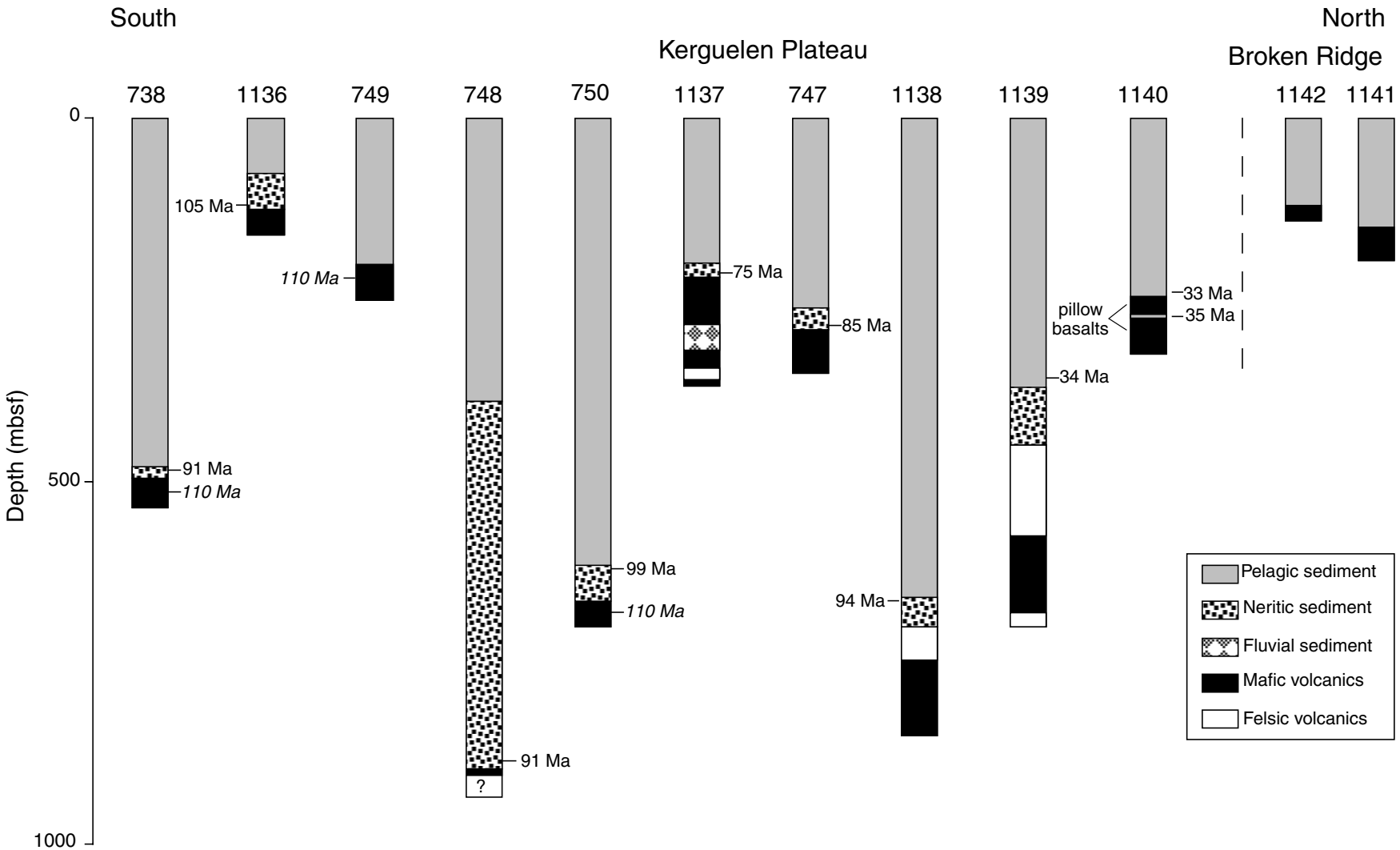

Figure F16. *Rig Seismic* RS180/201 multichannel seismic profile across Site 1135. CDP = common depth point. Vertical exaggeration = ~16 at seafloor.

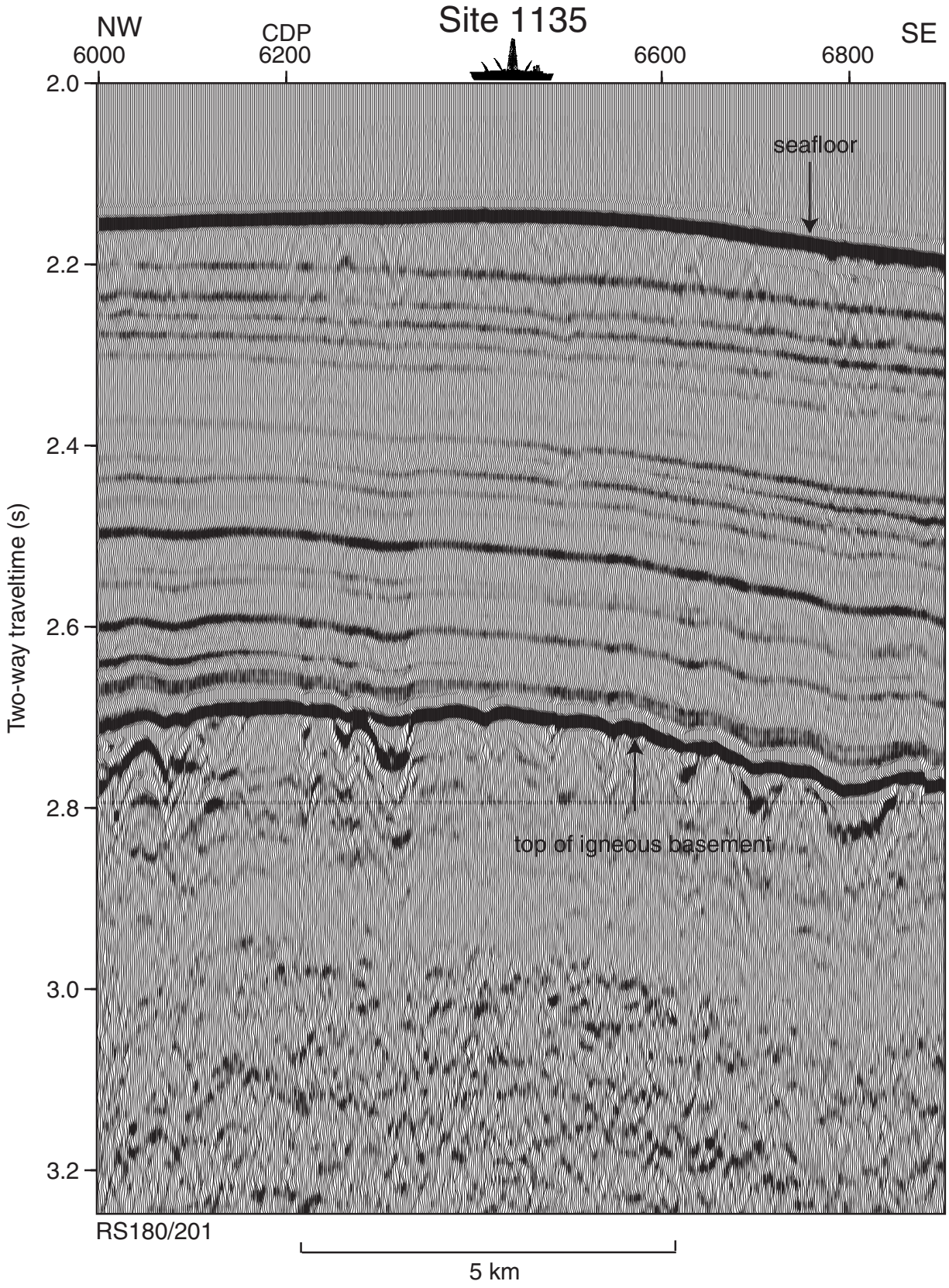

Figure F17. *Marion Dufresne* MD47/10 multichannel seismic profile across Site 1136. Vertical exaggeration = ~6.67 at seafloor.

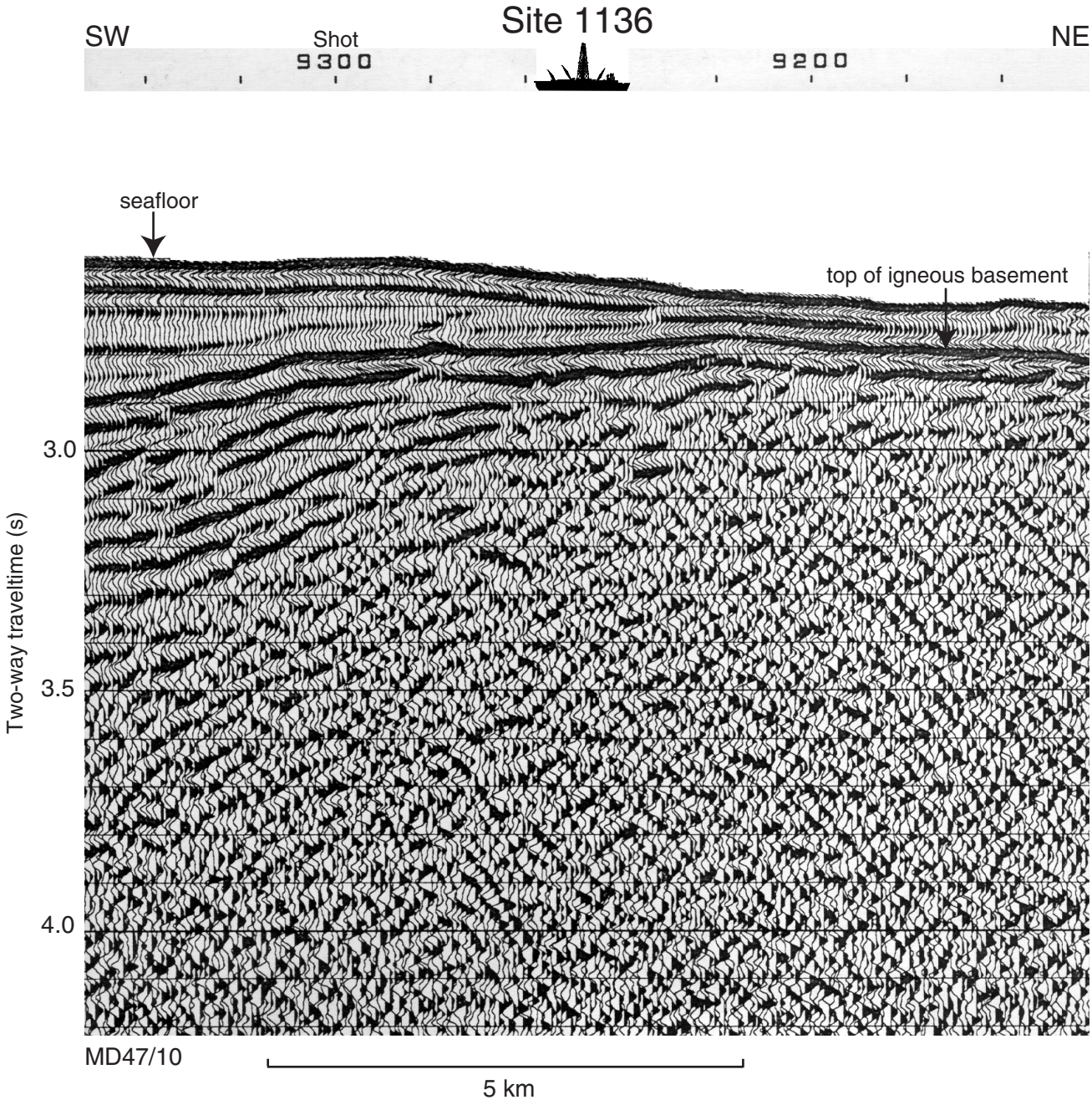

Figure F18. Composite stratigraphic section for Site 1135 showing core recovery, a simplified summary of lithology, lithologic unit boundaries, ages of units, names of lithologies, and total carbonate contents expressed as $CaCO_3$ weight percent. (Table T4, p. 51, in the "Site 1135" chapter).

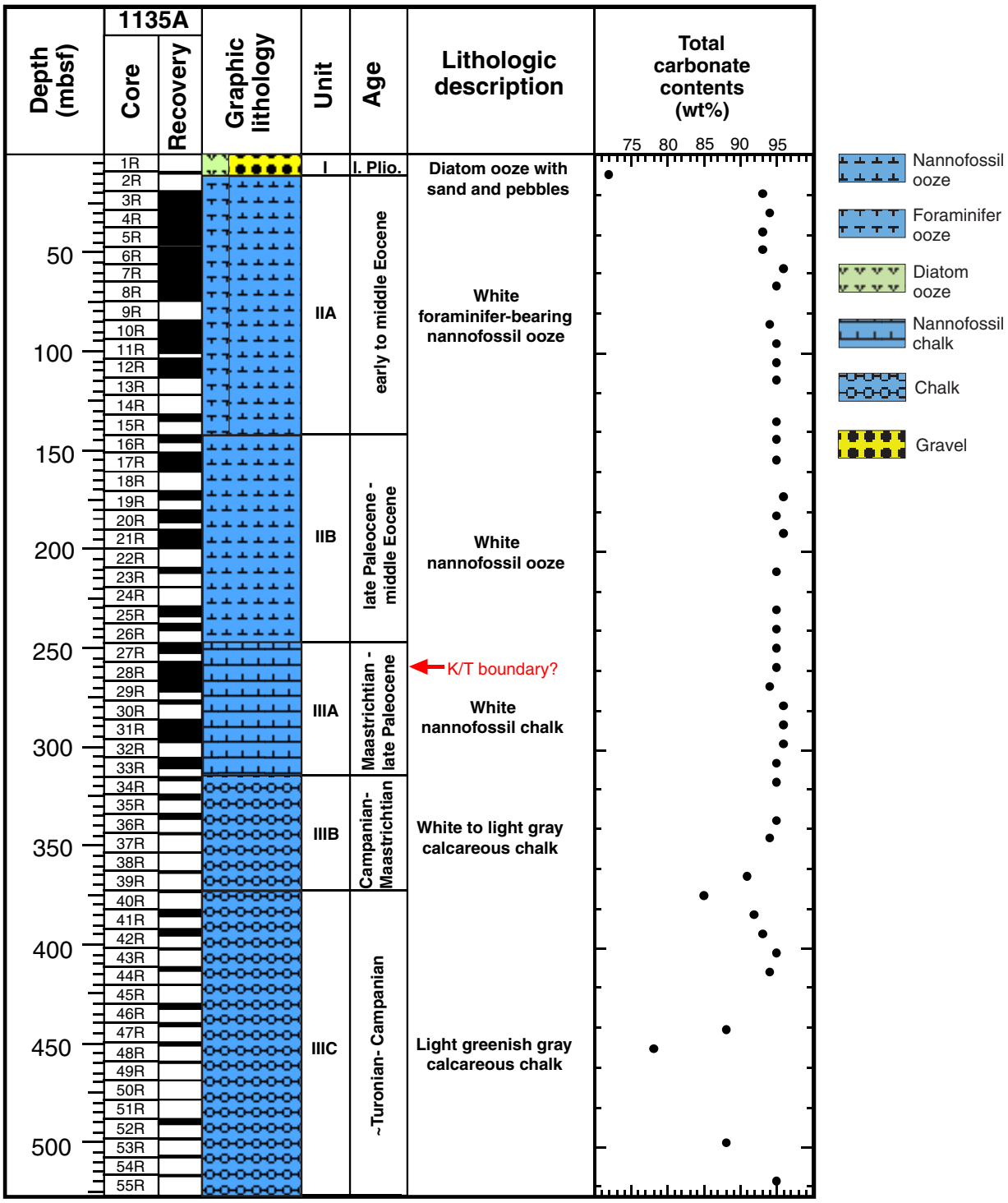

Figure F19. Composite stratigraphic section for Site 1136 showing core recovery, a simplified summary of lithology, lithologic unit boundaries, ages of units, names of lithologies, and total carbonate contents expressed as $CaCO_3$ weight percent.

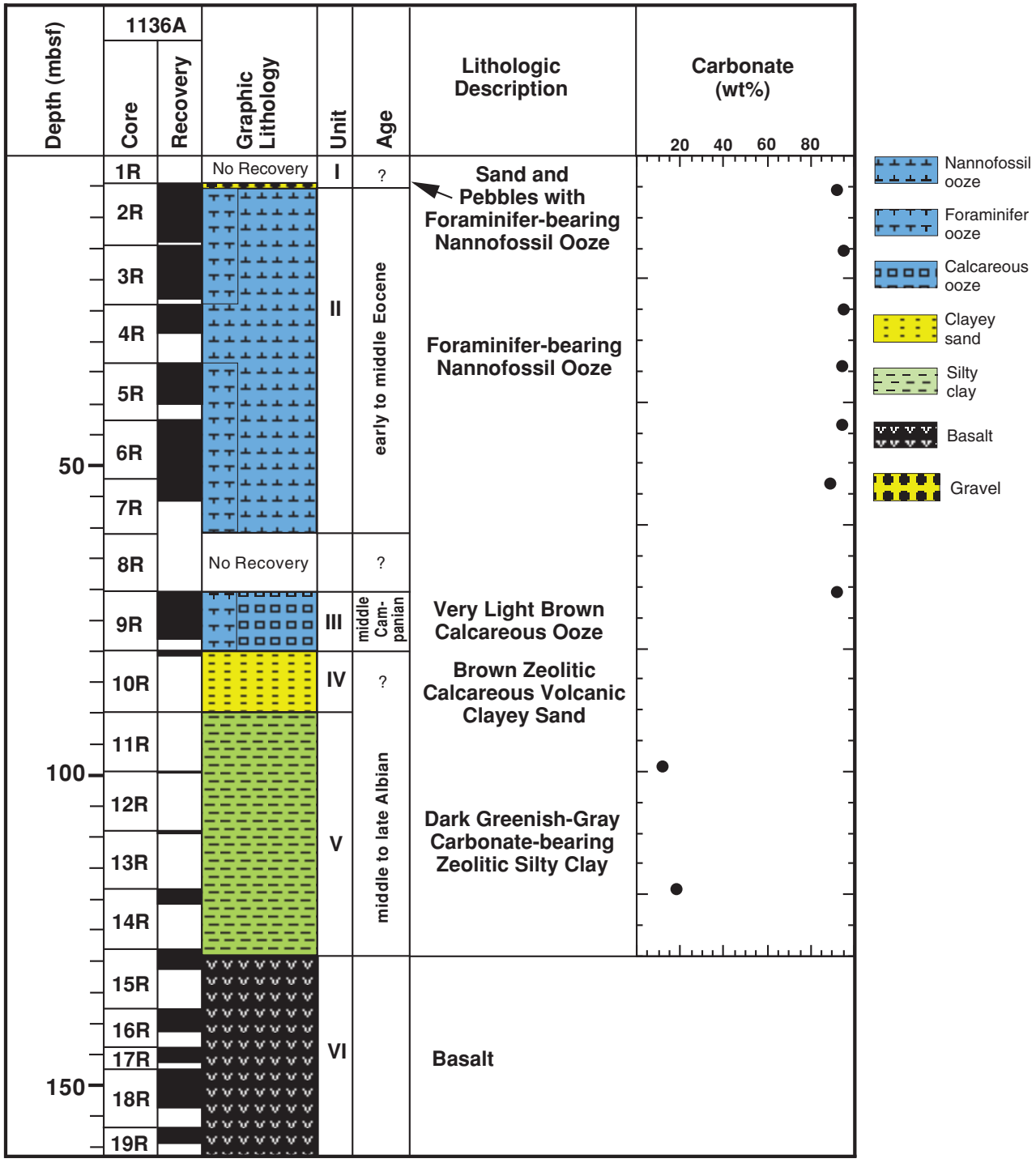

Figure F20. Compositions of volcanic rocks from Sites 1136, 1137, 1138, and 1140 on the $Na_2O + K_2O$ vs. SiO_2 classification diagram. Alkalic and tholeiitic basalt fields are separated according to Macdonald and Katsura (1964). Compositions of basalts from southern and central Kerguelen Plateau locations are shown as fields for Sites 738, 747, 749, and 750 (Alibert, 1991; Mehl et al., 1991; Salters et al., 1992; Storey et al., 1992) and dredge samples (Davies et al., 1989; Weis et al., 1989). Open circles and diamond indicate highly altered samples from Sites 1137 and 1138, respectively.

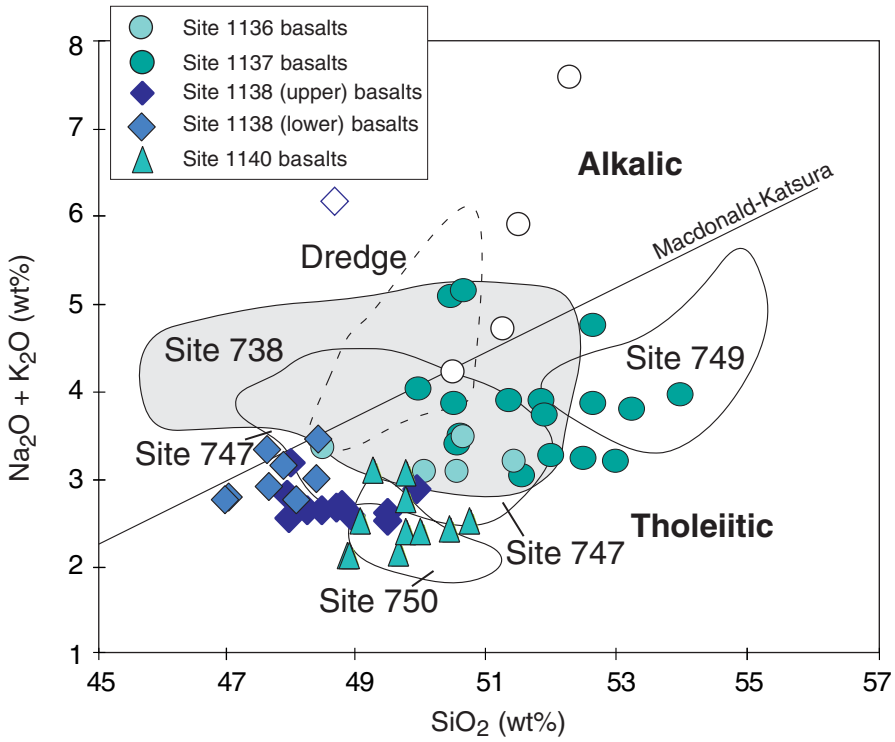

Figure F21. Mantle-normalized $(Nb/Ce)_N$, $(Zr/Ti)_N$, and $(Nb/Zr)_N$ vs. $(Zr/Y)_N$ ratio or Zr content (subscript N indicates ratios normalized to primitive mantle abundances of Sun and McDonough, 1989). These ratios are sensitive to the presence of a component from the continental crust. Note that basalts from Site 738, which are thought to contain a continental component, have the lowest Nb/Ce and Nb/Zr and highest Zr/Ti values. Site 1137 basalts have a comparable Zr/Ti range but higher Nb and Zr contents and, consequently, higher Zr/Y, Nb/Ce, and Nb/Zr. In contrast, Site 1136 basalts most closely resemble basalts from Site 749. Data sources are given in the Figure F20 caption, p. 71.

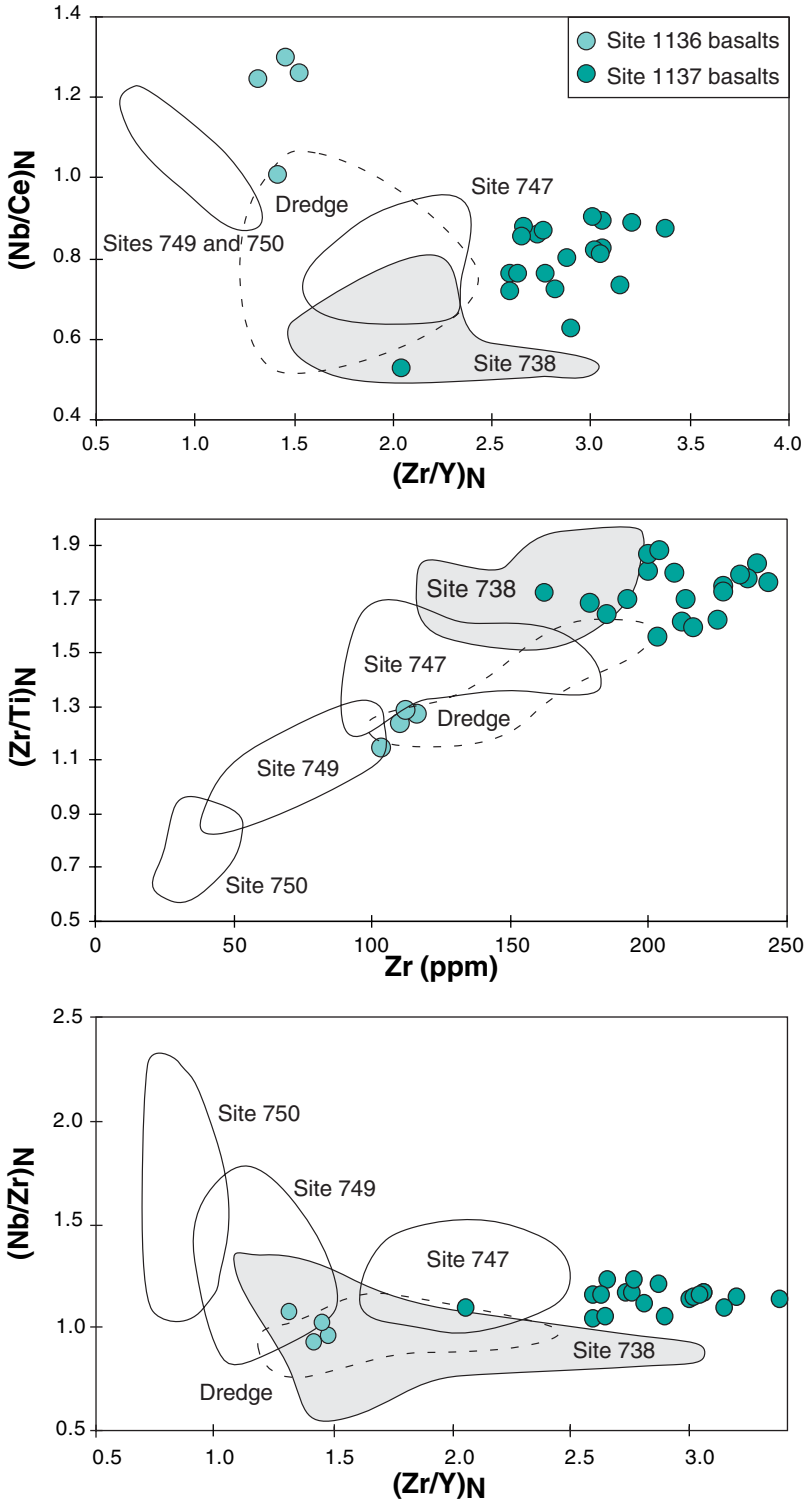

Figure F22. *Rig Seismic* RS179/601 multichannel seismic profile across Site 1137. CDP = common depth point. Vertical exaggeration = ~16 at seafloor.

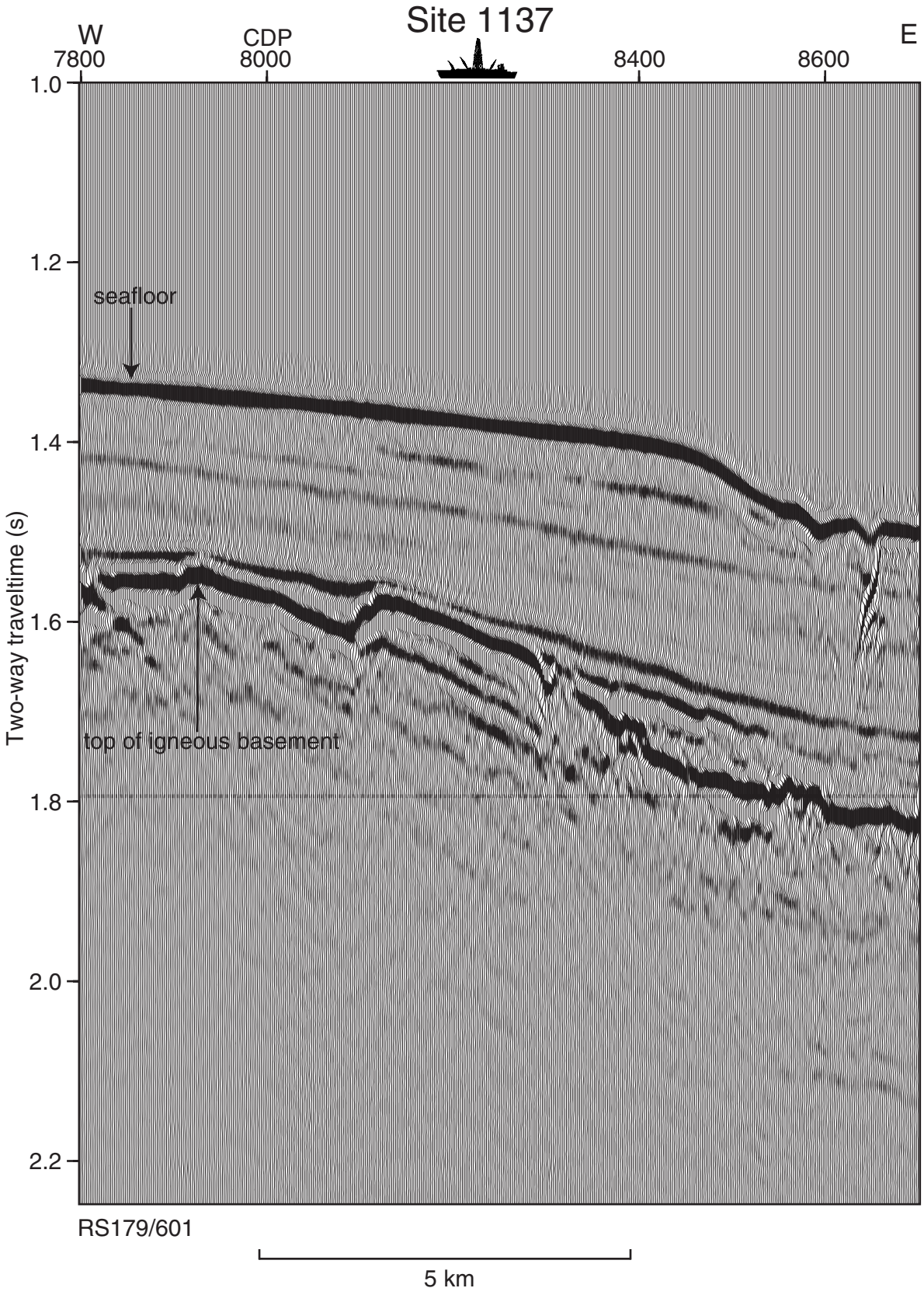

Figure F23. Composite stratigraphic section for Site 1137 showing core recovery, a simplified summary of lithology, lithologic unit boundaries, basement unit boundaries, ages of units, and names of lithologies.

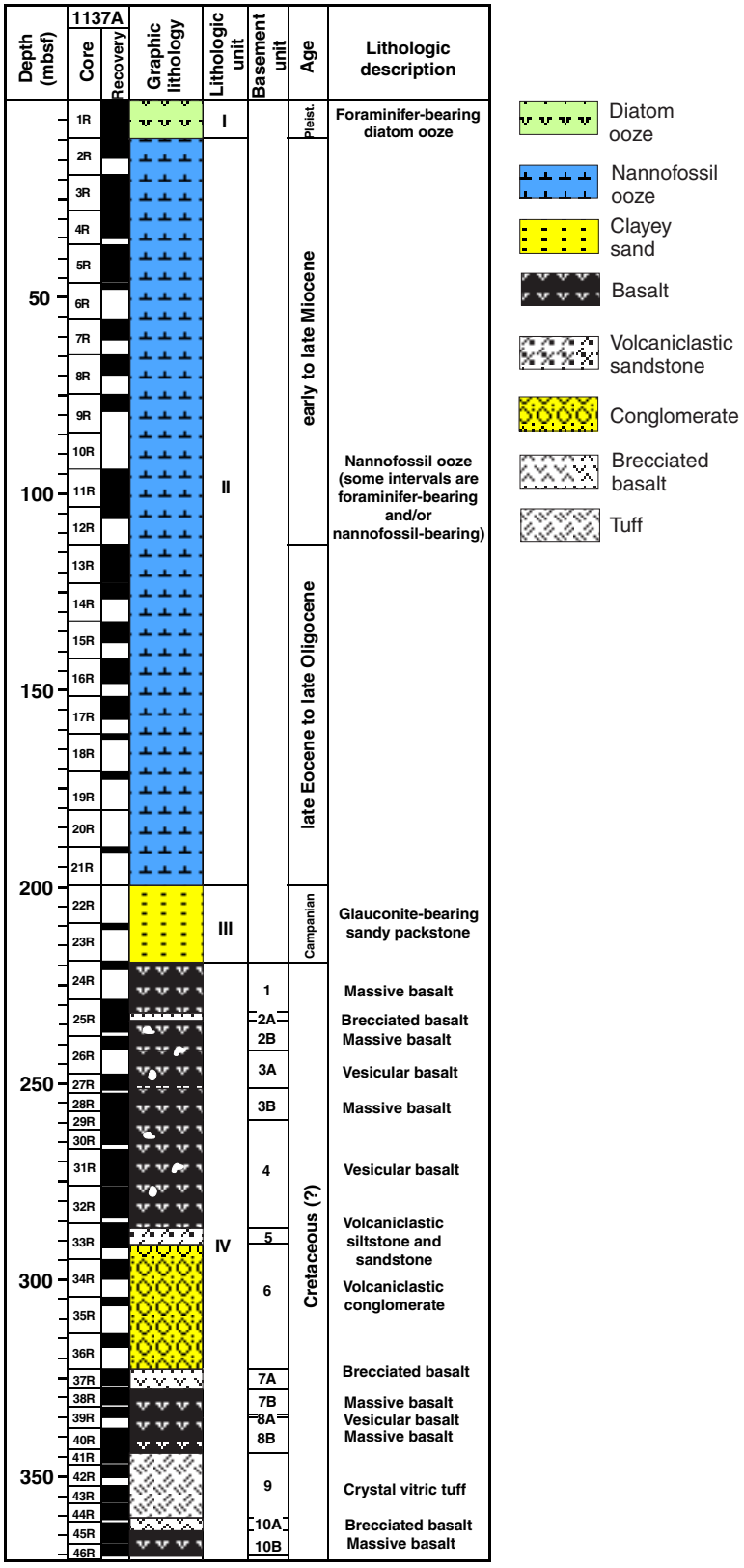

Figure F24. Incompatible trace element compositions of basalts from Sites 1136 and 1137 compared with pre-Leg 183 basalt samples from other parts of the Kerguelen Plateau. Data sources are given in the caption to Figure F20, p. 71.

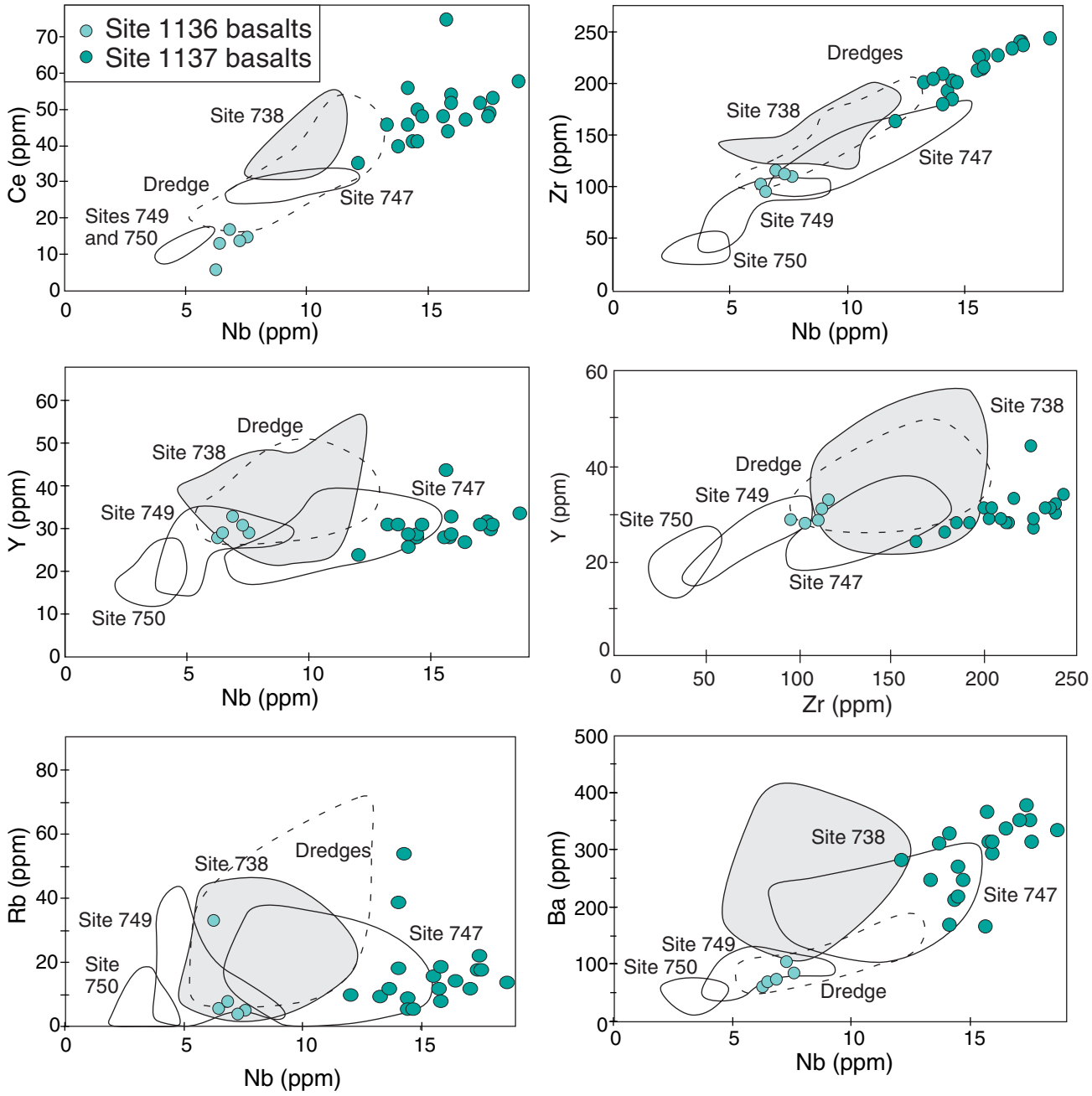

Figure F25. Nb/Y vs. Zr/Y for Kerguelen Plateau basement basalt from Sites 738, 747, 749, 750, 1136, and 1137. The two diagonal lines delimit the field of plume-derived Icelandic lavas; MORB plots to the right of this field as do plume-derived basalts that have been contaminated by upper continental crust. Fitton et al. (1997) argue that melts derived by a varying extent of melting from a common peridotite source define trajectories nearly parallel to these boundary lines. Average MORB and oceanic island basalt (OIB) (Sun and McDonough, 1989), average lower and upper continental crust (LCC and UCC, respectively, Rudnick and Fountain, 1995), alkalic basalts from Site 748 (recovered above basement), and the evolved rocks from Site 1137 are shown for reference.

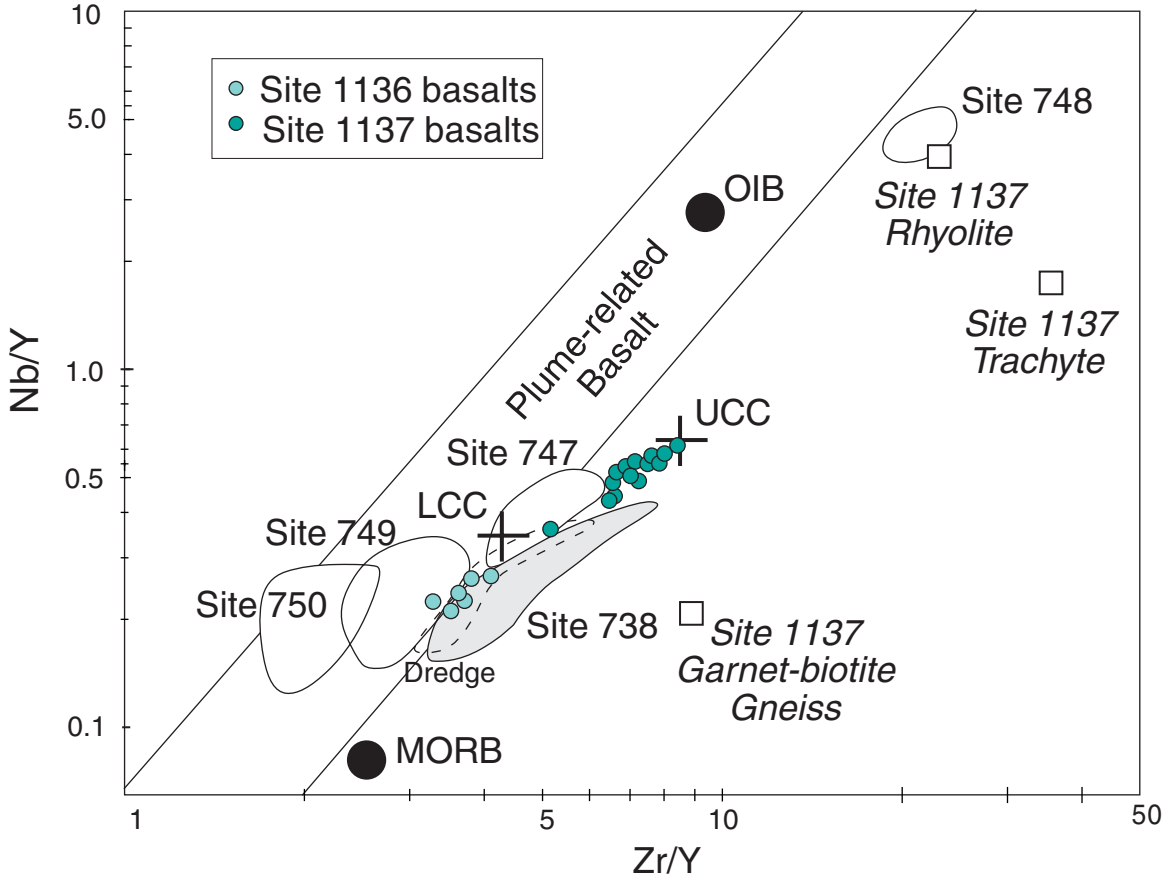

Figure F26. Trace element contents of basalts from Site 1137, normalized to primitive mantle values of Sun and McDonough (1989). All Site 1137 basalts are enriched in incompatible elements. The wide range of Rb and K shows the mobility of these elements during postmagmatic alteration.

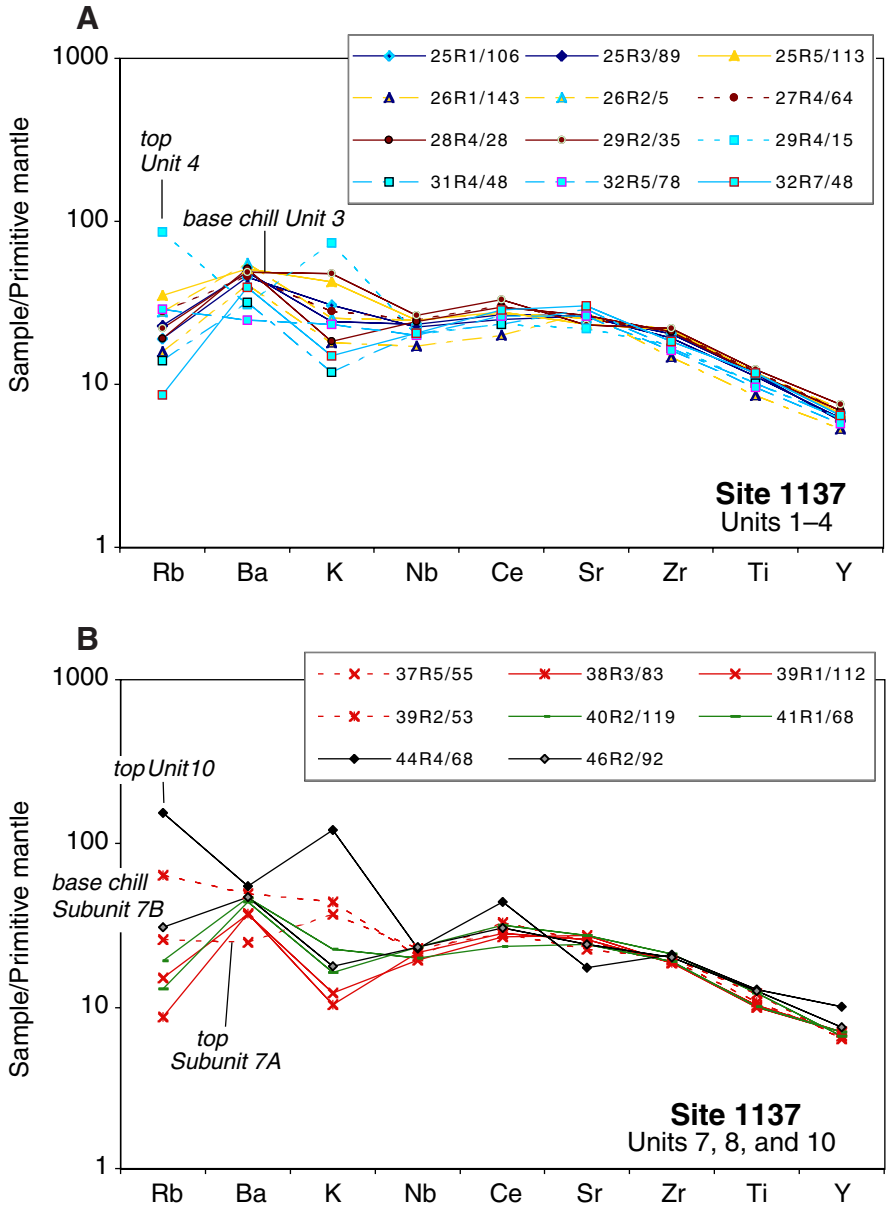

Figure F27. *Rig Seismic* RS179/101 multichannel seismic profile across Site 1138. CDP = common depth point. Vertical exaggeration = ~16 at seafloor.

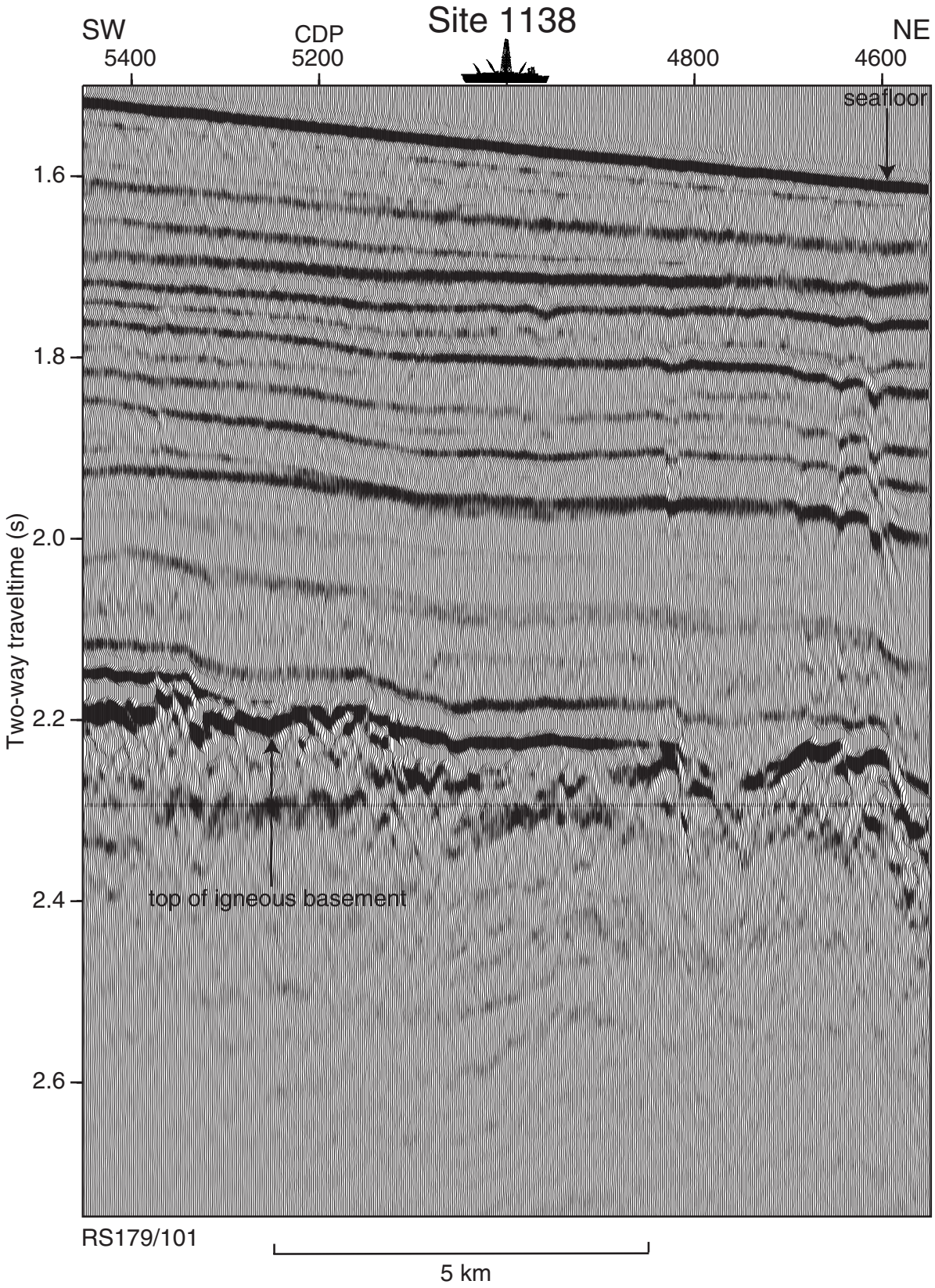

Figure F28. Composite stratigraphic section for Site 1138 showing core recovery, a simplified summary of lithology, lithologic unit boundaries, ages of units, and names of lithologies.

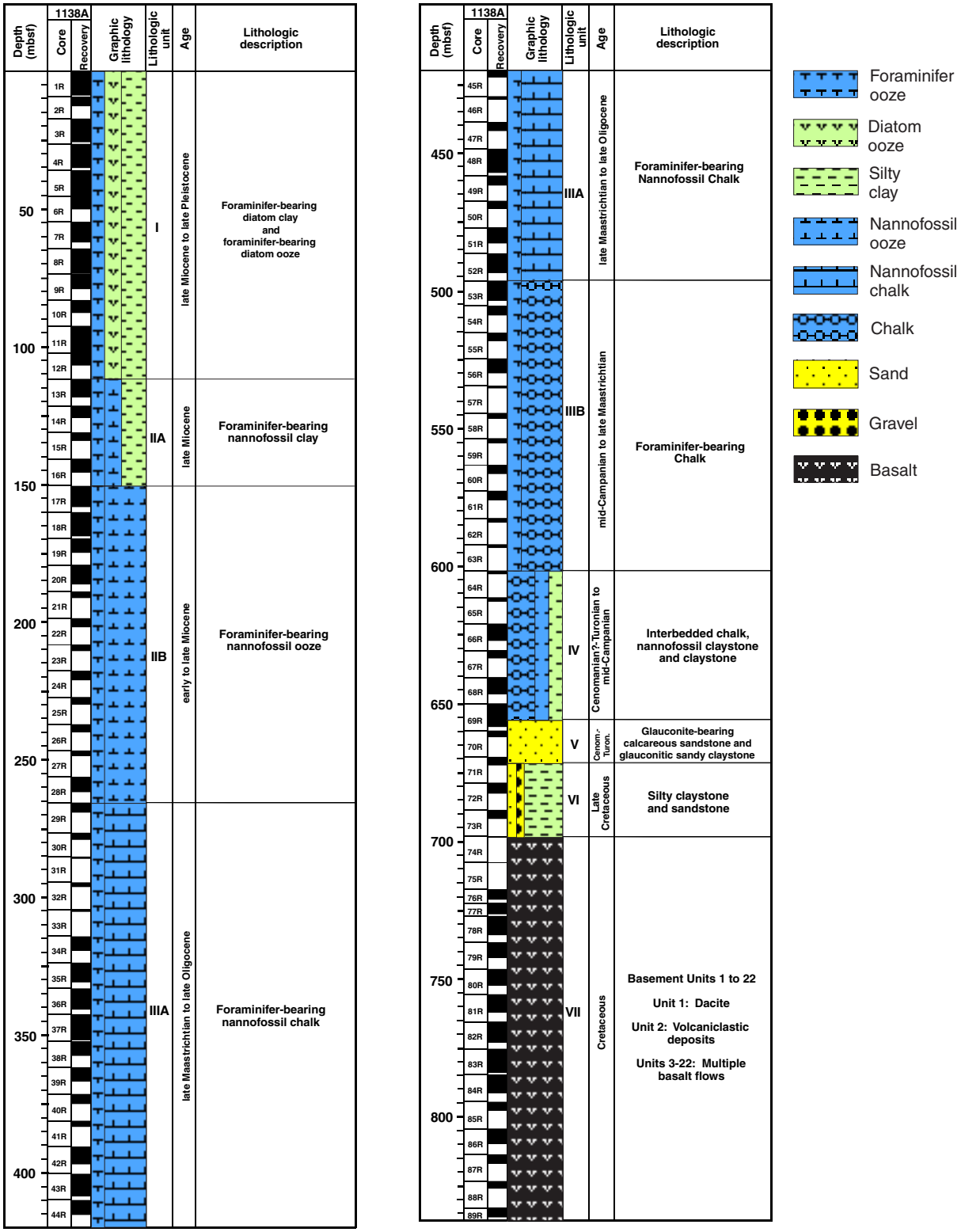

Figure F29. Site 1138 igneous rock compositions in the $Na_2O + K_2O$ vs. SiO_2 classification diagram (Le Bas et al., 1986). Unit 1 cobbles are dacites, whereas the pumice-rich portion of the Unit 2 breccia has a trachytic composition (squares). Units 3–22 are tholeiitic to transitional basalts (solid diamonds = upper series lavas; shaded diamonds = lower series lavas). A highly altered sample is indicated by the open diamond. Alkalic and tholeiitic basalt fields are separated by the Macdonald-Katsura (1964) line.

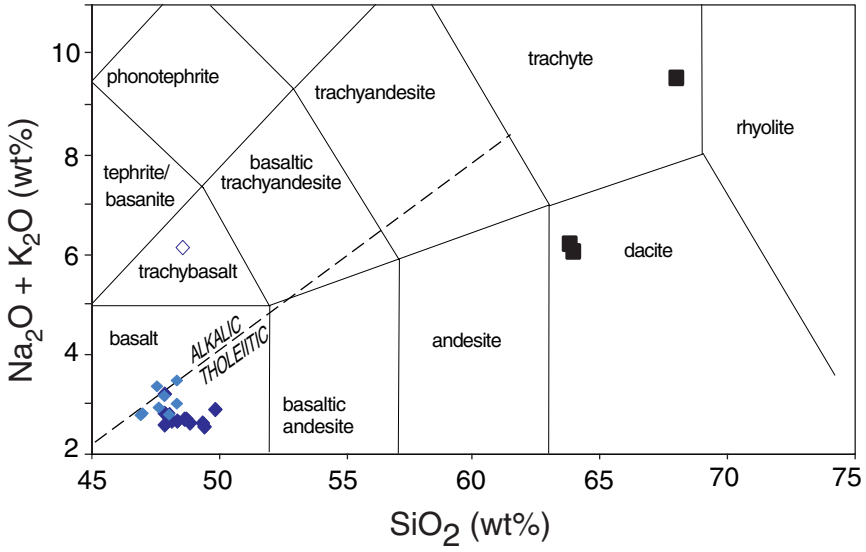

Figure F30. Downhole variations in trace element abundances and abundance ratios for Site 1138 basalts (subscript N indicates values normalized to primitive mantle abundances of Sun and McDonough, 1989). Symbols as in Figure F29, p. 80.

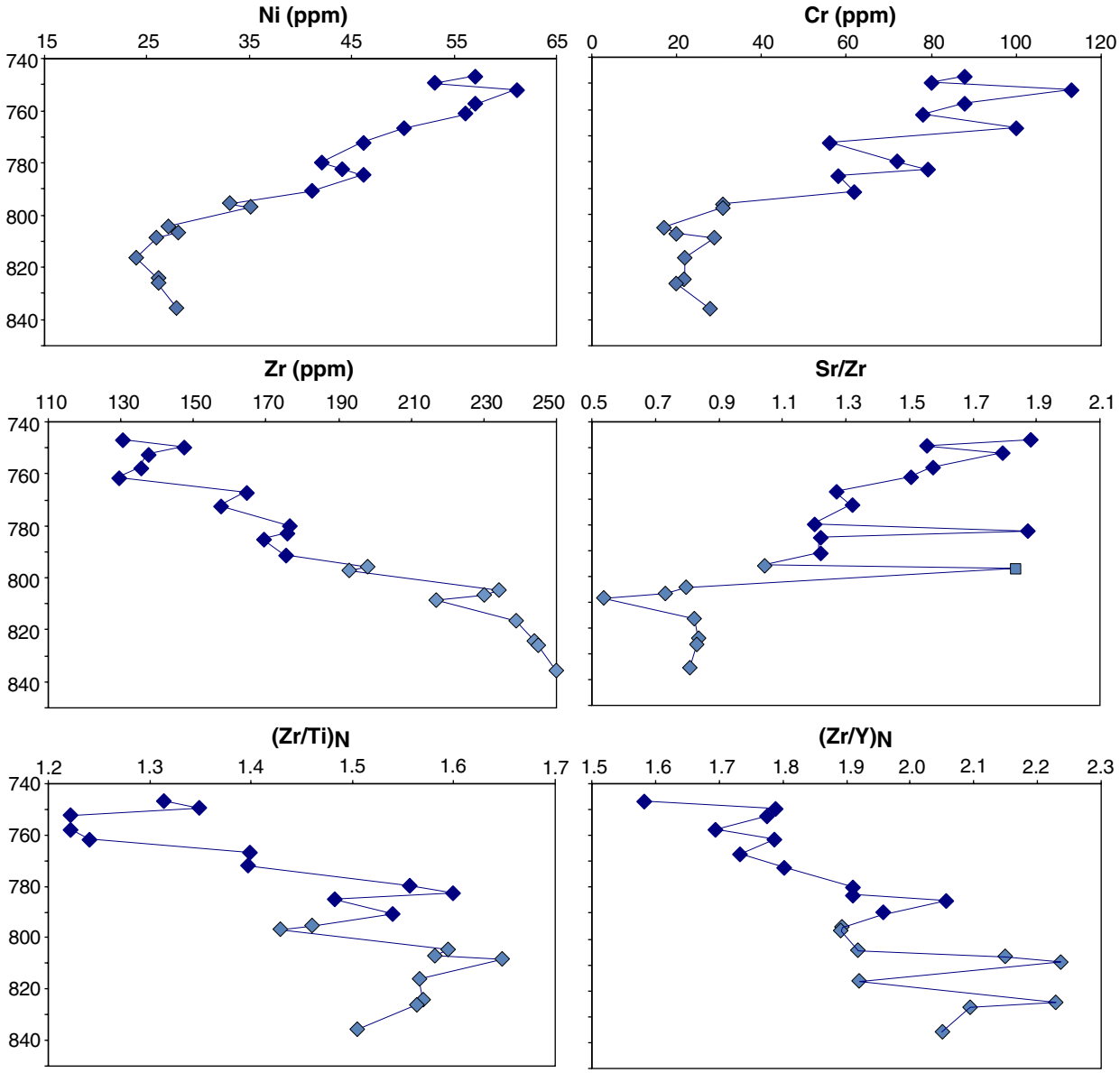

Figure F31. A. The Nb/Y vs. Zr/Y plot (Fitton et al., 1997) has been used to distinguish between basalts derived from the Icelandic plume (data within the diagonal lines labeled "Icelandic plume") and mid-ocean ridge basalt (MORB) derived from the North Atlantic asthenosphere (data below the lower diagonal line). Fitton et al. (1997) showed that basalts derived from a common peridotite source by variable extent of melting define a trend parallel to these lines (see arrow labeled "melting"; melts formed by low extents of melting will have relatively high Nb/Y and Zr/Y and these ratios will decrease along this trend as extent of melting increases). Mantle heterogeneity is dominantly expressed by variations in Nb/Y (see arrow labeled "source heterogeneity"). The fields show 82-Ma to Holocene lavas associated with the Kerguelen plume. These lavas, tholeiitic basalts from Sites 756, 757, and 758 on the Ninetyeast Ridge and transitional to alkalic basalts from the Kerguelen Archipelago, define a trend that overlaps the lower boundary line. We infer that the Nb/Y and Zr/Y of the Kerguelen plume lie on this line. A representative field for Southeast Indian Ridge (SEIR) MORB is shown for comparison (see Fig. **F8,** p. 58, caption for data sources). **B.** Fields for pre-Leg 183 sampling of basaltic basement from the Kerguelen Plateau. Dredge basalts from the CKP (dashed field) and drill sites 738, 747, 749, and 750. For comparison, averages are shown for MORB, primitive mantle (PM), lower and upper continental crust (LCC and UCC, respectively), and ocean-island basalt (OIB) (see captions for Figs. **F20,** p. 71, and **F25,** p. 76, for data sources). **C.** Fields for pre-Leg 183 sampling (dredges) of basaltic basement from Broken Ridge (Mahoney et al., 1995) and data for basalts from Sites 1141 and 1142. Except for one sample, the Broken Ridge basalts from Sites 1141 and 1142 lie at higher Nb/Y and Zr/Y, but all basalts from Broken Ridge lie along the lower boundary line, much like the 82-Ma to Holocene lavas shown in A. **D.** Data for basement lavas from the Kerguelen Plateau obtained at five Leg 183 drill sites. Generally, lavas from each site define distinct fields lying along the lower boundary line of the plume field. An exception is lava from Site 1137, which defines a trend toward UCC, much like basalts from SKP Site 738 in B. Basalts from these two sites are inferred to contain a component derived from continental crust. (**Figure shown on next page.** Continued on next two pages.)

Figure F31 (continued). (Caption shown on previous page.)

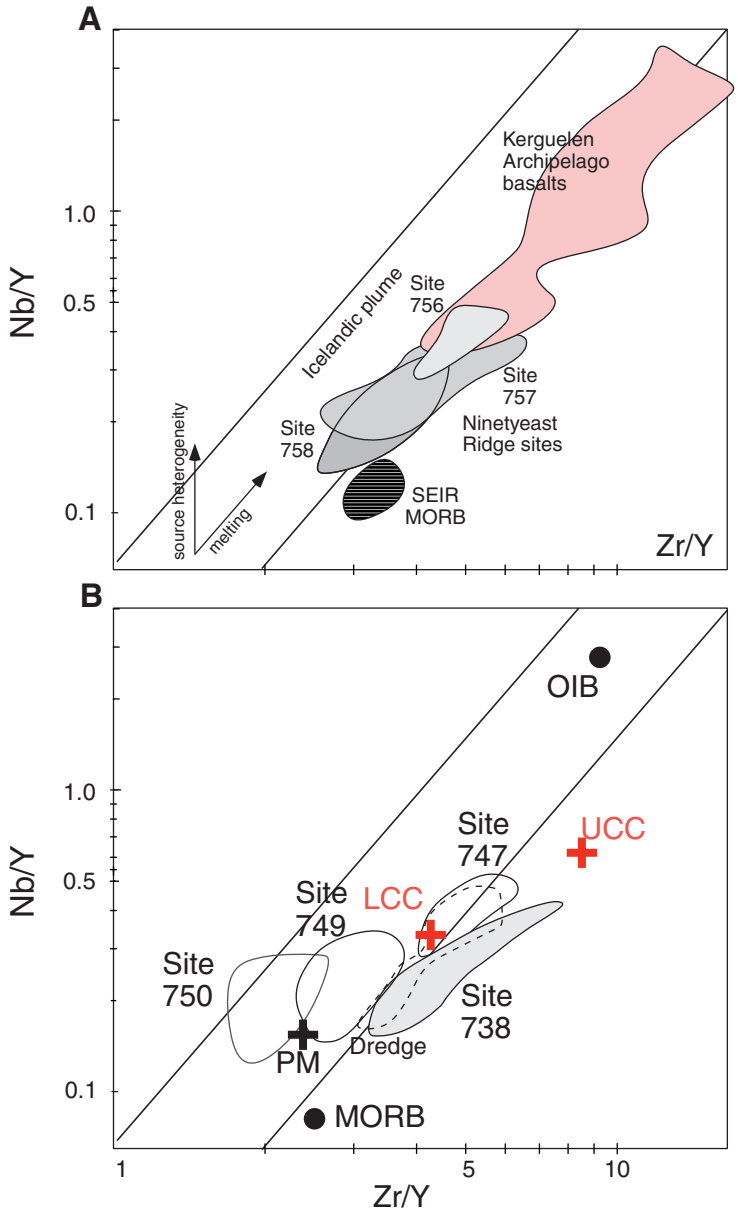

Figure F31 (continued).

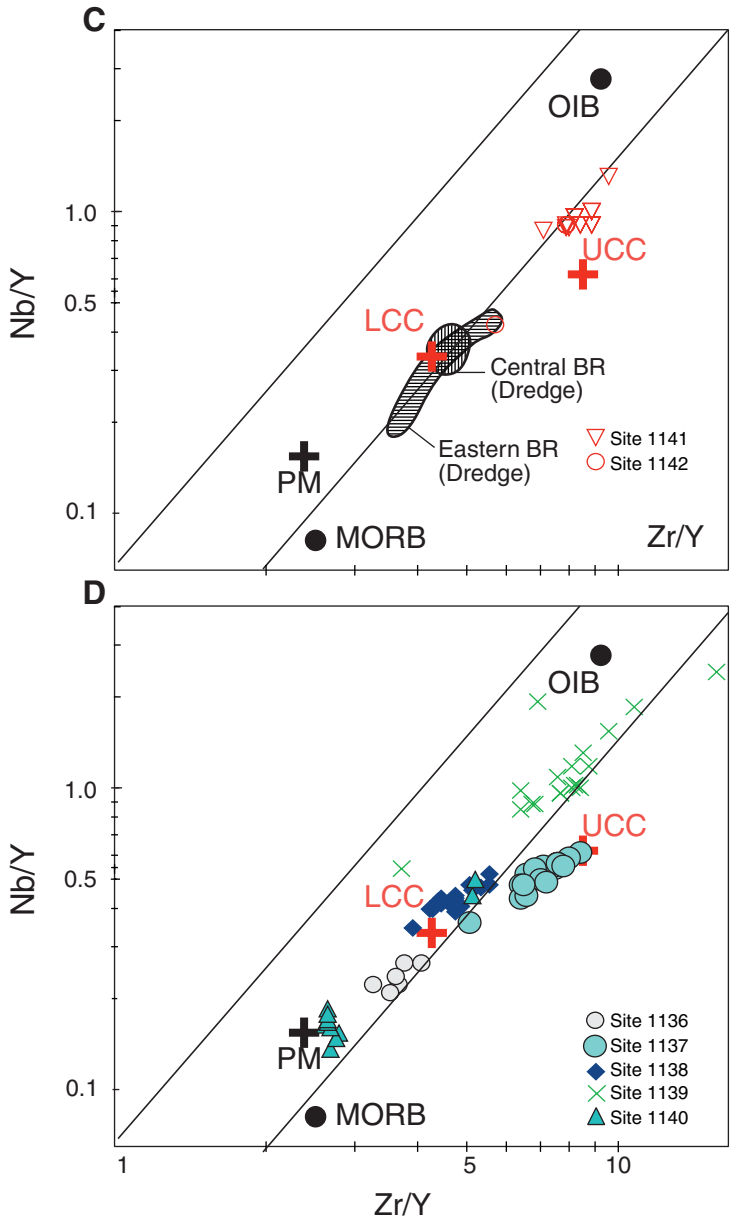

Figure F32. *Marion Dufresne* MD109-05 multichannel seismic profile across Site 1139. CDP = common depth point. Vertical exaggeration = ~16 at seafloor.

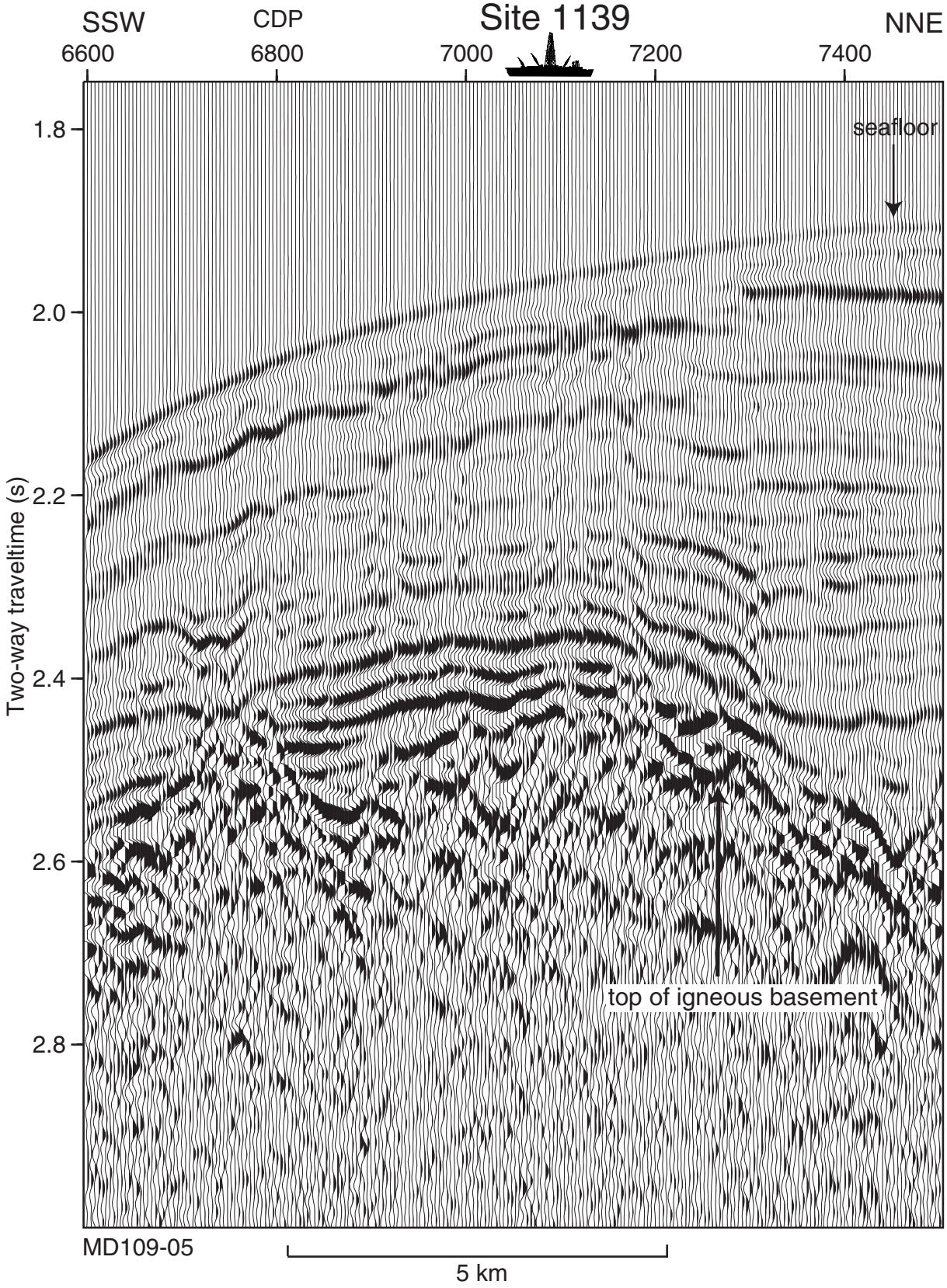

Figure F33. Composite stratigraphic section for Site 1139 showing core recovery, a simplified summary of lithology, lithologic unit boundaries, ages of units, and names of lithologies.

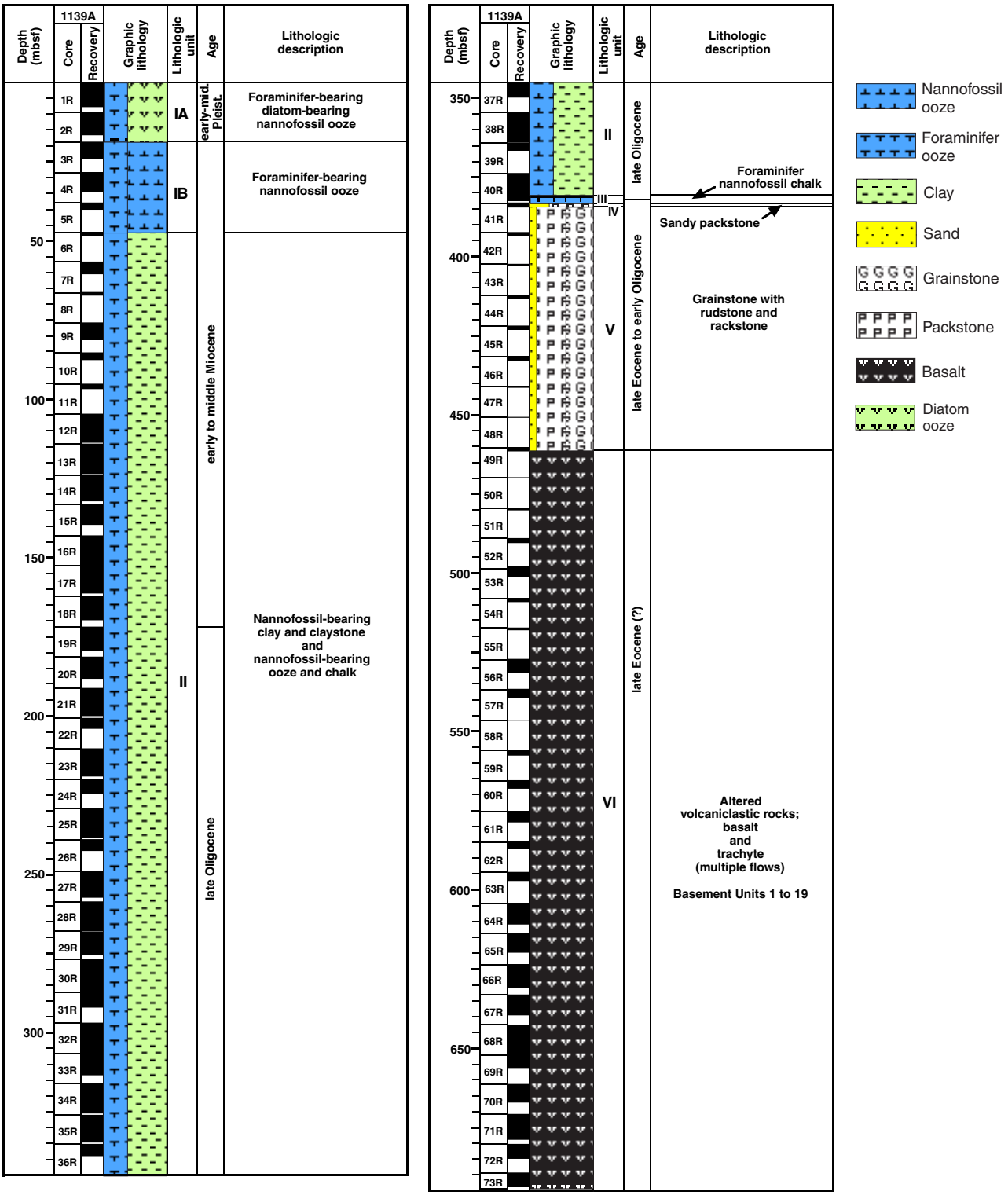

Figure F34. Interpretative summary diagram for Site 1139 showing 19 igneous units that include trachytic to rhyolite volcanic and volcaniclastic rocks and basaltic to trachytic lava flows. In general, the primary vesicularity of the lava flows and marginal breccias is obscured by the effects of alteration. Sanidine xenocrysts are distributed throughout the more mafic flows. Although changes in potassium concentration from downhole natural gamma measurements correlate generally with the defined igneous units, the logging data show more complexity, indicating unrecovered changes in lithology.

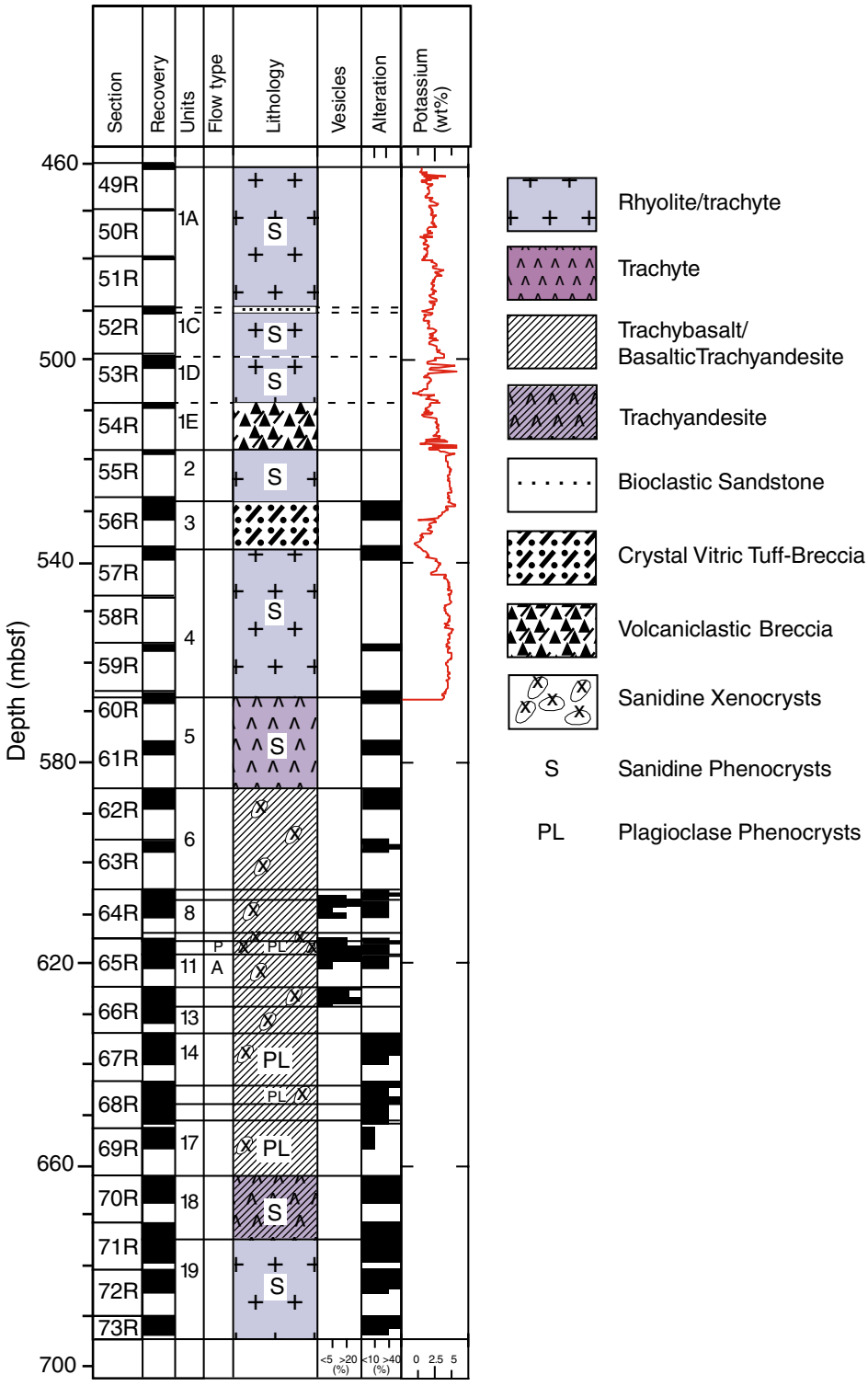

Figure F35. A. Site 1139 igneous rock compositions on the $Na_2O + K_2O$ vs. SiO_2 classification diagram (Le Bas et al., 1986); alkalic and tholeiitic basalt fields are separated by the Macdonald-Katsura (1964) line. Note that there is one chemical analysis per igneous unit except for Units 5, 18, and 19 from which two, two, and four samples were analyzed, respectively. The less altered Units 18 and 19 samples are marked in bold and other samples from these units show considerable spread because of alteration. **B.** Site 1139 mafic compositions compared to samples from Kerguelen Plateau Sites 1136, 1137, 1138. The fields represent data from previous dredging and drilling on the southern and central Kerguelen Plateau (Sites 738, 747, 749, and 750 and dredge locations reported by Weis et al.,1989). Data sources are Davies et al. (1989), Weis et al. (1989), Alibert (1991), Mehl et al. (1991), Salters et al. (1992), Storey et al. (1992), Mahoney et al. (1995), and this study.

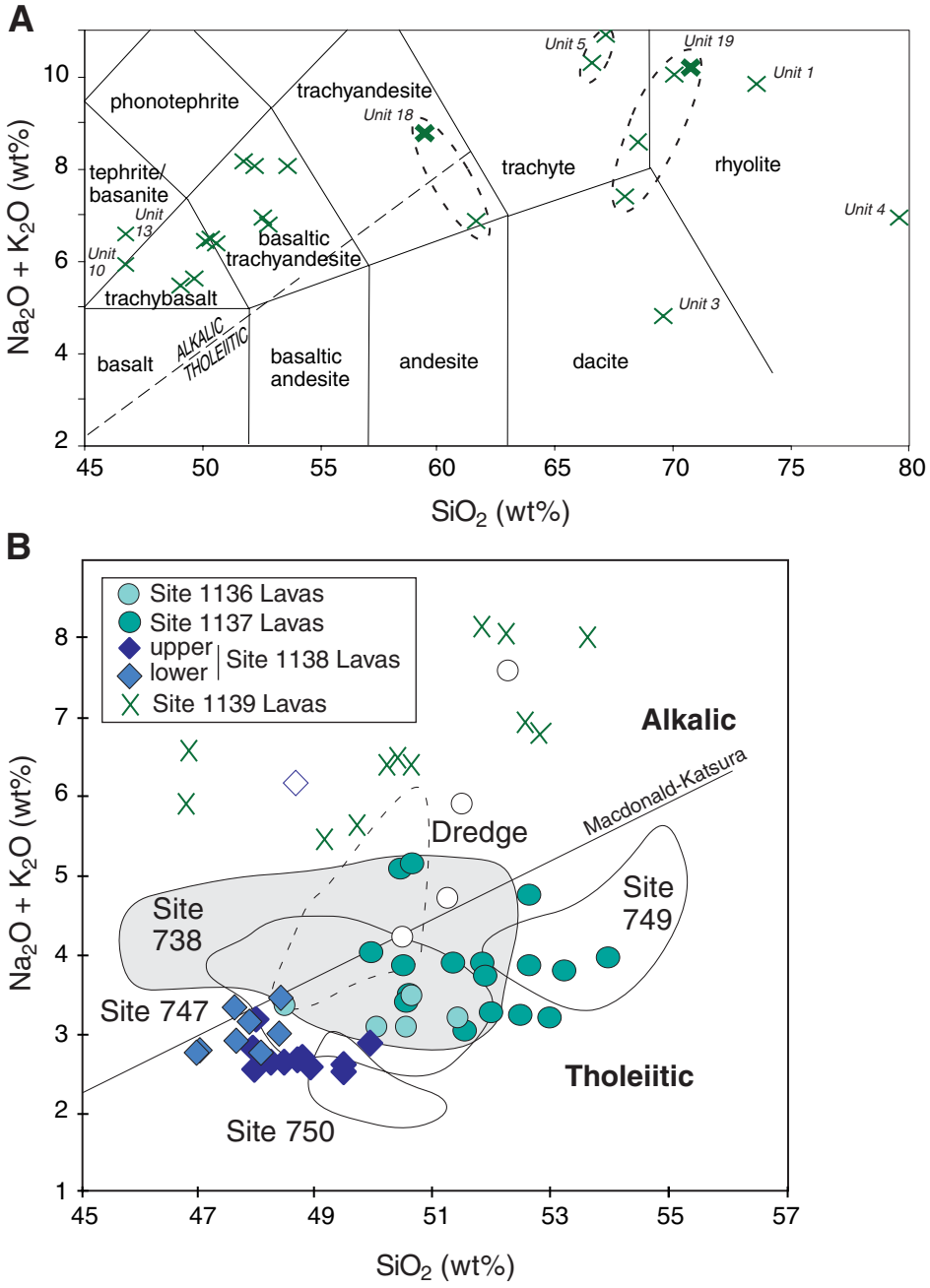

Figure F36. *Marion Dufresne* MD109-06 multichannel seismic profile across Site 1140. CDP = common depth point. Vertical exaggeration = ~16 at seafloor.

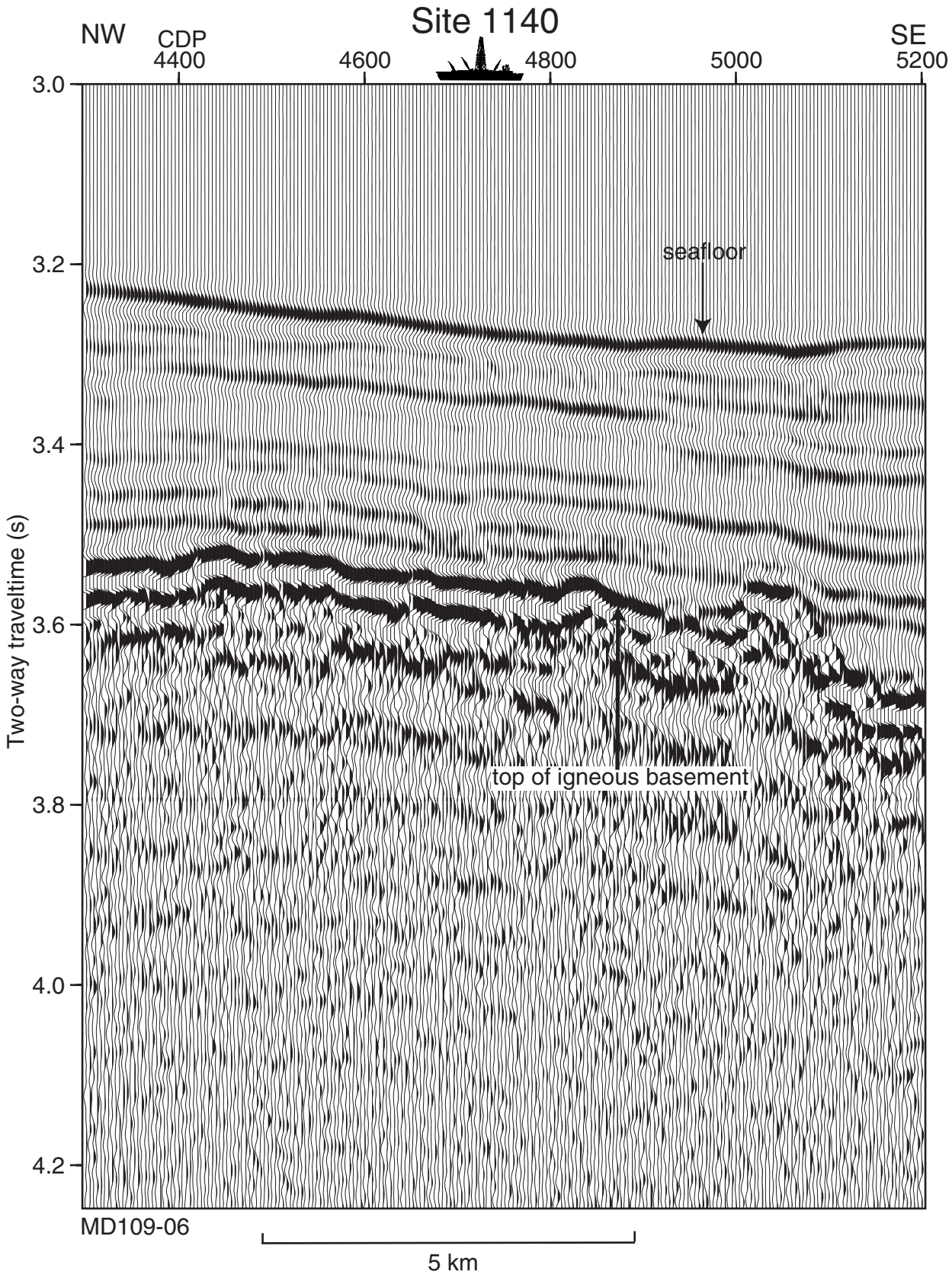

Figure F37. Composite stratigraphic section for Site 1140 showing core recovery, a simplified summary of lithology, lithologic unit boundaries, ages of units, and names of lithologies.

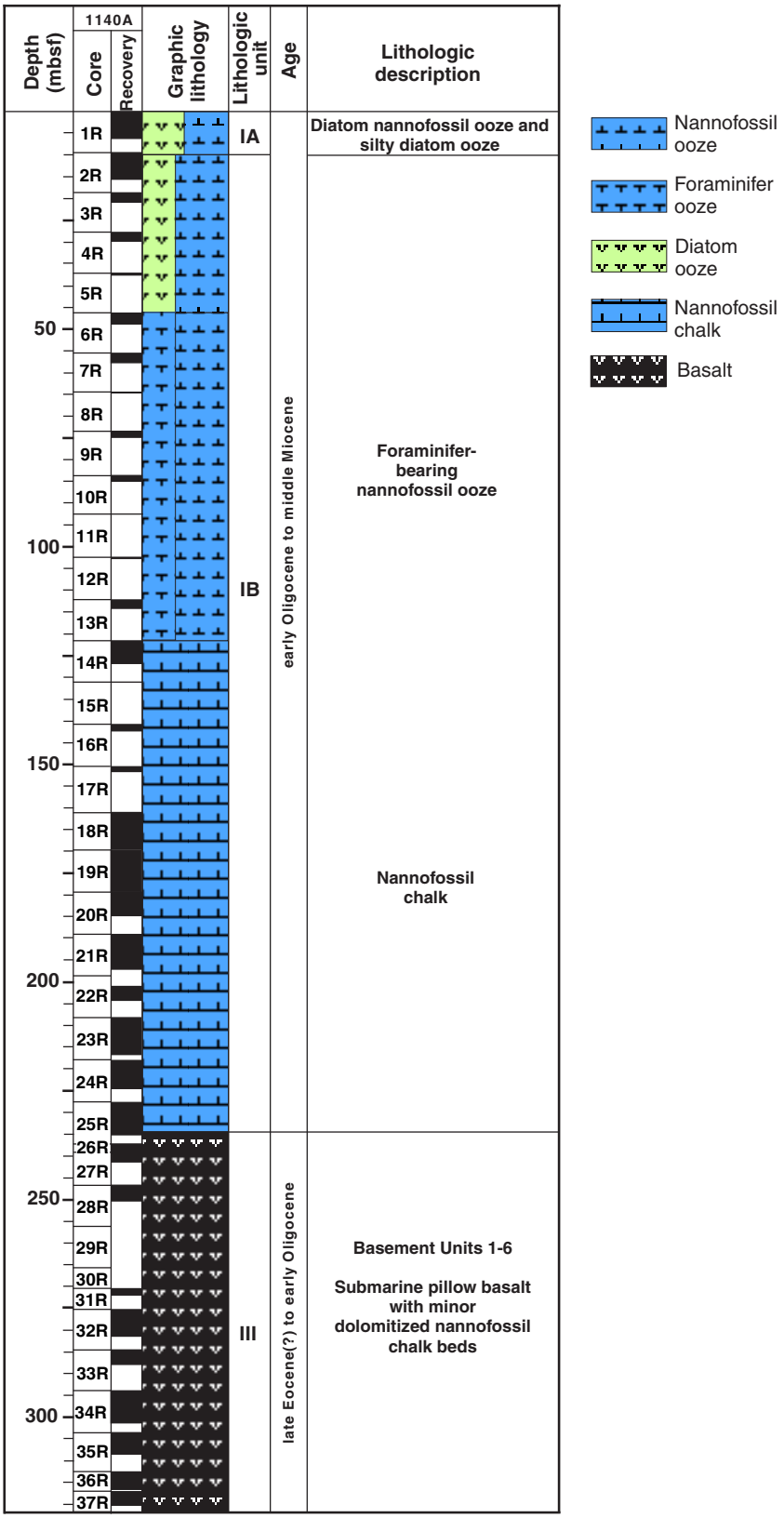

Figure F38. Close-up photograph of Section 183-1140A-28R-3 (Piece 2, 86–101 cm) showing glassy pillow rinds with calcite filling vesicles, veins, and space between adjoining pillows. Open space-filled dolomite and baked white sediment are along the margin with the glass.

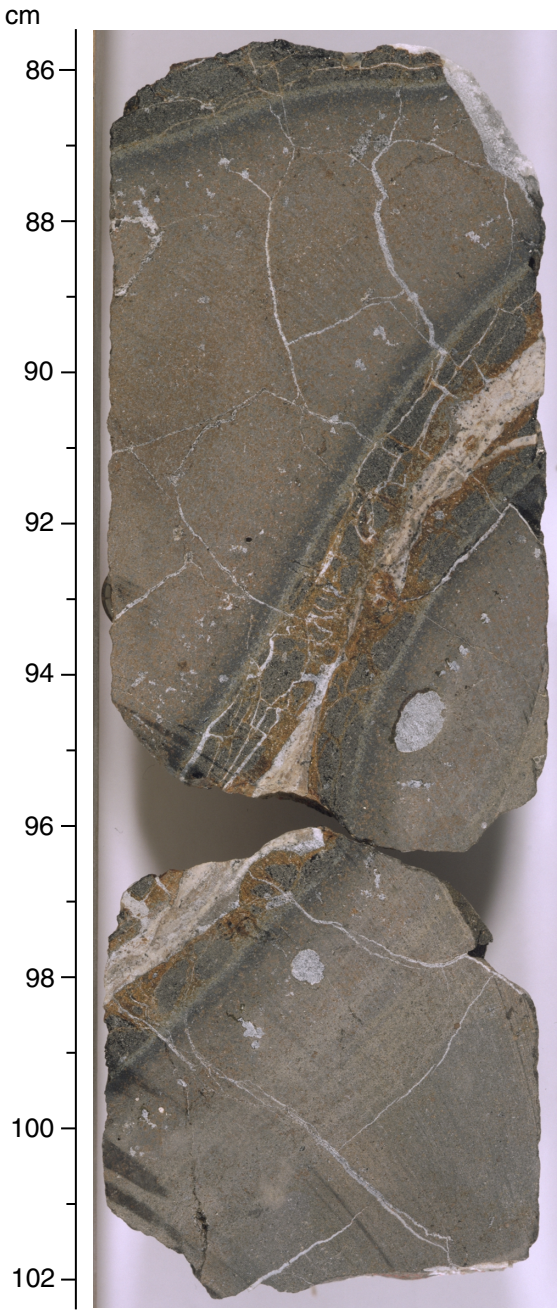

Figure F39. Photomicrograph (plane-polarized light) of glass in a chilled pillow margin from Unit 1 containing fresh, euhedral olivine phenocrysts (center) with inclusions of chromite and glass (left side of chromite crystals). The chromite inclusions in the olivine indicate early oxide precipitation. Sample 183-1140A-26R-1 (Piece 1A, 5–18 cm).

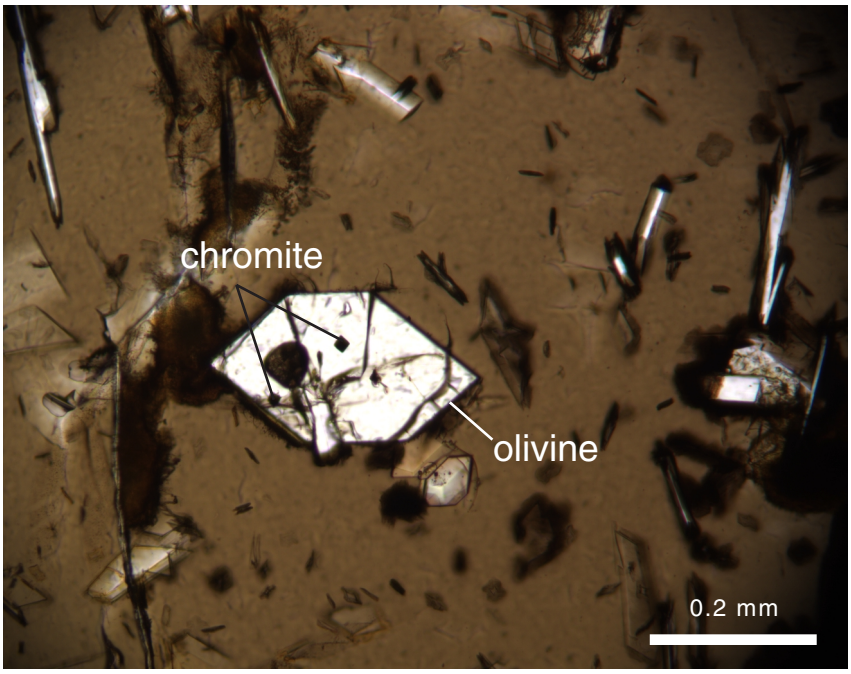

Figure F40. Nb, $(Zr/Ti)_N$, and Ni vs. Zr (subscript N indicates ratios normalized to primitive mantle values of Sun and McDonough, 1989). Data for basalts from Leg 183 Sites 1136, 1137, 1138, 1140, 1141, and 1142 are compared with fields for basalts dredged and cored from the Kerguelen Plateau (Sites 738, 747, 749, and 750) and dredged basalts from Eastern and Central Broken Ridge (BR) (Data from Alibert, 1991; Davies et al., 1989; Mahoney et al., 1995; Mehl et al., 1991; Salters et al., 1992; Storey et al., 1992; and Weis et al., 1989). Note that basalts from Site 1141 have the highest Nb, Zr, and Ni contents, basalts from Sites 1138 and 1140 range widely in Nb and Zr contents, and basalts from Sites 738, 1137, 1141, and 1142 have the highest $(Zr/Ti)_N$. (Continued on next page.)

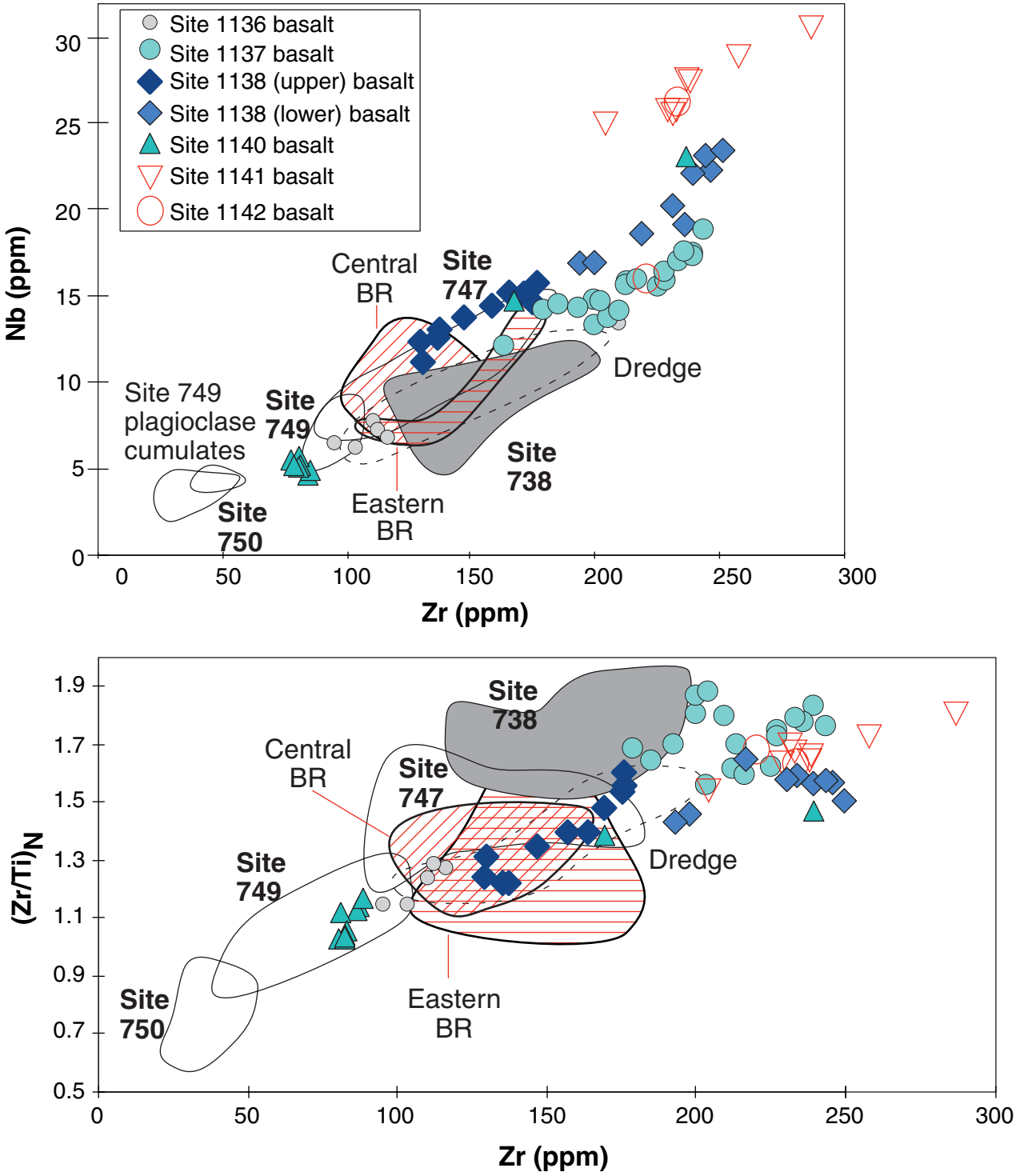

Figure F40 (continued).

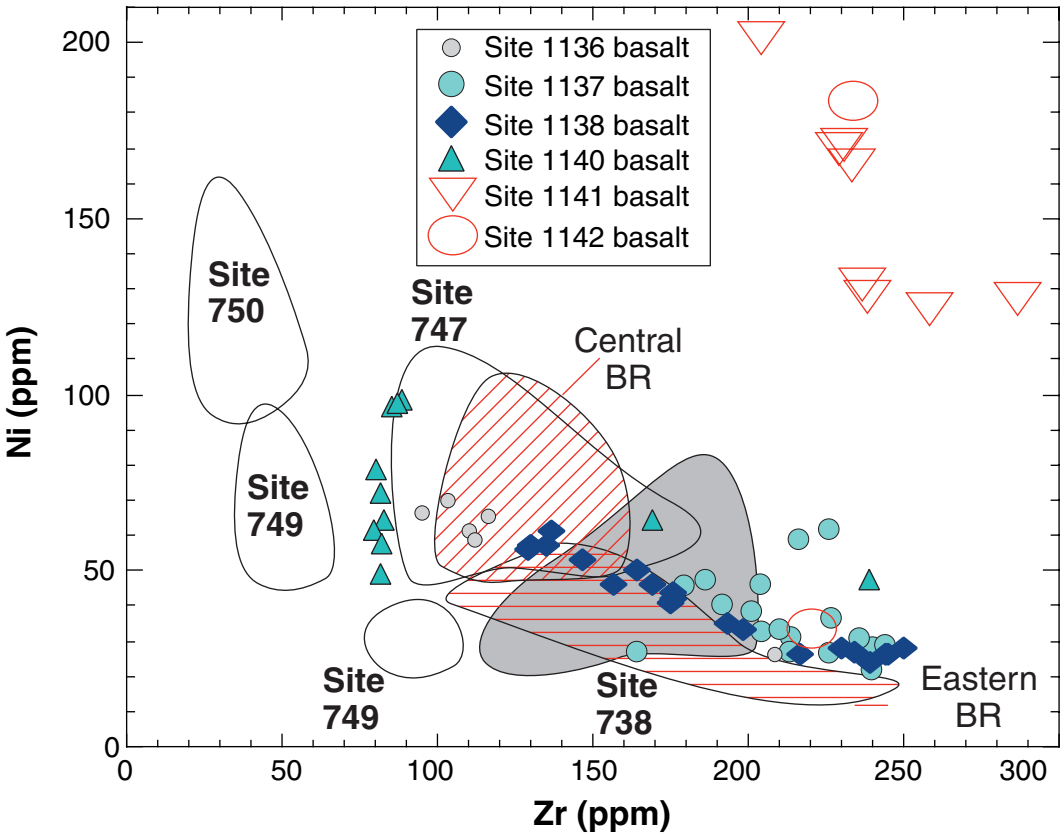

Figure F41. *JOIDES Resolution* JR183-101 single-channel seismic profile across Sites 1141 and 1142. SP = shotpoint. Vertical exaggeration = ~20 at seafloor.

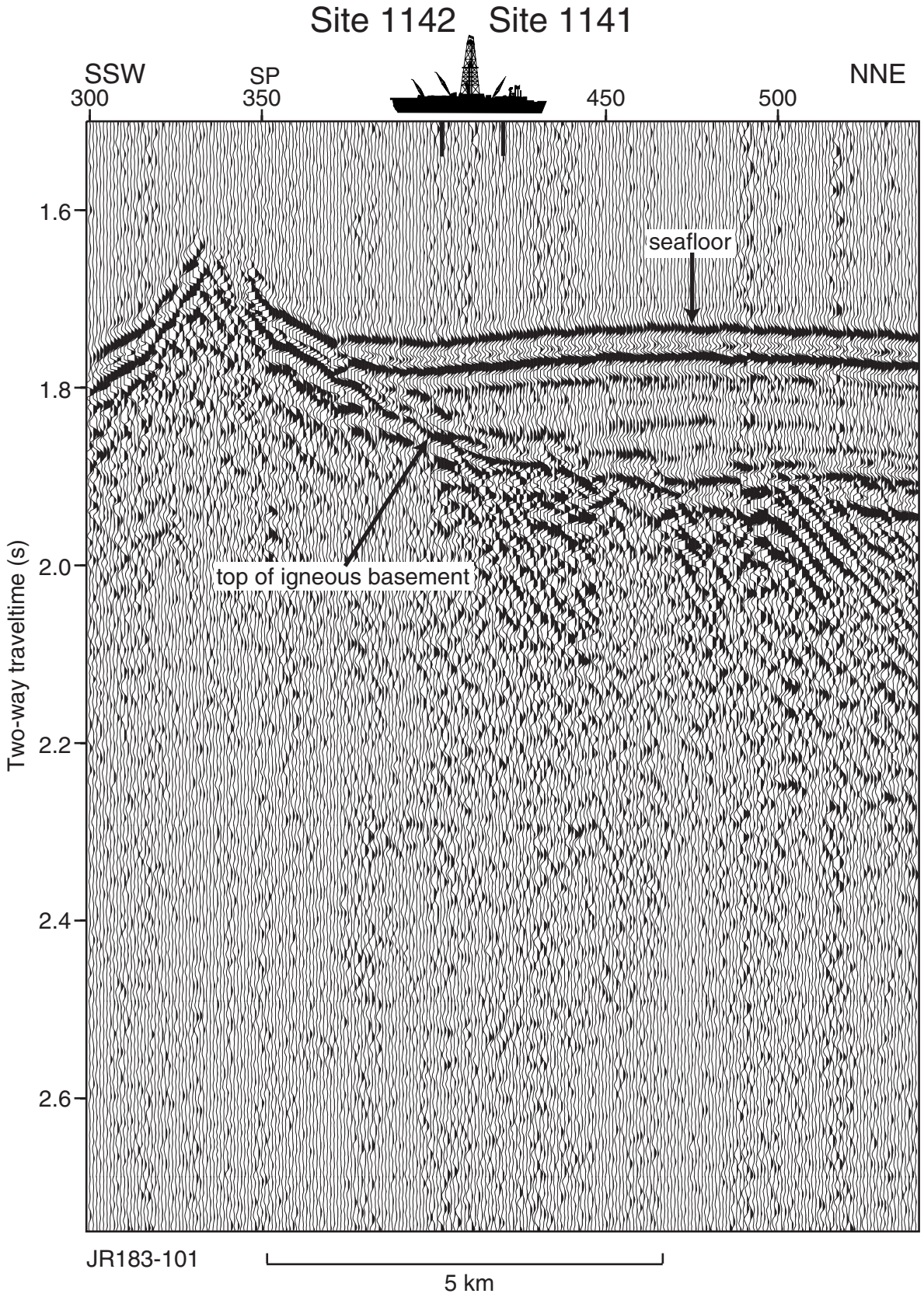

Figure F42. Composite stratigraphic section for Site 1141 showing core recovery, a simplified summary of lithology, lithologic unit boundaries, ages of units, and names of lithologies.

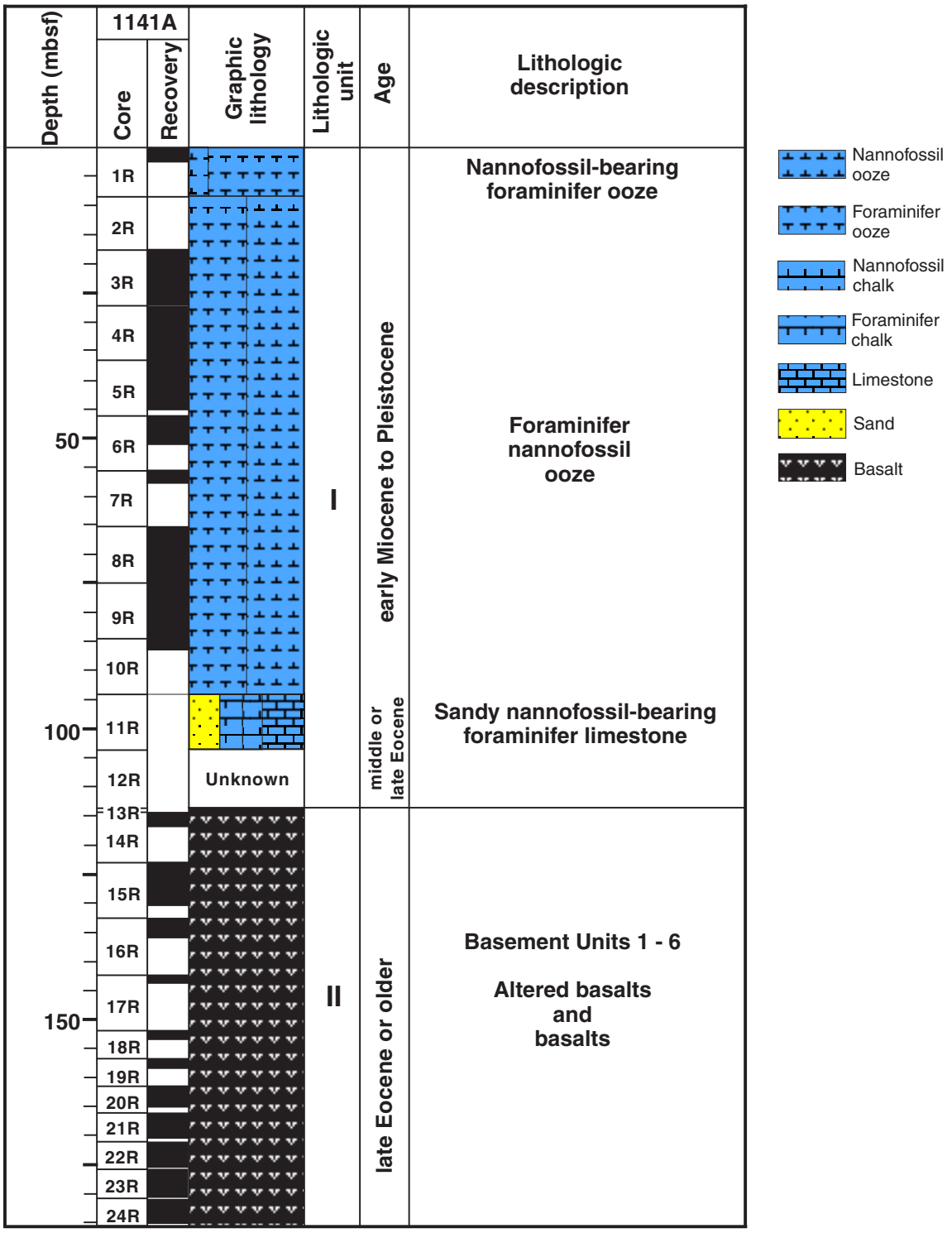

Figure F43. Composite stratigraphic section for Site 1142 showing core recovery, a simplified summary of basement lithology, basement unit boundaries, and names of basement lithologies. The interval from the seafloor to top basement rocks was washed, and the sedimentary section was not cored.

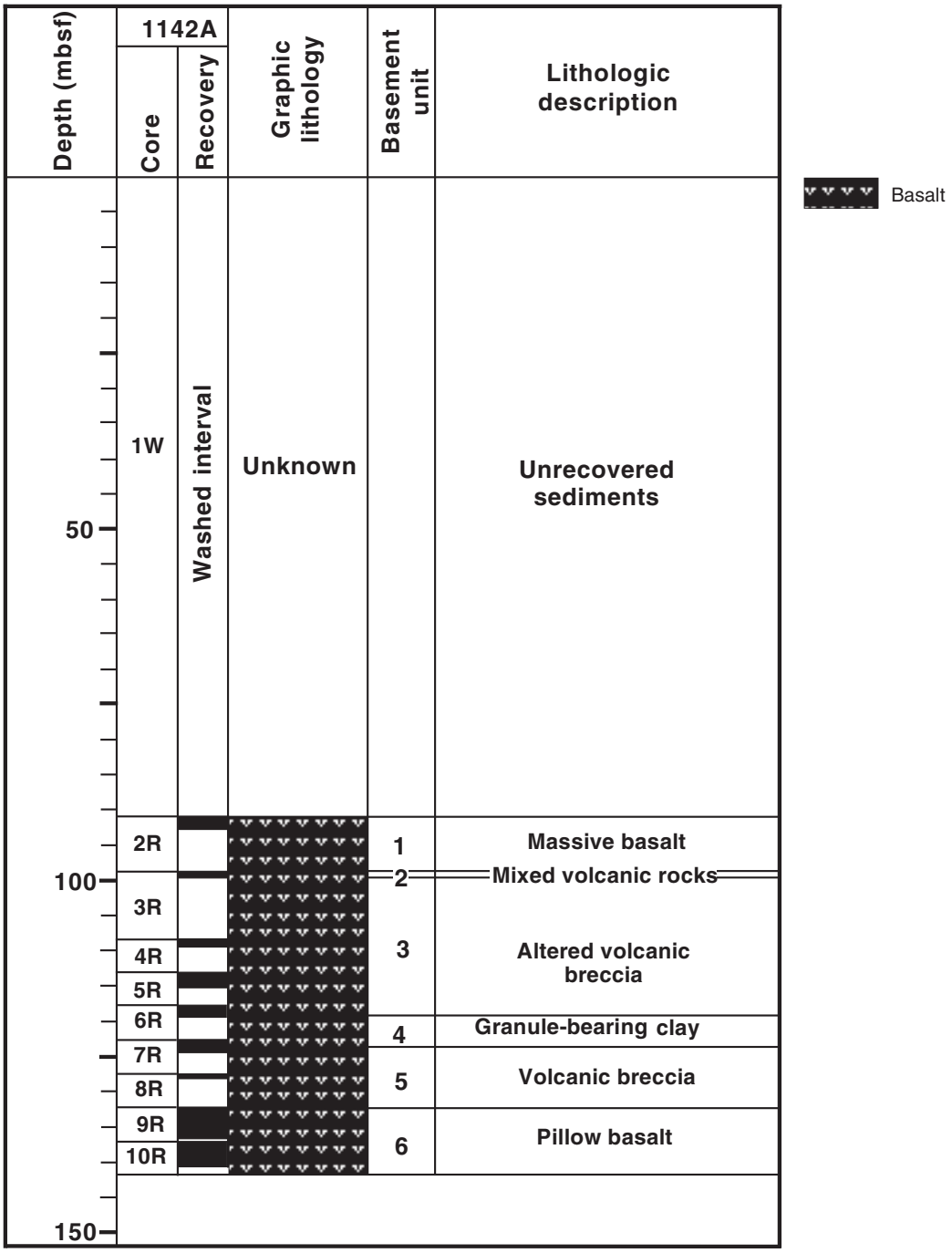

Figure F44. Compositions of volcanic rocks from all Leg 183 basement recovery sites (Fig. F15, p. 66) on the $Na_2O + K_2O$ vs. SiO_2 classification diagram of Le Bas et al. (1986). For comparison, fields are also indicated for volcanic rocks recovered from Kerguelen Plateau drill sites 738, 747, 748, 749, and 750 (Alibert, 1991; Davies et al., 1989; Mehl et al., 1991; Salters et al., 1992; Storey et al., 1992; Weis et al., 1989).

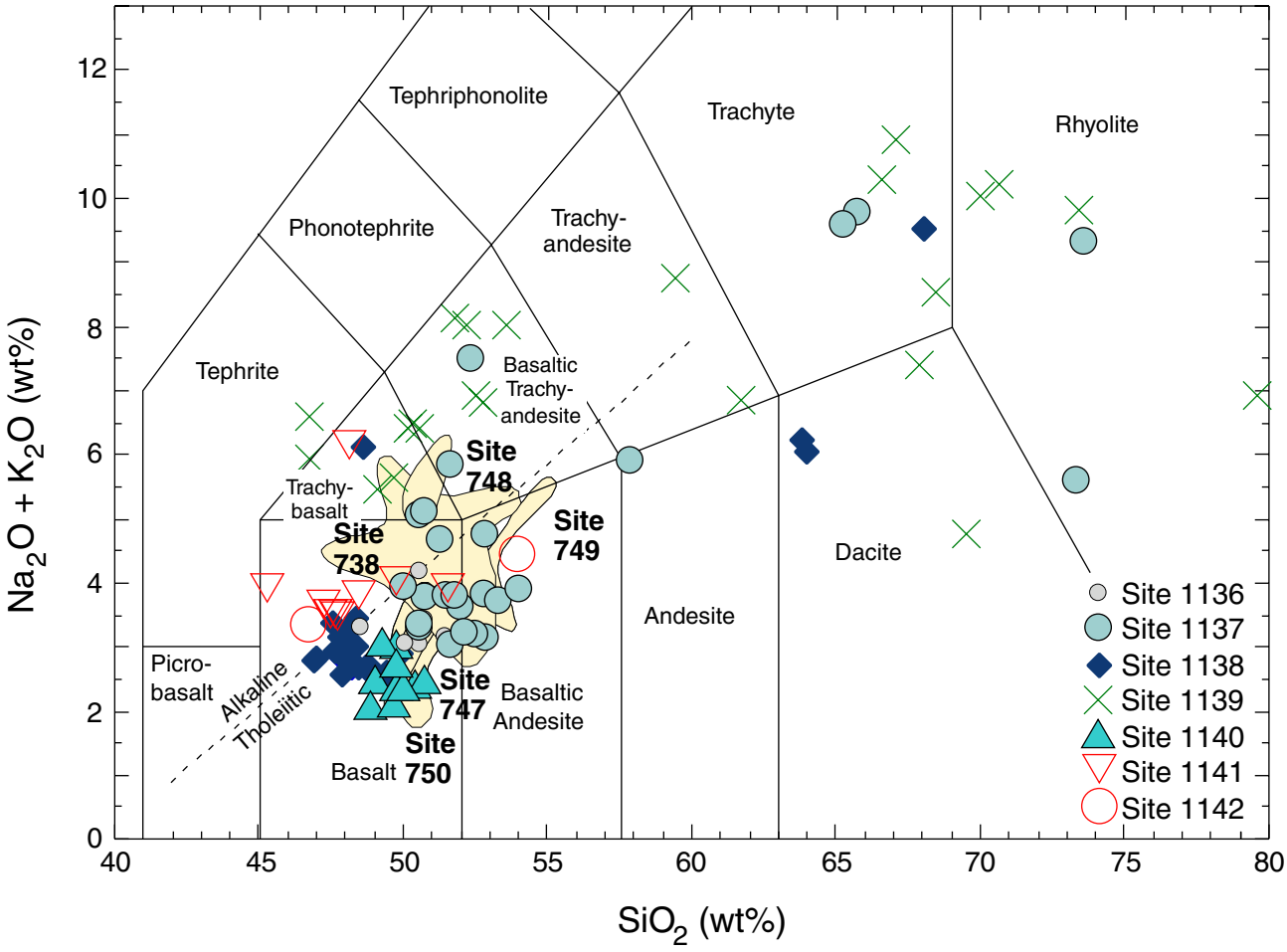

Figure F45. Color close-up photograph of Site 1137 conglomerate (interval 183-1137A-34R-3, 57–80 cm).

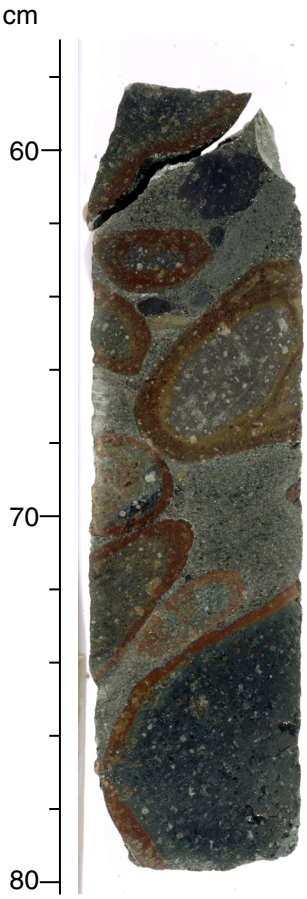

Figure F46. Photomicrographs of garnet gneiss. **A.** Poikiloblastic garnet (gt) in Unit 6 (clast in conglomerate, Sample 183-1137A-35R-2, 46–47 cm). Field of view = 1.4 mm (plane-polarized light). **B.** Porphyroblastic garnet (gt) and biotite (bi) from Unit 9 (clast in tuff, Sample 183-1137A-44R-4, 44–46 cm). Field of view = 2.8 mm (plane-polarized light).

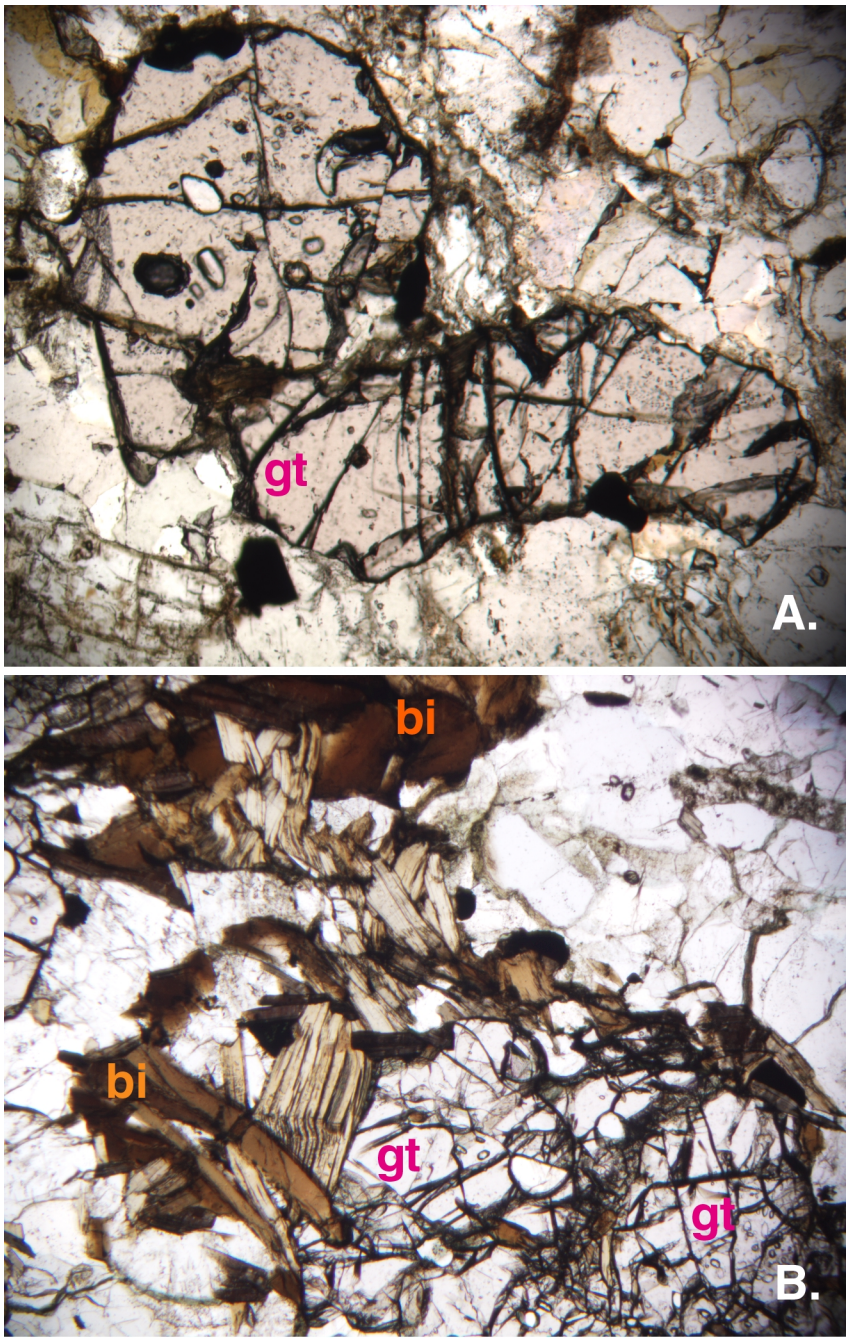

Table T1. Leg 183 drill sites, locations, water depths, subseafloor penetration, recovery, and age.

Site	Location	Coordinates	Water depth (m)	Sediment penetration (m)	Sediment recovery (m)	Basement penetration (m)	Basement recovery (m)	Total penetration (m)	Age* (Ma)
1135	Southern Kerguelen Plateau	59°42.0′S 84°16.4′E	1566.6	526.0	208.7	0	0	526.0	NA
1136	Southern Kerguelen Plateau	59°39.1′S 84°50.1′E	1930.6	128.1	54.2	33.3	18.4	161.4	105
1137	Elan Bank	56°50.0′S 68°05.6′E	1004.5	219.5	113.9	151.7	105.5	371.2	74
1138	Central Kerguelen Plateau	53°33.1′S 75°58.5′E	1141.4	698.2	343.0	144.5	69.0	842.7	94
1139	Skiff Bank	50°11.1′S 63°56.2′E	1415.3	461.7	269.6	232.5	87.3	694.2	33
1140	Northern Kerguelen Plateau	46°15.6′S 68°29.5′E	2394.1	234.0	95.8	87.9	49.1	321.9	35
1141	Broken Ridge	32°13.6′S 97°07.7′E	1196.9	113.5	57.7	71.2	39.1	185.6	NA
1142	Broken Ridge	32°13.9′S 97°07.5′E	1200.8	91.0	No coring	50.9	17.3	141.9	NA

Notes: * = minimum age of basement is oldest biostratigraphic age in overlying sediment. NA = not available.